Petroleum generation and migration modelling for the Capel and Faust basins, eastern offshore Australia

R. Funnell
V. Stagpoole

GNS Science Report 2011/22
November 2011

BIBLIOGRAPHIC REFERENCE

Funnell, R.; Stagpoole, V. Petroleum generation and migration modelling for the Capel and Faust basins, eastern offshore Australia, 2011. *GNS Science Report* 2011/22. 54 p.

R. Funnell, GNS Science, PO Box 30368, Lower Hutt 5040, New Zealand
V. Stagpoole, GNS Science, PO Box 30368, Lower Hutt 5040, New Zealand

ISSN 1177-2425
ISBN 978-0-478-19725-9

CONTENTS

FIGURES

TABLES

ACKNOWLEDGEMENTS

We gratefully acknowledge the input from Geoscience Australia staff on this project, especially Riko Hashimoto who contributed significantly to the modelling exercise through his knowledge of the basins and in reviewing drafts of the report. We thank Chris Boreham for supplying kinetic data on lacustrine source rocks. The authors received helpful reviews from Greg Browne, Karsten Kroeger and Rosemary Quinn and we thank Kat Hammond for formatting the document.

ABSTRACT

The Capel and Faust basins, located on the Lord Howe Rise in water depths between 1,300 m and 2,500 m, were the focus of a series of marine surveys by Geoscience Australia in 2006 and 2007. Their interpretation of high-fold 2D seismic reflection, gravity and magnetic, multi-beam bathymetry, sonobuoy refraction, heat flow and geological sample data suggested the basins have petroleum potential. Analysis of petroleum generation and migration, based on structural maps, lithological and other data supplied by Geoscience Australia, is the focus of this study. Basin models predict that most of the deeper depocentres in the Capel and Faust basins, mapped as containing Jurassic-aged pre-rift and Cretaceous-aged syn-rift source rocks, have the potential to expel oil and gas, and charge nearby syn-rift and post-rift reservoir formations from Cretaceous time to the present day.

Multi-1D thermal and petroleum generation models predict:

- Pre-rift (215 – 165 Ma) and Syn-rift 1 (130 – 100 Ma) megasequences within the deeper depocentres are within the oil or gas generation window;
- Based on the expected presence of petroleum-generative coaly source rocks, total oil and gas expulsion from the major depocentres exceeds 5 MMbbl/km^2 and 25 Bcf/km^2 respectively from the Pre-rift source rocks, and 20 MMbbl/km^2, and 300 Bcf/km^2 respectively from the Syn-rift 1 source rocks. In terms of timing, 80% of total hydrocarbon expulsion is predicted by the end of the Eocene, with maximum expulsion taking place between the Late Cretaceous and the Late Eocene (c. 68–36 Ma);
- A significant increase in paleo-water depth in late Cenozoic time has supressed further heating related to post-Eocene burial. However, modelling predicts post-Eocene expulsion of oil and gas may have been partly enhanced by post-rift magmatism.

In this study total expelled oil and gas volumes are “migrated across” mapped horizons to assess charge of and fill-spill relationships between structural traps. This map-based charge modelling assumes certain reservoir properties with no migration losses and predicts that:

- Accumulations within potential reservoir facies, such as deltaic, shoreline and turbidite sandstones of the lower Post-rift unit (70 – 68 Ma) are dominantly gas with volumes generally about 5 to 9 Tcf at burial depths of 400 – 700 m;
- Accumulations within similar sandstones of the upper Syn-rift 2 unit are mixed oil and gas (about 2 to 3 billion bbl oil and 10 Tcf gas) at burial depths of 400 – 800 m;
- Similar accumulations are present in the lower Syn-rift 2 and Syn-rift 1 fluvial sands;
- Most of the mapped structural traps are buried to relatively shallow depths and seal effectiveness for containment must therefore be a significant risk. Deeper structures and stratigraphic plays may further contribute to the petroleum potential in the basins.

The model presented here illustrates the potential for petroleum charge of structural traps in the Capel and Faust basins and highlights the risks associated with source rock distribution and type, reservoir distribution and quality, and seal effectiveness. Volumetric and charge assessments could be further refined using higher density seismic data and appropriate rock property data for reservoir and seal rocks in combination with 3D modelling.

KEYWORDS

Lord Howe Rise, Capel Basin, Faust Basin, multi-1D basin modelling, hydrocarbon maturity, hydrocarbon migration

1.0 INTRODUCTION

The Capel and Faust basins are located on the Lord Howe Rise in Australian territory between 25 and 30°S (Figure 1). Water depths range between 1,300 m and 2,500 m. Prior to 2006, the basins had only been lightly explored: the only well in the region is the Deep Sea Drilling Program (DSDP) drill-hole 208, drilled in the southern Faust Basin in 1971 to a depth of 594 m below seabed and terminating in Late Cretaceous nannofossil chalk. (Figure 1). In 2006 and 2007 Geoscience Australia completed a series of marine surveys (Figure 1) with the goal of investigating the petroleum potential of the region. Approximately 6,000 line km of high-fold 2D seismic reflection, 17,000 line km of gravity and magnetic, 24,000 km^2 of high-resolution multi-beam bathymetry, sonobuoy refraction, heat flow and geological sample data were acquired over a 300 x 350 km^2 area. Interpretation of the new seismic data, utilising 3D visualisation of the basin, has led to a better understanding of the geological history of the region. Findings on the petroleum potential of the basins by Colwell et al. (2010) and Higgins et al. (2011) was the impetus for the multi-1D basin modelling described in this report. These models examine source rock maturity, timing of expulsion and inferred petroleum migration and accumulation in the Capel and Faust basins.

Our modelling was based on paleobathymetry and structural maps of eight horizons, (including seabed and basement).supplied by Geoscience Australia (Van de Beuque et al. 2003, Colwell et al. 2010, Higgins et al. 2011). Source rock properties were based on data from the Taranaki Basin (King & Thrasher 1996), Clarence-Moreton Basin (O'Brien et al. 1994) and other Mesozoic Australian basins (Powell et al. 1991, Boreham et al. 2003). Simple map-based maturity and migration modelling was undertaken to define regional scale source - trap relationships. However, the wide data spacing and lack of constraints only allowed a basin-wide overview of the source rock maturity and migration.

This report is divided into two sections. The first section describes the multi-1D basin models used to predict basin-wide maturity, the volumes of expelled petroleum and the timing of expulsion from mapped kitchen areas. The second section describes map-based migration models used to provide a reconnaissance level assessment of possible migration and entrapment in the two basins.

1.1 GEOLOGY OF THE CAPEL AND FAUST BASINS

Interpretation of seismic and gravity data indicates that large sub basins (up to 125 km long) with a maximum sediment thickness of over 7 km in the northwest of the study area, developed in the Mesozoic. Rifting is interpreted to have been associated with the Early Cretaceous regional magmatism in eastern Gondwana and the Late Cretaceous Tasman Sea opening (Norvick et al. 2008). Extension, oblique to pre-existing northwest-trending basement structure, resulted in the formation of en-echelon sub-basins (Bryan et al. 1997, Norvick et al. 2001, 2008).

Seismic interpretation by Hashimoto et al. (2008) suggests that two syn-rift megasequences and a post-rift megasequence overlie a heterogeneous pre-rift megasequence (Figure 2 and Table 1). Coaly and lacustrine source rocks are inferred to have been deposited in predominantly fluvial environments during the ?Paleozoic to Mesozoic pre-rift and syn-rift megasequences (Hashimoto et al. 2010). Reservoir and seal rocks are likely to have been deposited in marginal marine to deep-water environments (including turbidite/submarine fan systems) during the Cretaceous and younger syn-rift and post-rift megasequences (Table 1).

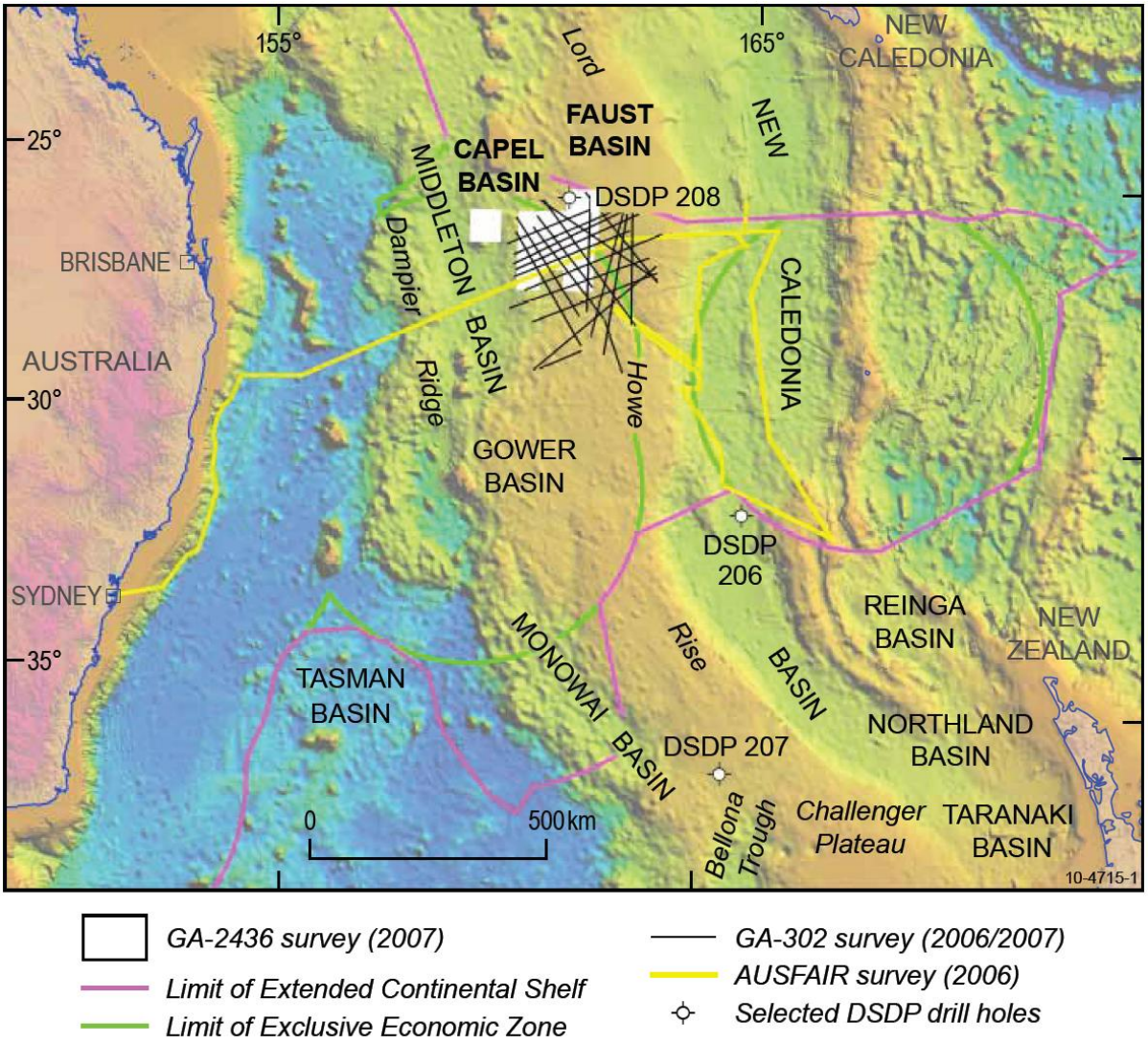

Figure 1 Capel and Faust basin location map showing DSDP wells, recent survey data and territorial boundaries (from Hashimoto et al. 2010).

The regional seal is expected to be provided by calcareous bathyal sediments of the upper Post-rift succession that overlie the transgressive systems tract formed during the initial stages of the Late Cretaceous marine transgression (Hashimoto et al. 2010). Potential structural traps are formed by rifting-related, tilted fault blocks and drape over horsts, as well as later anticlinal structures associated with Cretaceous and Cenozoic deformation. Hashimoto et al. (2010) suggest that variability in seismic facies and the presence of several unconformities point toward the presence of stratigraphic traps within the syn-rift and lower post-rift successions. However, widespread Cenozoic magmatism may have created a potential risk to reservoir quality and seal integrity and is proposed as the likely cause of fluid migration features visible on seismic sections (Hashimoto et al. 2010).

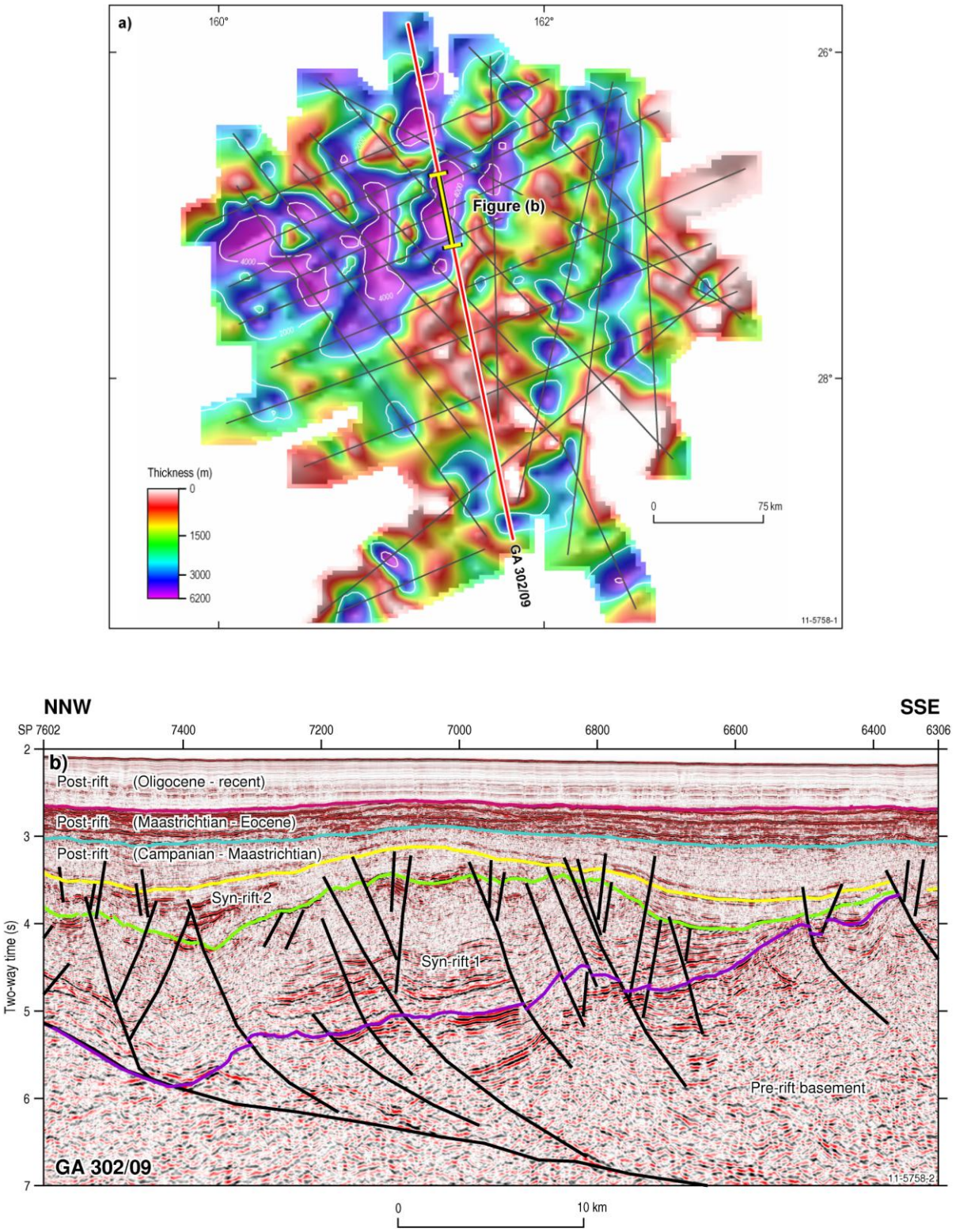

Figure 2 (a) Interpreted total syn-rift and post-rift sediment thickness based on seismic, gravity and magnetic data and, (b); the seismic stratigraphy along line GA-302/09 (from Hashimoto et al. 2010). Line location is shown in (a).

Table 1 Seismic megasequences in the Capel and Faust basins. Age, lithology and depositional environment of the syn-rift megasequences and lower post-rift successions are inferred from regional tectonic reconstructions and analogues in the Gippsland, Maryborough and Taranaki basins (from Hashimoto et al. 2010).

Seismic megasequence	Inferred age	Inferred lithology	Depositional environment	Potential petroleum system elements
Post-rift	Oligocene–Recent	Calcareous chalk and ooze, volcanics and intrusives	Bathyal	Regional seal
	Late Maastrichtian–Eocene	Siliceous and calcareous chalk, marl, chert, volcanics and intrusives	Bathyal	Regional seal
	?Campanian–Late Maastrichtian	Siliciclastic to calcareous sandstone, fining upward to mudstone	Fluvio-deltaic and shallow marine (lower), bathyal (upper)	Reservoir, seal
Syn-rift 2	?Cenomanian–?Campanian	Sandstone, siltstone, mudstone, minor coal, volcanics and intrusives	Fluvial and lacustrine (lower), deltaic, shoreline and shallow marine (upper)	Reservoir, seal, source (coal, lacustrine) in lower parts
Syn-rift 1	?Early Cretaceous–?Cenomanian	Volcanics, intrusives, sandstone, siltstone, coal.	Fluvial, lacustrine and colluvial	Source (coal, lacustrine), reservoir
Pre-rift	Paleozoic-Mesozoic	E. Cretaceous volcanics, Mesozoic sedimentary, Paleozoic fold belt	Convergent margin, backarc rift, foreland and intracratonic basins	Source (coal)

2.0 MULTI-1D BASIN MODELLING

Multi-1D basin modelling was undertaken on grids of the Capel and Faust basins (supplied by Geoscience Australia) (Figure 3a, 3b). The multi-1D (pseudo-3D) BM1D basin modelling code used in this report is a GNS Science development based on the 1D finite-element conductive heat flow package Bassim (modified from Willett 1998, Armstrong et al. 1996), the application of which is described in Wood et al. (1998). The basin simulation code is applied to each 0.39 km^2 (625 x 625 m) cell across a grid covering the Capel and Faust basins. Thickness, age and paleobathymetric data associated with stratigraphic intervals are combined with simple mathematical relationships describing sediment properties during progressive compaction to derive burial and thermal maturity histories for each cell. Heat flow is applied at the base of the model (base lithosphere) using an approach consistent with that described in Armstrong et al. (1996) to fit thermal calibration data such as heat flow from sea-bed probes or temperatures when well data are available.

Using a one-dimensional conductive heat flow algorithm in a three-dimensional sense has limitations, especially in areas where lateral heat transfer is important. The effects on subsurface temperatures caused by heat transfer related to lateral fluid flow and refraction of heat across thermal conductivity boundaries, such as faults, should be considered, although in this case these effects are probably minor because of the regional scale of the modelling project.

The stack of sedimentary layers is decompacted to allow the reconstruction of the basin configuration and rate of sediment fill through time. Periods of non-deposition or erosion are also included to more accurately represent the burial and maturity history. Diachronous events related to sediment onlap or an unconformity may be accounted for, as necessary, by assigning age grids for the base of each interval. Geochemical parameters describing source rock properties (hydrogen index – HI, gas oil generation index – GOGI, saturation threshold – S_{th}) allow source rock maturity and volumes of expelled petroleum to be predicted. These BM1D model outputs are used as input to the map-based migration modelling (Section 3). Other outputs include predicted heat flow, vitrinite reflectance and temperatures within the basin, as well as paleo-structure maps for the evolving basin, which are used as surfaces suitable for paleo-charge modelling.

The methodology adopted for developing maps of expelled petroleum phases can be summarised as:

- Check data grids, trim and mask to a uniform area and derive isopach grids for input into the multi-1D modelling programme;
- Compile full input data set for multi-1D models (BM1D) and execute multiple runs using various scenarios to test model sensitivities;
- Convert BM1D petroleum volumetric data to maps for display, volumetric calculations and input to map-based migration models.

2.1 INPUT DATA

2.1.1 Burial history input

Burial history is represented in the model by combining a series of isopach grids. Initially, eight stratigraphic horizons (including seafloor depth) were provided by Geoscience Australia for modelling (Table 2, Figure 3a, 3b). Isopach grids were further sub-divided to represent source rock intervals, based on the suggested presence of coaly facies from strong seismic reflectors (Figure 2) in pre-rift and syn-rift successions. Both syn-rift isopachs (Syn-rift 1 and Syn-rift 2; Table 1) were subdivided into lower and upper units with the lower third of each unit assigned different source rock parameters. The Neogene-Oligocene isopach (Seabed – Base Oligocene) was also subdivided into three separate isopachs to provide greater flexibility in modifying recent burial history and heat flow scenarios. The Pre-rift sequence may correlate with the Clarence-Moreton or Maryborough basins in eastern Australia (Colwell et al. 2006, Hashimoto et al. 2010). Hence, the upper section of this unit (arbitrarily determined as 15% of total thickness) has been assigned as an equivalent of the Walloon Coal Measures of the Clarence-Moreton Basin, with a maximum thickness no greater than 500 m. The list of grids used in the modelling, in stratigraphic sequence, is shown in Table 2.

The age and lithologic composition for all units (Table 3), provided by Geoscience Australia, are based on seismic interpretation and analogues in other basins (Taranaki, Clarence-Morton, Gippsland and Maryborough basins; King & Thrasher 1996, Norvick et al. 2008, Colwell et al. 2010, Hashimoto et al. 2010). A cross-section of the multi-1D structural input along a line through the Capel and Faust basins illustrating the geometry of the structural grids is shown in Figure 4.

2.1.2 Erosion

The seismic data indicate two significant unconformities in the stratigraphic record that are interpreted to be:

- at the start of the Late Cretaceous separating the two syn-rift megasequences (100 - 95 Ma), and
- in the Late Cretaceous at the transition between syn-rift and post-rift phases (80 - 70 Ma).

There is insufficient data to adequately estimate the thickness of the eroded section, so a series of approaches were applied for including erosion in the models.

The initial approach was to assume a uniformly distributed overlying unit (i.e., eroded thickness plus thickness of overlying sequence is constant), resulting in erosion of up to 700 m in the Late Cretaceous (~80 Ma) and 1,300 m at the beginning of the Late Cretaceous (~100 Ma). A 5 Myr period was not considered long enough to both deposit and erode up to 1,300 m of sediment (see Table 2), so ages were modified in the erosion models to accommodate more time (i.e., unconformities for 105 – 95 Ma and 85 – 70 Ma).

Next, this approach was updated with more complex calculations based on the thickness of both overlying and underlying units, and the predicted paleo-depths, with further refinements that assumed maximum erosion occurred on the flanks of bald highs in the basin. These calculations resulted in complex distributions of erosion which were difficult to justify from the available data. Hence, it was finally decided to determine model sensitivity to erosion by adopting a constant value for each erosional event. For the earlier event 1,000 m was

deposited from 105 to 97 Ma and eroded prior to 95 Ma. In the later event, 500 m was deposited from 85 to 75 Ma and eroded prior to 70 Ma. This erosion scenario was tested against a hiatus scenario with no sedimentation or erosion modelled over the two periods 100 – 95 Ma and 80 – 70 Ma (Hiatus 2 and Hiatus 3 in Table 2).

Hashimoto et al. (2010) identified additional periods of non-deposition related to further restructuring events. These unconformities were input in the model separating pre-rift and syn-rift megasequences, as well as near the base-Eocene and base-Oligocene sequences (Tables 2 and 3).

Table 2 Input deck for BM1D relating units to grids, and nomenclature used in the hiatus scenario model.

Unit	Grid for base unit	Modelled unit name	Age at base Ma	Paleo-water depth
Waterdepth	depth_CF_wb_1km	Water0Ma	0	Water0Ma
Seafloor to early Miocene		Late Neogene	18	Water15Ma
Miocene - Oligocene		Early Miocene	27	Water36Ma
Early Oligocene	depth_CF_Olig_1km	Early Oligocene	36	Water36Ma
Hiatus		Hiatus5	40	Water40Ma
Base Oligocene – near base Eocene	depth_CF_Eoc_1km	Eocene Oligocene	50	Water50Ma
Hiatus		Hiatus4	60	Water60Ma
Post-rift Upper sag	depth_CF_Usag_1km	Paleocene Eocene	68	Water64Ma
Post-rift Lower sag	depth_CF_SR2B_1km	Lower Sag	70	Water69Ma
Hiatus		Hiatus3	80	Water70Ma
Upper Syn-rift 2		Upper SR2B	90	Water80Ma
Lower Syn-rift 2	depth_CF_SR1B_1km	Lower SR2B	95	Water80Ma
Hiatus		Hiatus2	100	Water90Ma
Upper Syn-rift 1		Upper SR1B	120	Water90Ma
Lower Syn-rift 1	depth_CF_CretRift_1km	Lower SR1B	130	Water90Ma
Hiatus		Hiatus1	165	Water90Ma
Upper Pre-rift (Walloon eq.)		Walloon	175	Water90Ma
Lower Pre-rift	depth_CF_Bus_1km	Pre-rift	215	Water90Ma

Table 3 Age and lithology (proportion of sand, silt, mud, lime, coal and volcanic rock) for each unit used as input to multi-1D modelling.

Modelled unit name	Age at base Ma	Lithologic composition					
		Sand	Silt	Mud	Lime	Coal	Volc.
Water0Ma	0						
Neogene_Oligocene	36	0	0	0.1	0.9	0	0
Hiatus5	40						
Eocene Oligocene	50	0	0	0.1	0.9	0	0
Hiatus4	60						
Paleocene Eocene	68	0	0	0.2	0.8	0	0
Lower Sag	70	0.1	0.1	0.3	0.5	0	0
Hiatus3	80						
Upper SR2B	90	0.39	0.2	0.35	0	0.01	0.05
Lower SR2B	95	0.4	0.15	0.35	0	0.05	0.05
Hiatus2	100						
Upper SR1B	120	0.29	0.2	0.35	0	0.01	0.15
Lower SR1B	130	0.45	0.15	0.2	0	0.05	0.15
Hiatus1	165						
Walloon	175	0.25	0.3	0.35	0	0.1	0
Pre-rift	215	0.4	0.15	0.4	0	0	0.05

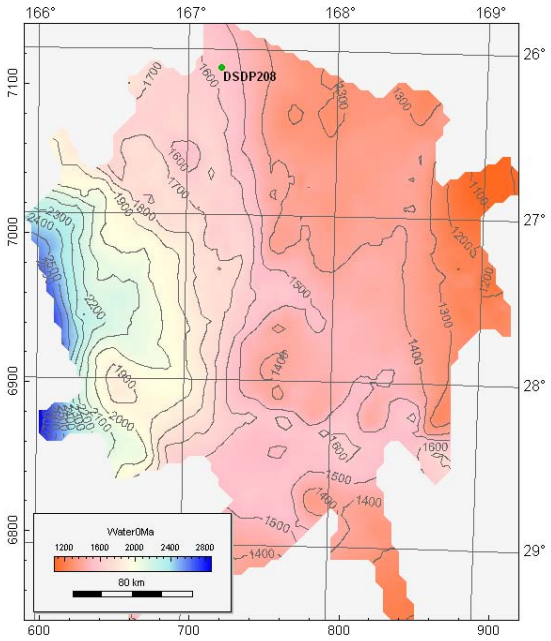

Present day seabed depth

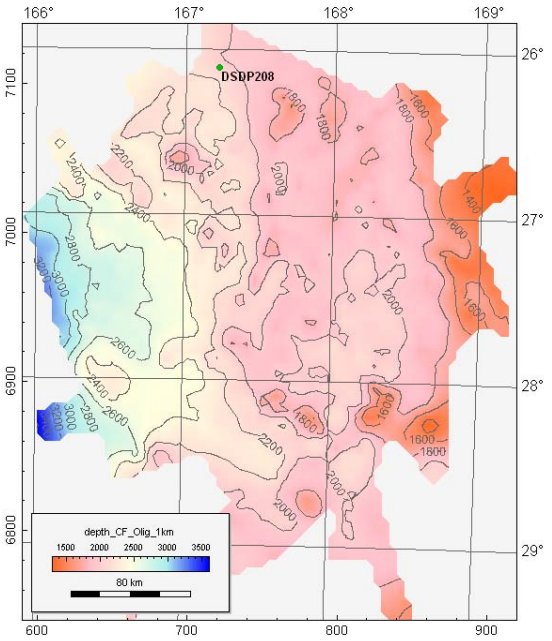

Base Oligocene horizon (36 Ma)

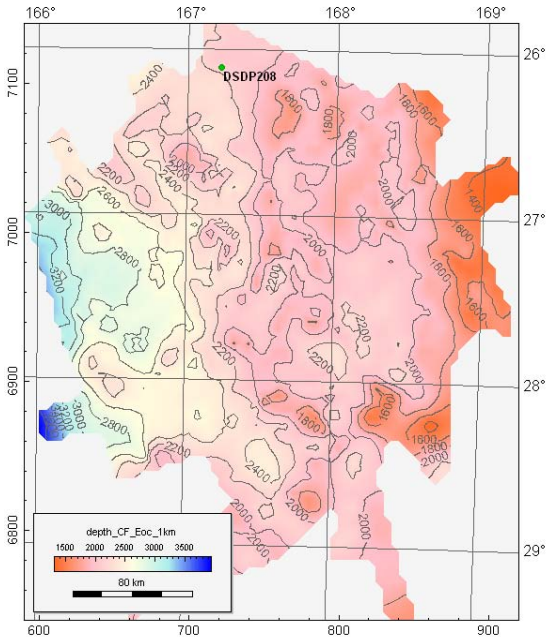

Near base Eocene horizon (50 Ma)

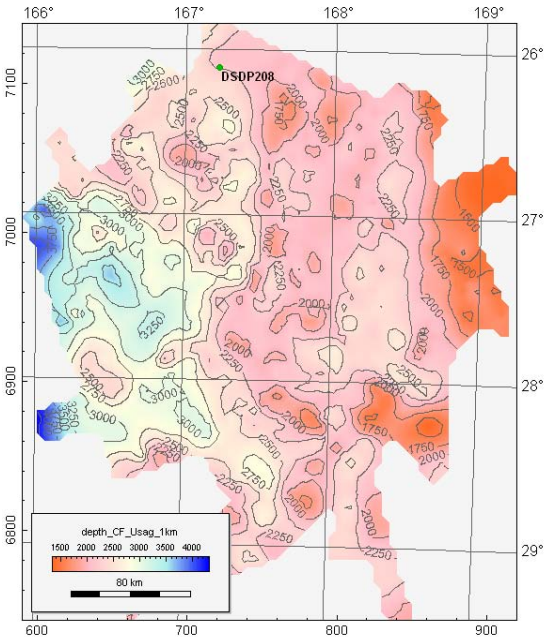

Base Paleocene – Lower Post-rift (68 Ma)

Figure 3a Structural depth maps (m) for input to multi-1D modelling (note different depth scales for each map). Co-ordinates on left and lower axes are UTM 58S in km and on right and upper axes are latitude (S) and longitude (E).

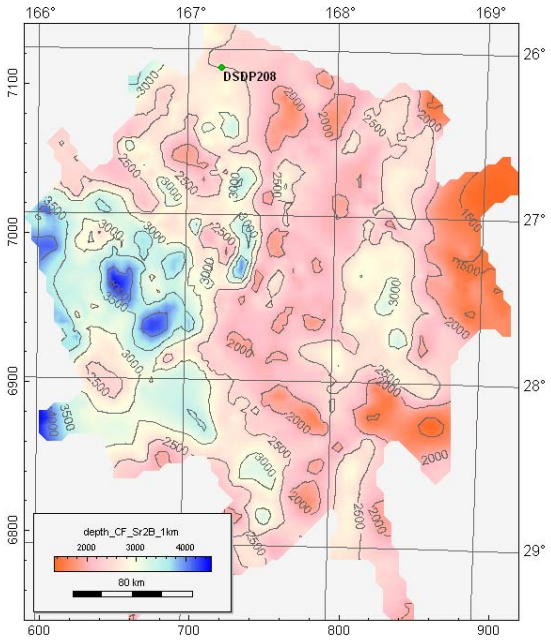

Syn-rift 2 (80 Ma)

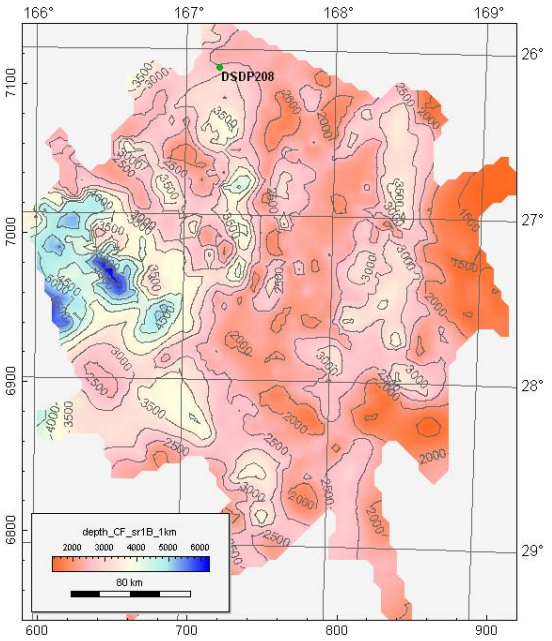

Top Syn-rift 1 (100 Ma)

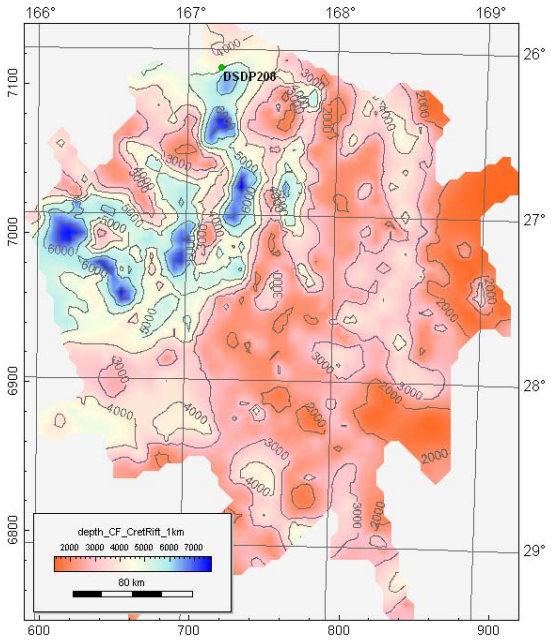

Pre-rift megasequence (165 Ma)

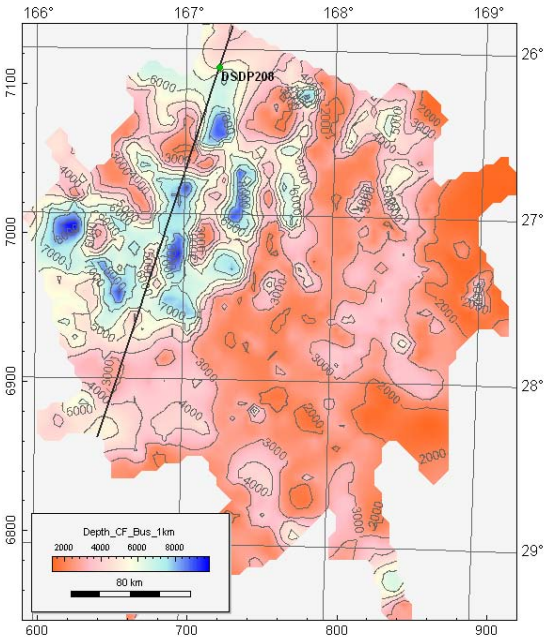

Basement (215 Ma)

Figure 3b Structural depth maps (m) for input to multi-1D modelling (note different depth scales for each map). The location of cross-section in Figure 4 is shown on the basement map (lower right). Co-ordinates on left and lower axes are UTM 58S in km and on right and upper axes are latitude (S) and longitude (E). Note the Capel Basin lies to the south and west, and the Faust Basin to the south and east of the DSDP208 well on these maps.

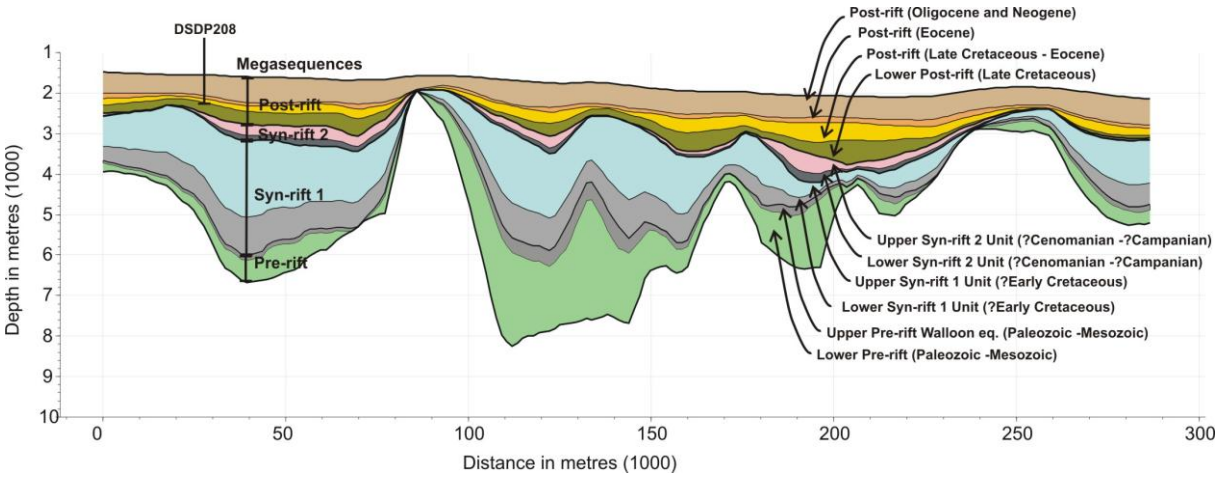

Figure 4 Cross-section through the multi-1D structural input along a line through the DSDP208 well site. Modelled source rock units are in grey colours. See Figure 3b for cross-section location.

2.1.3 Paleobathymetry

Bathymetry (water depth) maps were provided by Geoscience Australia for the present day and for Late Eocene time (Figure 5). Average water depth for other times was inferred from the tectonic setting and seismic facies character. Paleobathymetry maps were derived, as a ratio of either of these two maps, to best represent the estimated average bathymetry of the study area for a particular time. The uncertainty in these derived maps is assessed to be ± 50%, which at bathyal depths may be significant in terms of paleo-structure, although is less significant for paleo-temperature.

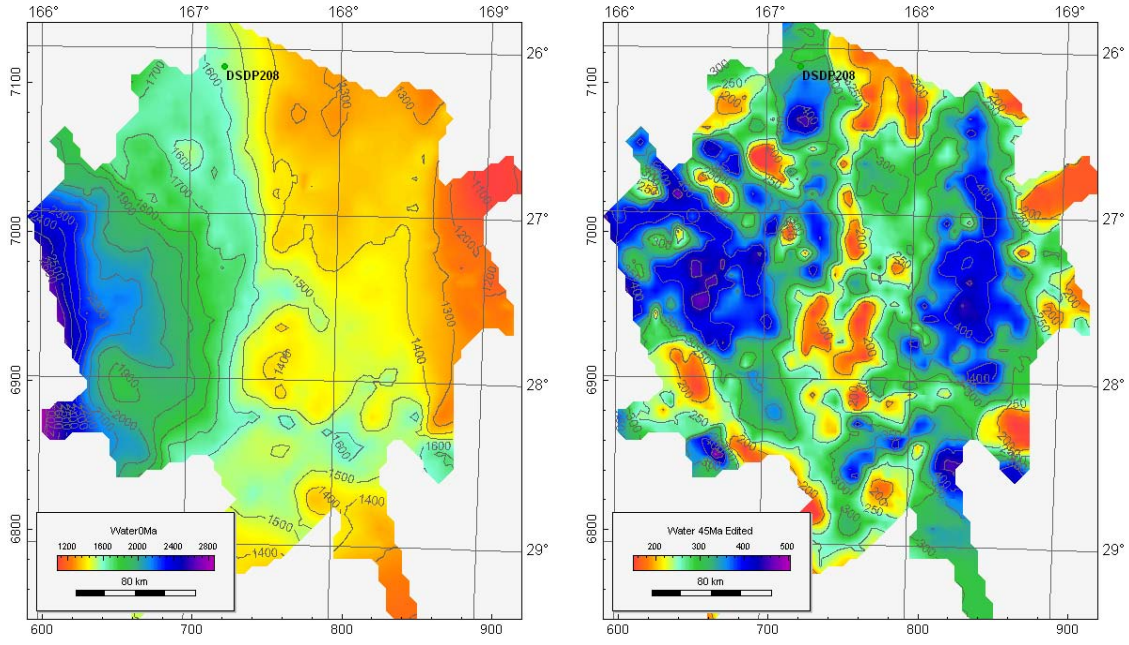

Figure 5 Present day bathymetry (left) and Late Eocene (45 Ma) paleobathymetry (right) for input to multi-1D modelling. Paleobathymetry for other times were derived from these maps. Co-ordinates on left and lower axes are UTM 58S in km and on right and upper axes are latitude (S) and longitude (E).

2.1.4 Source rocks and hydrocarbon generation parameters

There are no proven source rocks in the Capel and Faust basins. Source rock distribution has been inferred from seismic interpretation and inferences based on analogue basins and regional tectonic reconstructions. General source rock parameters, similar to those of the

Taranaki Basin were used, with hydrogen indices (HI) of 300 mg_{HC}/g_{TOC} and total organic carbon (TOC) contents of 1.0 to 5.0% (Table 3). Coaly source rocks were modelled in both syn-rift megasequences as well as the uppermost part of the Pre-rift megasequence. Lacustrine source rocks were modelled in the lower third of both syn-rift megasequences (Lower Syn-rift 1 and Lower Syn-rift 2 units). The lower syn-rift coaly and lacustrine units were interpreted to be richer in organic matter (3% TOC), with the upper syn-rift units being much leaner (1% TOC). The Pre-rift coaly unit was interpreted to be equivalent to Walloon Coal Measures and assigned a TOC value of 5% in all models.

The rate of transformation of kerogen to oil and gas was modelled using two-component (oil and gas) Arrhenius-type kinetics, specified with a single frequency factor and a distribution of activation energies. Source rock kinetics of Pepper & Corvi (1995a) were used due to their widespread global use and proven application for matching generation in the Taranaki Basin (Funnell et al. 2004). Coaly source rocks were modelled as sub-type DE organofacies (type III waxy, terrigenous kerogen) for oil and gas generation and cracking of oil to gas (secondary gas generation). Lacustrine source rocks were modelled as both sub-type C organofacies (type I aquatic, terrigenous kerogen) and using kinetic data derived from a lacustrine shale sampled in the Carnarvon Basin of northwestern Australia (Woodleigh 2A kinetic data supplied by Chris Boreham, Geoscience Australia). A simple saturation-controlled expulsion threshold (S_{th}) for oil (Pepper & Corvi 1995b) was adopted that required the generation of a certain amount of oil to fill pore space and overcome the adsorption capacity before expulsion occurred (Table 4).

Table 4 Hydrocarbon generation parameters for source rock units used as input to multi-1D modelling. Parameters are presented for both coaly and lacustrine source rocks for units modelled as containing both organofacies.

Unit	Age at base (Ma)	TOC (%)	GOGI	Sth (mg_{HC}/g_{TOC})	HI (mg_{HC}/g_{TOC})	Kinetics for organofacies
Upper Syn-rift 2	90	1.0	0.37	100	300	Pepper & Corvi (1995a) sub-type DE
Lower Syn-rift 2	95	3.0	0.37	100	300	Pepper & Corvi (1995a) sub-type DE,
Lower Syn-rift 2	95	3.0	0.16	100	548	sub-type C and Woodleigh shale
Upper Syn-rift 1	120	1.0	0.37	100	300	Pepper & Corvi (1995a) sub-type DE
Lower Syn-rift 1	130	3.0	0.37	100	300	Pepper & Corvi (1995a) sub-type DE,
Lower Syn-rift 1	130	3.0	0.16	100	548	sub-type C and Woodleigh shale
Upper Pre-rift Walloon eq.	175	5.0	0.37	100	300	Pepper & Corvi (1995a) sub-type DE

The multi-1D basin modelling used simplified algorithms to estimate volumes of oil and gas expelled from the modelled source rock units. These are presented below as equations 1 and 2, respectively:

$$Vol_{oil} = \frac{TOC}{15900} \left[TR_{oil} \cdot HI_o - S_r \right] \rho_{rock} \cdot vol_{source} / \rho_{oil} \qquad 1$$

where Vol_{oil} is the volume of expelled oil (bbl); TOC is the percentage of total organic carbon; HI_o is the initial Hydrogen Index for oil (mg_{OIL}/g_{TOC}); TR is the transformation ratio determined from maturity modelling; S_r is the retained oil in the source rock (mg_{OIL}/g_{TOC}); vol_{source} is the volume of source rock (m^3) and ρ_{rock} and ρ_{oil} are the

densities of the dry source rock and oil (kg/m^3), respectively. A standard value of 800 kg/m^3 is used throughout this report as the density of oil.

Gas volumes are estimated using a similar approach, except that no residual gas is modelled as being retained in the source rock:

$$Vol_{gas} = \frac{TOC}{2832} \left[TR_{gas} \cdot HI_g + TR_{crack} \cdot S_r \right] \cdot \rho_{rock} \cdot vol_{source} / \rho_{gas}, \quad 2$$

where Vol_{gas} is the volume of expelled gas (cu ft); HI_g is the initial Hydrogen Index for gas (mg_{GAS}/g_{TOC}) and ρ_{gas} is the gas density, assumed to be 0.86 kg/m^3 at standard temperature and pressure (STP) conditions. While this represents an average density for dry gas, it is recognised that density varies considerably with gas composition and its thermodynamic properties.

In the two-component petroleum system model used for this study, gas is modelled to be expelled much more efficiently than oil. In coaly source rocks with a high oil expulsion threshold, this can result in gas being expelled prior to oil expulsion. Generated oil retained within the source rock is subjected to secondary cracking processes (Pepper & Dodd 1995), which generates and expels additional gas, contributing to the total gas yield in equation 2.

The influence of different kinetic parameters is illustrated in Figure 6 for an assumed uniform heating rate of 3°C/My. Transformation ratio (TR), or the proportion of kerogen converted to oil and gas, is plotted against temperature for different source rock types. It is worth noting the very similar oil and gas curves for the Woodleigh shale which are considerably different to the widely spaced oil and gas trends using Pepper & Corvi (1995a) kinetic parameters. The combination of kinetic parameters and other source rock properties on two-phase expulsion histories using the zero-dimensional maturity simulator (Kinex[1]) is illustrated in Figure 7. The proportions of oil and gas generated and expelled are combined in cumulative plots (with a maturity dependent saturation threshold and uniform heating at a rate of 3°C/My) for both DE (type III) and C (type I) organofacies (Pepper & Corvi 1995a). For lacustrine source rocks (sub-type C organofacies) oil starts to be expelled at about 130°C, with cracking of retained oil commencing at about 154°C (Figure 7). For coaly source rocks (sub-type DE organofacies) oil starts to be expelled at about 133°C, with cracking of retained oil commencing at about 165°C (Figure 7).

Graphs of source rocks productivity, assuming total conversion of the available kerogen, are shown in Figure 8. For coaly source rocks an estimated 2.3 MMbbl/km^2 of oil and about 33 Bcf/km^2 of gas are expelled from a 50 m interval with a HI of 300 mg_{HC}/g_{TOC} and a TOC of 3%. For comparison, a 50 m interval of lacustrine source rock with similar properties is expected to produce about 4 MMbbl/km^2 oil and 23 Bcf/km^2 gas. However, the multi-1D modelling used a more productive HI of 548 mg_{HC}/g_{TOC} consistent with values from the Woodleigh shale and a TOC of 3.0% (Table 4). Using these properties a 50 m interval of lacustrine source rock is predicted to yield about 10.6 MMbbl/km^2 oil and 21 Bcf/km^2 gas (Figure 8).

[1] Zero-dimensional maturity modelling software by Zetaware, Inc. http://www.zetaware.com

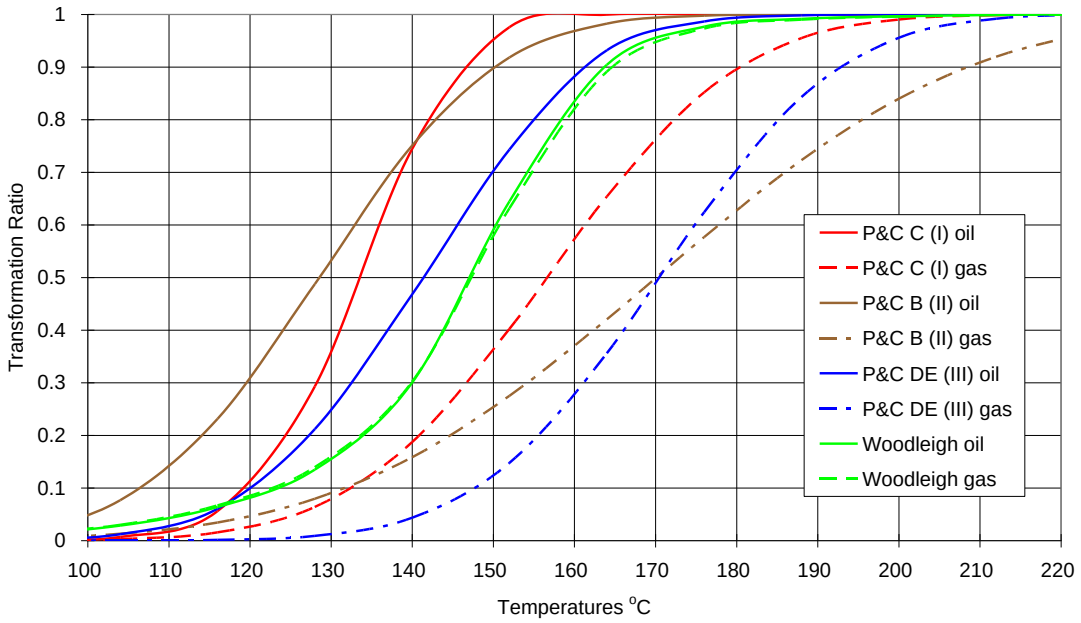

Figure 6 Comparison of transformation ratios for oil and gas with various kerogen types using a linear heating rate of 3°C / My.

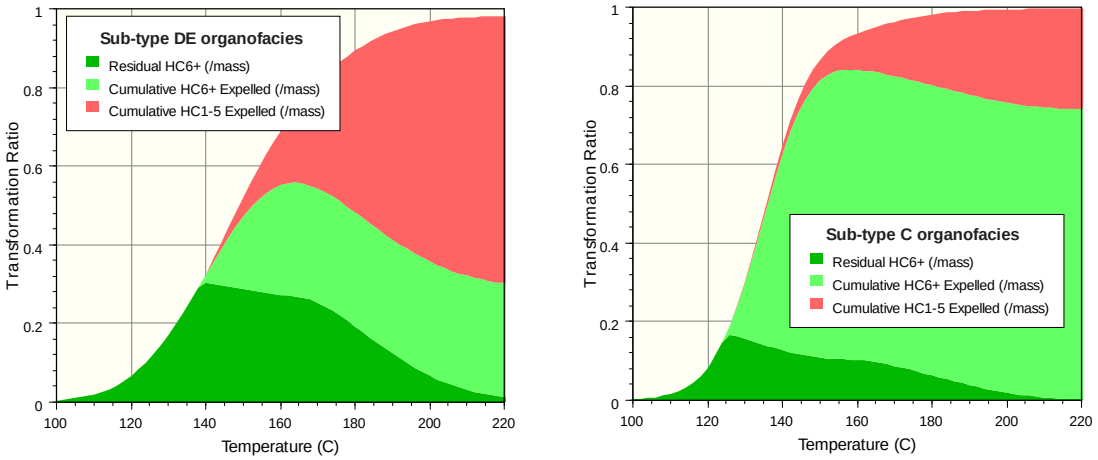

Figure 7 Illustration of oil and gas expulsion history (plot from Kinex) for a linear heating rate of 3°C/My using the kinetics of Pepper & Corvi (1995a).

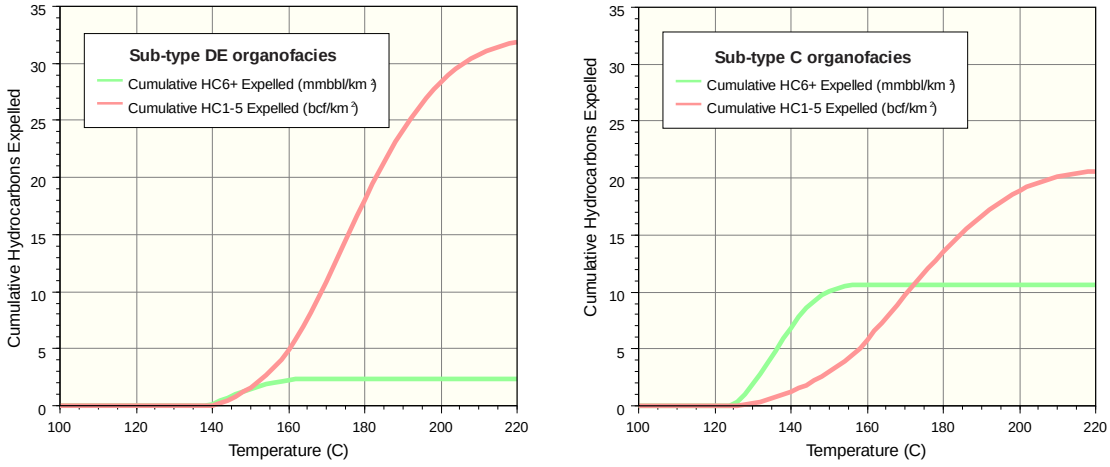

Figure 8 Productivity history for a 50 m thick source rock (plot from Kinex) using a linear heating rate of 3°C/My and 3.0% TOC; for sub-type DE organofacies with HI of 300 mg_{HC}/g_{TOC} (left) and sub-type C organofacies with HI of 548 mg_{HC}/g_{TOC} (right). Oil yield (green line) in MMbbl/km^2 and gas yield (red line) in Bcf/km^2.

2.1.5 Heat flow

Heat flow data from the Lord Howe Rise region are sparse. Available data, derived from downhole temperature measurements in DSDP wells and heat flow probes, are listed in Table 5. There were no reliable downhole temperature measurements from DSDP 207, and 208 on the Lord Howe Rise. Morin & Von Herzen (1986) compute a surface heat flow of 56.9 ± 5.2 mW/m^2 for DSDP 587 in the north of the Lord Howe Rise, and Von Herzen (1973) calculated a surface heat flow of 57.8 ± 5.9 mW/m^2 for DSDP 206 in the New Caledonia Basin to the southeast of the study area. Grim (1969) made two heat flow measurements south and southeast of Lord Howe Island using a 6 metre core barrel. Both measurements gave high heat flow values (c. 100 mW/m^2) with high measurement uncertainties. Four heat flow measurements (identified with MD06 numbers in Table 5) were obtained using a heat probe on the 2006 AUSFAIR survey (Colwell et al. 2006). Calculated heat flow values vary from 59 to 82 mW/m^2, with the three observations made on the Lord Howe Rise and in the Capel Basin having an average heat flow of 65 mW/m^2.

Table 5 Heat flow measurements from heat flow probes and DSDP boreholes on the Lord Howe Rise and in the New Caledonia Basin (see text for details).

Site	Depth (m TVD bsf)	Penetration (m)	Heat Flow (mW/m^2)	Est. Error (mW/m^2)
MD06-3035	1937	14	61.9	3.8
MD06-3038-1	2587	14	65.8	5.86
MD06-3038-2	2587	14	66.9	6.05
MD06-3031	2928	7.2	81.0	11.5
Grim (1969) site 6	3609	6	100	15
Grim (1969) site 7	1529	6	97	25
DSDP 587	1100	108.7	56.9	5.2
DSDP 207	No reliable data			
DSDP 208	No reliable data			
DSDP 206	3191	304	57.8	5.9

The multi-1D models used a constant heat flow at base of the lithosphere of 40 mW/m^2 with an initial lithospheric thickness (before rifting) of 85 km. The models incorporated heat productivity in the crust that initially contributes about 21 mW/m^2 to the surface heat flow. This, however, reduces to 11 mW/m^2 as a consequence of rifting. These effects, plus surficial processes such as varying water depth and sedimentation rate, influence the transient thermal regime and the surface heat flow through time. Figure 9 illustrates the variation in heat flow for both the base sediment interface and at the sediment surface and clearly shows the impact of surficial processes.

Two phases of rifting, based on seismic interpretation, were incorporated in all models; in the Early Cretaceous (130 – 100 Ma) with an extension factor of 1.60 and in the Late Cretaceous (95 – 80 Ma) with an extension factor of 1.25. Scenarios run to test the effects of possible Cenozoic magmatism included two heating pulses at the base of the lithosphere between 68 and 60 Ma (applying 80 mW/m^2) and between 27 and 18 Ma (applying 60 mW/m^2). The surface heat flow in response to these magmatic events is predicted to still be increasing up to the present day (Figure 9).

A scenario including rifting and Cenozoic magmatism, without erosion, is presented as the red line in Figure 9 and subsequently referred to as the ‘base case’ model. All scenarios shown in Figure 9 result in a similar present day heat flow, mainly due to the competing effects of rifting and the corresponding reduction in crustal heat production for the ‘rifting and

magmatism', or base case, and 'rifting' scenarios. Apart from effects related to rifting and magmatism in Figure 9, the abrupt changes and inflections in the heat flow curve are due to variations in sedimentation rate and changes in paleo-water depth: notably even at significant burial depths for basement heat flow (e.g., 6 km by 68 Ma for this site).

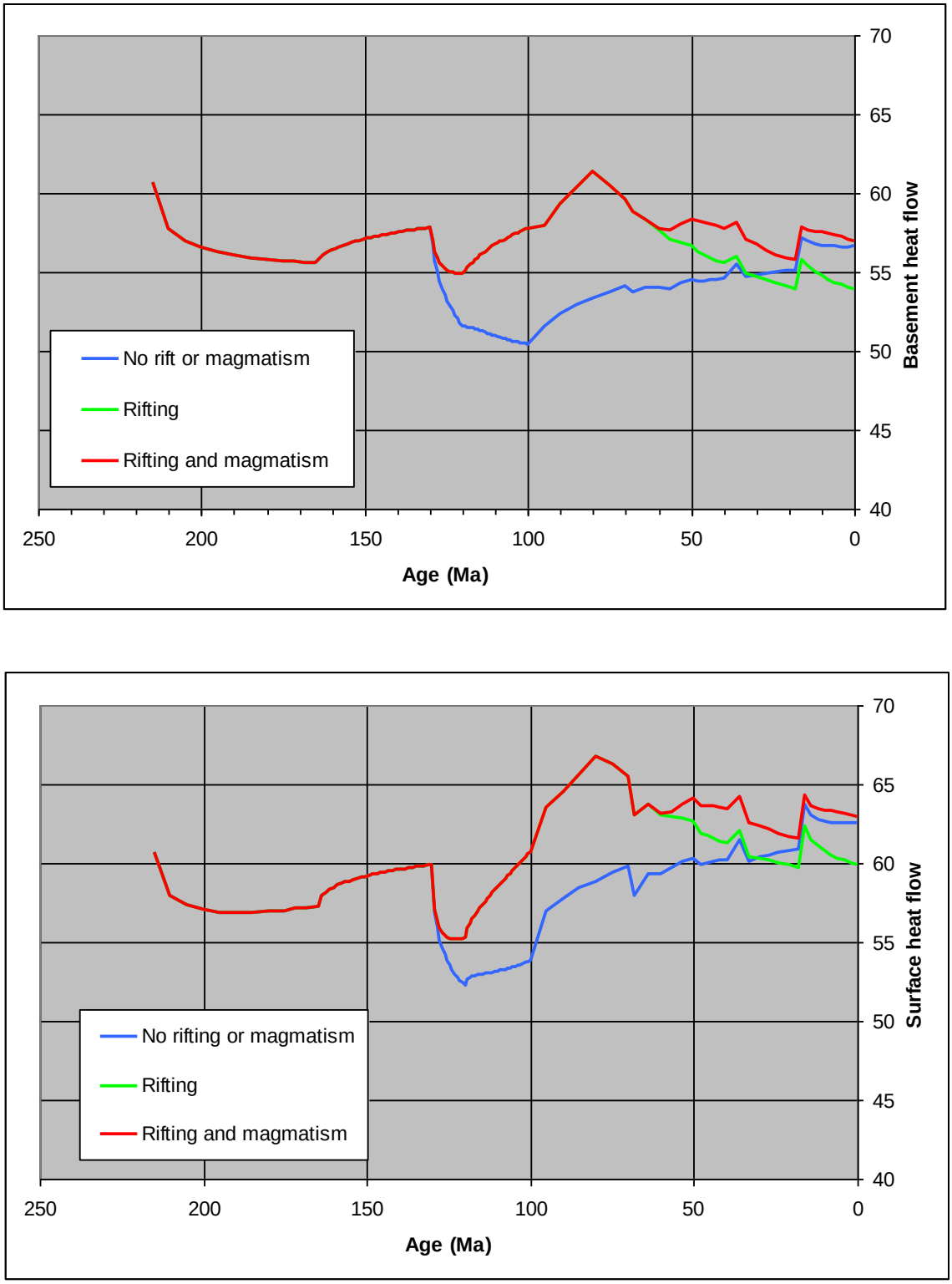

Figure 9 Heat flow (in mW/m^2) scenarios in one of the syn-rift depocentres comparing the effect of rifting (130 – 100 and 95 – 80 Ma) and magmatism (68 – 40 and 27 – 18 Ma) at the sediment surface (lower plot) and base sediment (basement) (upper plot). Note that the green and blue lines underlie the red line in the plots.

2.2 PREDICTED MATURITY

Predicted temperature at the base of the syn-rift megasequences for various times are shown for two scenarios; the 'base case' model in Figure 10 which incorporates rifting and Cenozoic magmatism and the 'no Cenozoic magmatism' scenario in Figure 11 incorporating only rifting. These paleo-temperature maps display identical predicted sediment temperatures throughout the Cretaceous. Temperatures are up to 7°C hotter at 36 Ma, and 11°C hotter at the present day, for the base case scenario compared to the 'no Cenozoic magmatism' scenario. Temperature differences tend to be greatest where the syn-rift megasequences are deepest, but generally average less than 5°C for the whole mapped region. A similar set of maps illustrating temperature of the Pre-rift megasequence for the base case at the base of the modelled upper Pre-rift Walloon equivalent coal measures is presented in Figure 12. The actual time periods presented in this series of maps are based on ages of mapped and interpolated horizons (see Table 2) used in the modelling.

Predicted vitrinite reflectance, which is often used as a maturity indicator, is presented in Figures 13 – 15 for the base case model. Maturity is presented irrespective of source rock presence. The maximum vitrinite reflectance through the syn-rift megasequences varies from 0.7% at top Syn-rift 2 to 3.2% at the base of Lower Syn-rift 1 unit; Figure 13 shows the predicted vitrinite reflectance for the present day at four levels within the syn-rift megasequences. The base of the upper section of Syn-rift 2 exhibits present day maturity consistent with oil generation in isolated depocentres mainly in the western Capel Basin, although the top of this section is considered immature for petroleum generation. The progressive increase in maturity through time for the middle and base of the Lower Syn-rift 1 unit is illustrated in Figures 14 and 15, respectively. A similar map for the upper Pre-rift Walloon equivalent coal measures is not presented because maturity is very similar to the base of the Lower Syn-rift 1 unit in Figure 15.

The base case heating model includes hiatuses related to non-deposition for five periods in the basin history (Table 2). The sensitivity of the model to erosion was tested by replacing the hiatuses with periods of deposition followed by periods of erosion for the two most significant unconformities (see section 2.1.2 justifying extension of affected periods to 105 – 95 Ma and 85 – 70 Ma). The effects of erosion were most noticeable immediately following the 85 – 70 Ma event. Somewhat surprisingly the model with no erosion, termed the hiatus model, exhibits higher maturity during post-rift sedimentation following the period of erosion/hiatus. Figure 16 compares temperature and reflectance for the two models (with and without erosion) showing the lower maturity predicted immediately following cessation of erosion compared to a hiatus model. This is explained as the interaction of two processes. Firstly, the combined thermal effects of depositing an additional unit and then eroding it tends to suppress heat flow at the base of the sediments, compared to a hiatus model (for the conditions applied in these models). Secondly, compaction effects result in shallower burial of the underlying sediments for a significant period of time following erosion compared to a hiatus model. This is because compaction is modelled to occur during burial of the eroded section: and following erosion, only when sediments once again reach a state of "maximum burial". This process causes deeper horizons to be uplifted to a shallower depth than they were buried immediately prior to deposition of the eroded interval. The combined effect of these processes causes a stratigraphic horizon to become more mature in a hiatus model than a corresponding model including deposition and erosion for the same period.

The transformation of kerogen to oil or gas (in terms of transformation ratio) is presented in Figures 17 – 22 using kinetic parameters specific to particular organofacies or source rock

types. Figures 17 and 18 present predicted present day transformation ratio of oil and gas for the base of the lower four modelled coaly source rock intervals. Transformation ratio and other thermal maturity parameters are presented irrespective of source rock presence. The Syn-rift 2 megasequence is generally immature for both oil and gas generation with only limited depocentres in the western Capel Basin displaying sufficient present day maturity to expel oil. The Syn-rift 1 megasequence displays sufficient maturity across a significant part of the Capel Basin to expel both oil and gas. The timing of maturation is illustrated through the progressive increase in maturity through time for the base of the Syn-rift 1 megasequence, shown in terms of transformation ratio for oil and gas in Figures 19 and 20, respectively. Only a limited increase in maturity is predicted from this base case model since 36 Ma. The centres of the depocentres are noticeably over-mature with only the edges or outer rims of depocentres predicted to be increasing in maturity, expanding the area of mature source rock.

To further test the model sensitivity to source rock type, both the Lower Syn-rift 1 and Lower Syn-rift 2 units have been modelled using two sets of kinetic parameters for lacustrine source rocks. Figure 21 shows present day predicted maturity using lacustrine source rock kinetics based on organofacies C classification (Pepper & Corvi 1995a), and Figure 22 shows predicted maturity based on data from the Woodleigh 2A shale (pers. comm. C Boreham, 2010). Both models predict sufficient maturity for significant oil and gas generation from the Lower Syn-rift 1 unit, although maturity for generation from the Lower Syn-rift 2 unit is predicted to be limited to only the western Capel Basin.

The Pre-rift Walloon equivalent coaly source rock unit is predicted to become over-mature for oil and gas generation in the deepest parts of the basin by 85 Ma in the Late Cretaceous. Possible source rocks in the Lower Syn-rift 1 unit are predicted to be over-mature for oil generation by 68 Ma at the end of the Cretaceous and gas generation by 36 Ma at the end of the Eocene in the deepest parts of the basin. However, models predict large (shallower) regions of both successions increase in maturity through to 36 Ma, and continue to mature at slower rates through to the present day. The overlying Upper Syn-rift 1 unit spans the range from over-mature in isolated depocentres in western Capel Basin to immature for both oil and gas generation in other regions. Within the Syn-rift 2 megasequence only the isolated depocentres in the western Capel Basin are predicted to be sufficiently mature to generate oil.

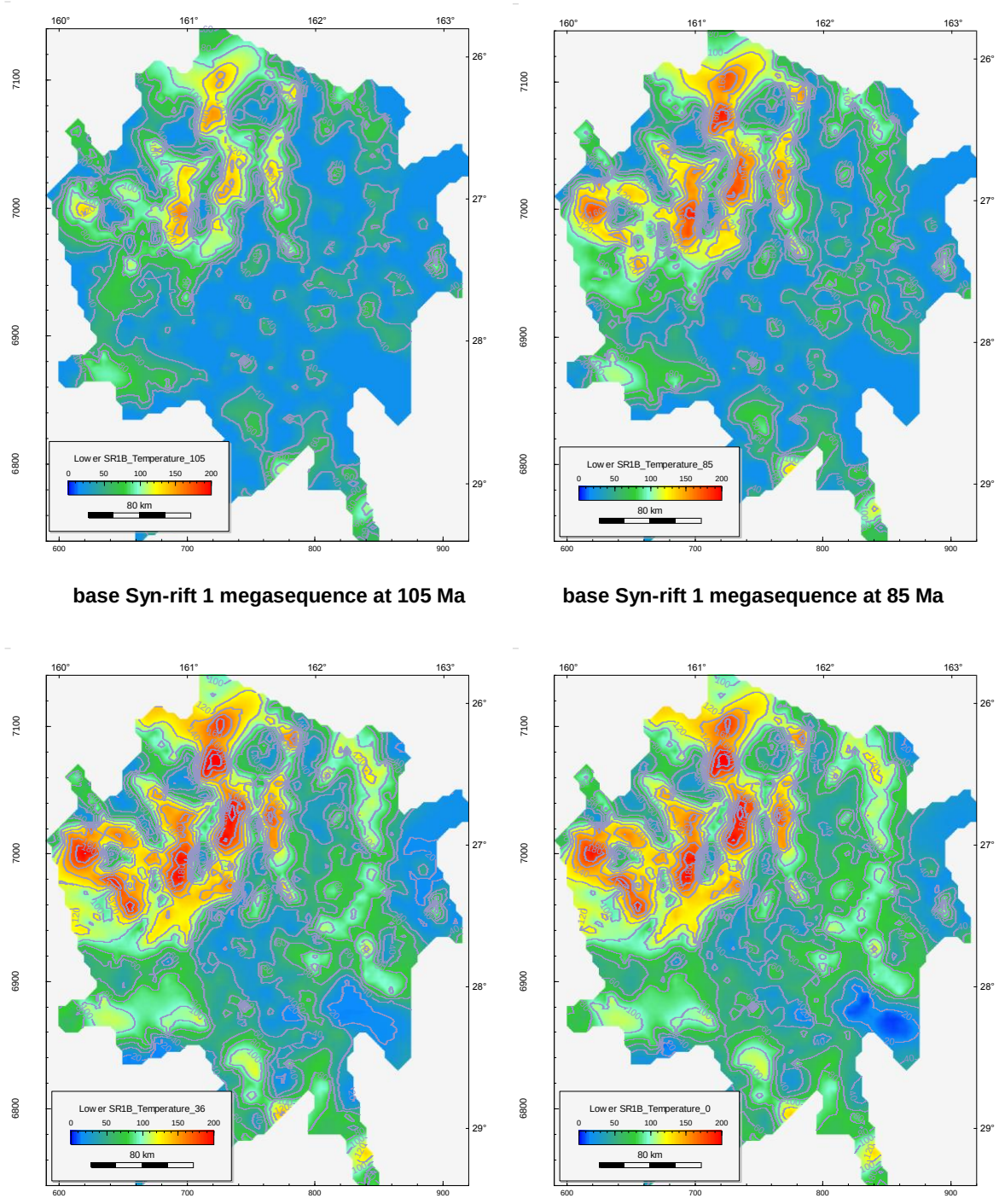

base Syn-rift 1 megasequence at 105 Ma

base Syn-rift 1 megasequence at 85 Ma

base Syn-rift 1 megasequence at 36 Ma

base Syn-rift 1 megasequence at 0 Ma

Figure 10 Predicted temperature of base Syn-rift 1 megasequence for 105 (top left), 85 (top right), 36 Ma (lower left) and present day (lower right) showing effects of burial, rifting and Cenozoic magmatism (base case model). Co-ordinates on left and lower axes are UTM 58S in km; the right and upper axes are latitude (S) and longitude (E).

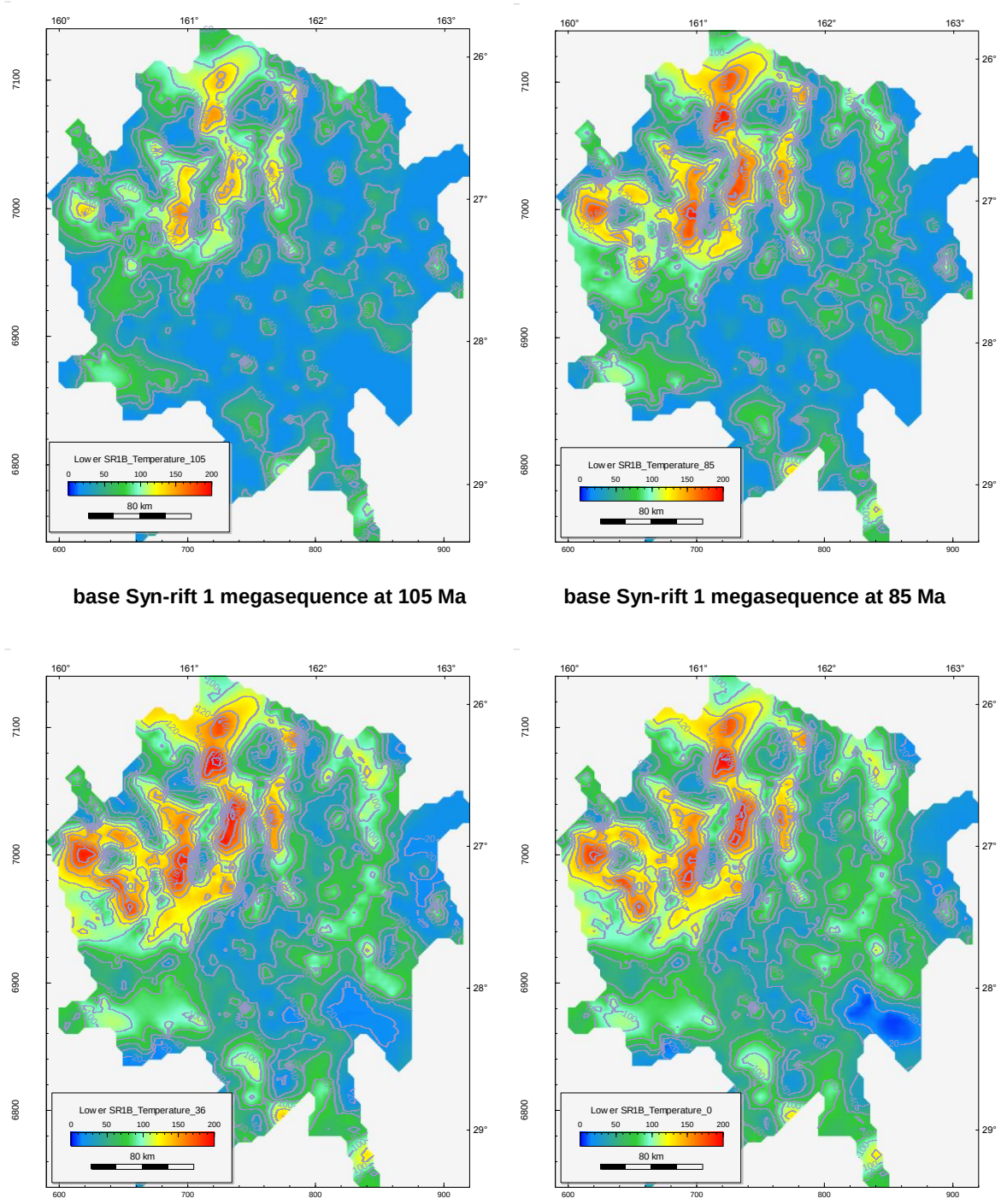

base Syn-rift 1 megasequence at 105 Ma

base Syn-rift 1 megasequence at 85 Ma

base Syn-rift 1 megasequence at 36 Ma

base Syn-rift 1 megasequence at 0 Ma

Figure 11 Predicted temperature of base Syn-rift 1 megasequence for 105 (top left), 85 (top right), 36 Ma (lower left) and present day (lower right) showing effects of burial and rifting (no Cenozoic magmatism). Co-ordinates on left and lower axes are UTM 58S in km; the right and upper axes are latitude (S) and longitude (E).

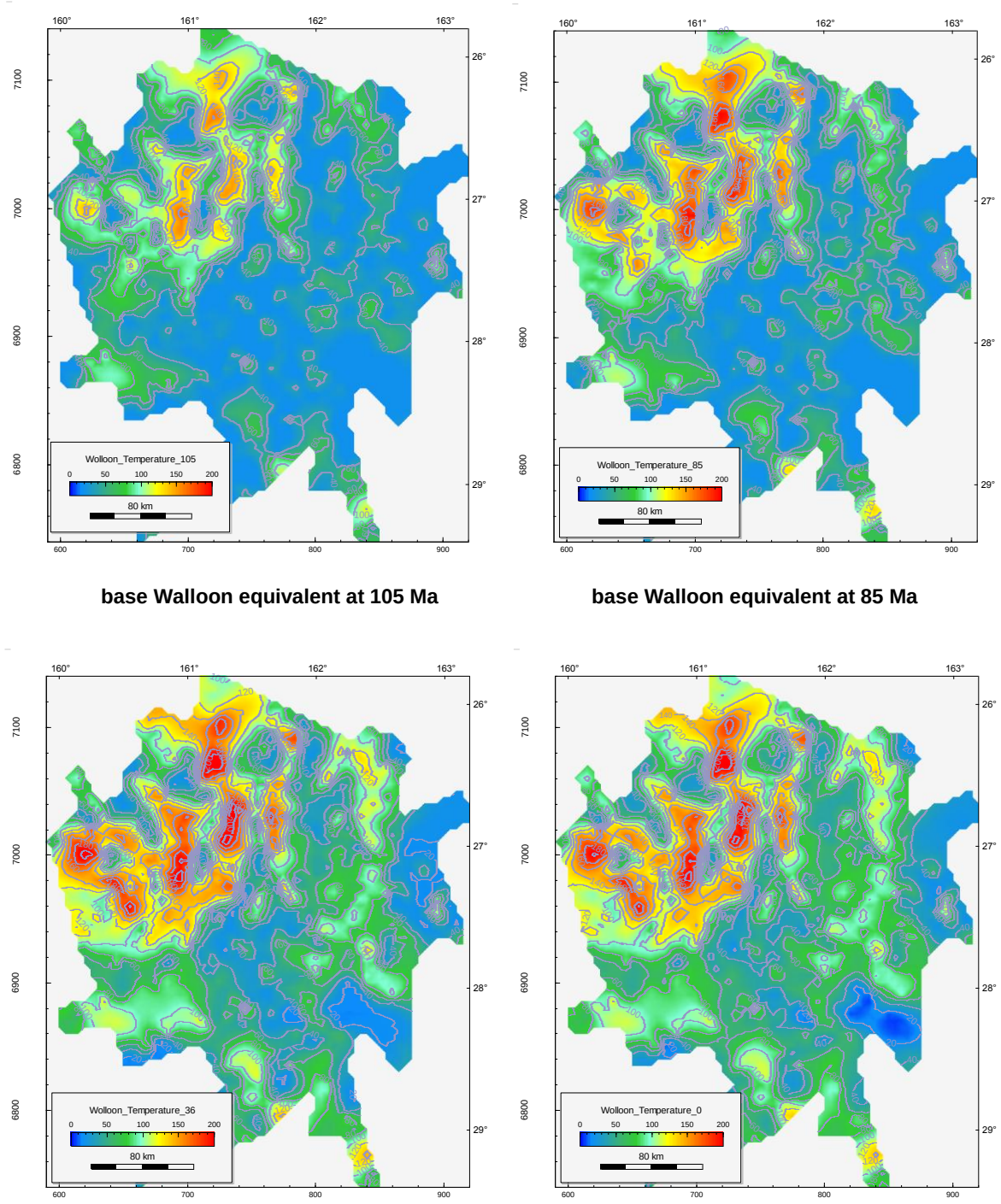

base Walloon equivalent at 105 Ma

base Walloon equivalent at 85 Ma

base Walloon equivalent at 36 Ma

base Walloon equivalent at 0 Ma

Figure 12 Predicted temperature of base Walloon Coal Measures equivalent in Upper Pre-rift megasequence for 105 (top left), 85 (top right), 36 Ma (lower left) and present day (lower right) showing effects of burial, rifting and Cenozoic magmatism. Co-ordinates on left and lower axes are UTM 58S in km; the right and upper axes are latitude (S) and longitude (E).

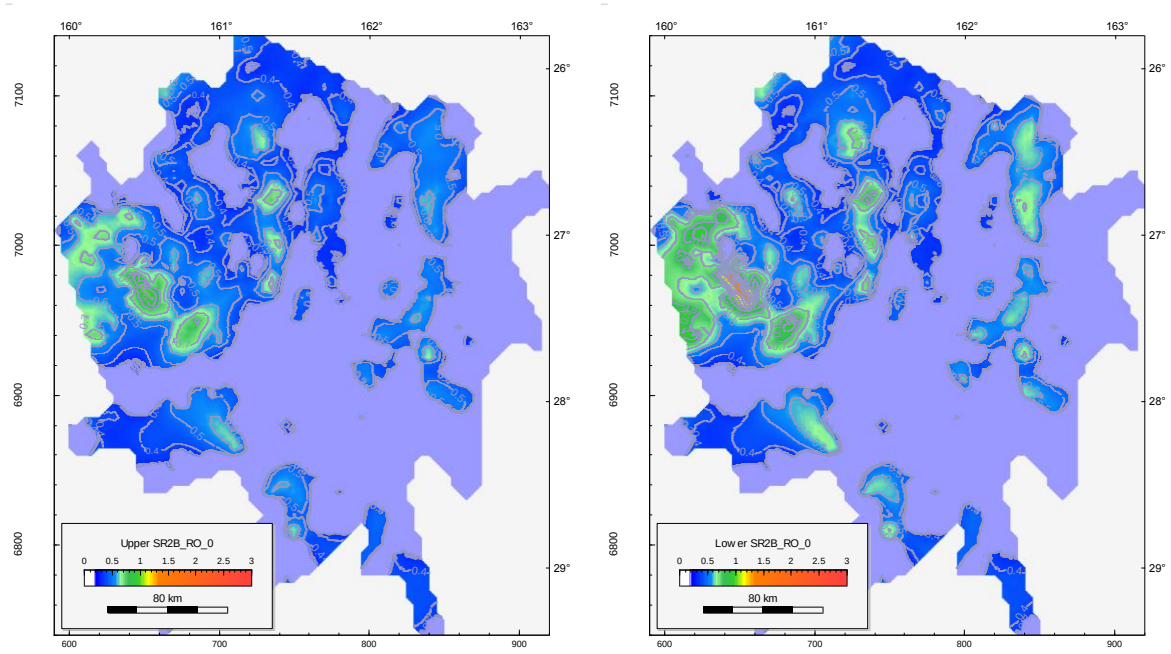

base Upper Syn-rift 2 unit at 0 Ma

base Lower Syn-rift 2 unit at 0 Ma

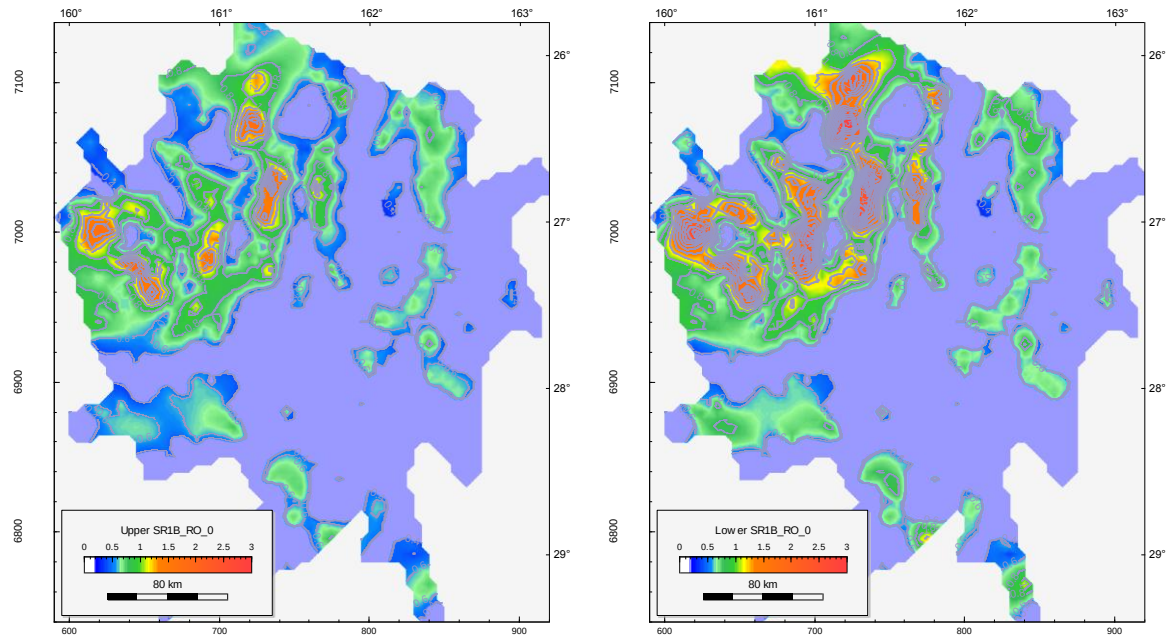

base Upper Syn-rift 1 unit at 0 Ma

base Lower Syn-rift 1 unit at 0 Ma

Figure 13 Predicted vitrinite reflectance maturity of syn-rift megasequences at present day for base case model; base Upper Syn-rift 2 unit (top left), base Lower Syn-rift 2 unit (top right), base Upper Syn-rift 1 unit (bottom left), and base Lower Syn-rift 1 unit (bottom right). Co-ordinates on left and lower axes are UTM 58S in km; the right and upper axes are latitude (S) and longitude (E).

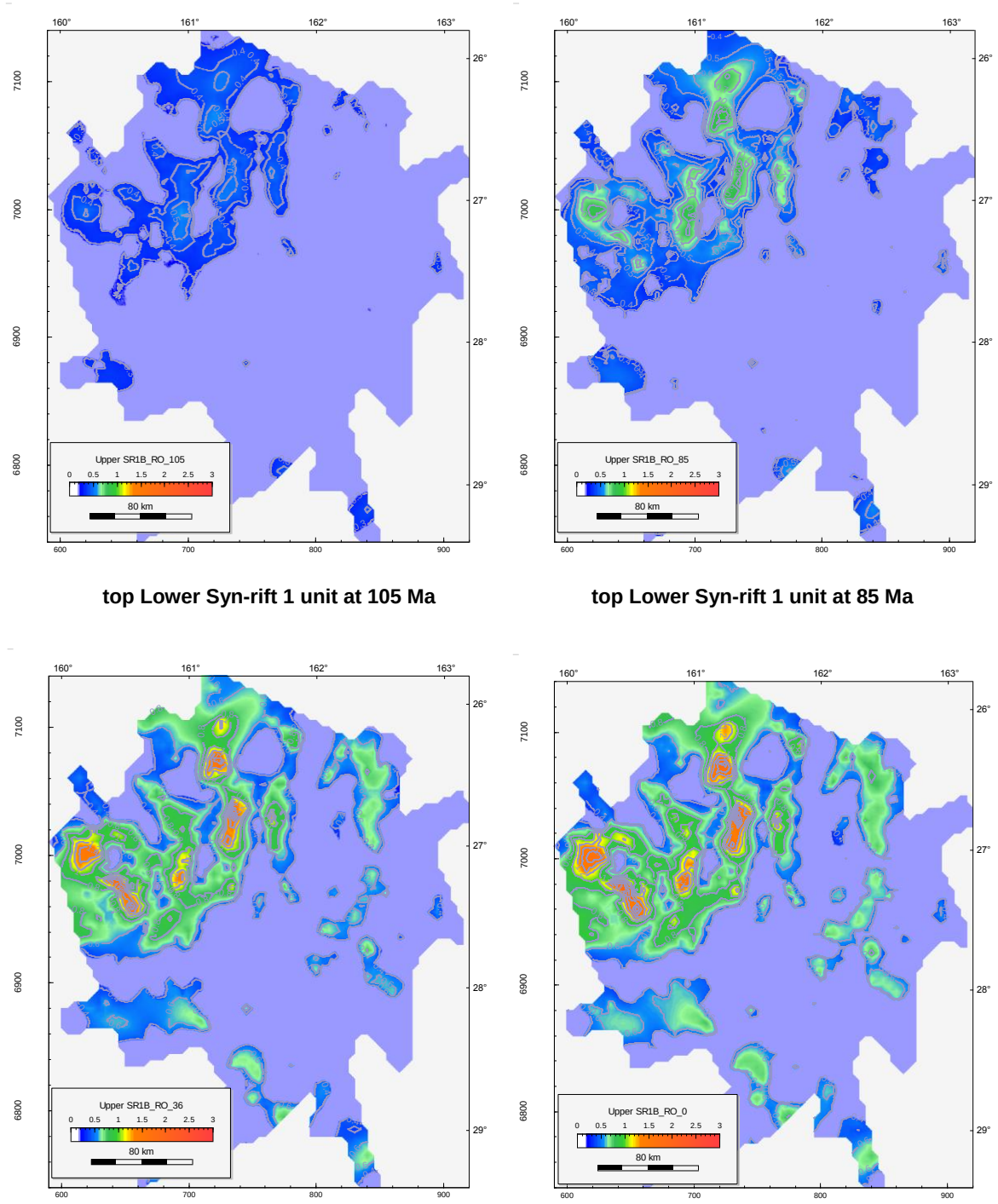

top Lower Syn-rift 1 unit at 105 Ma

top Lower Syn-rift 1 unit at 85 Ma

top Lower Syn-rift 1 unit at 36 Ma

top Lower Syn-rift 1 unit at 0 Ma

Figure 14 Predicted vitrinite reflectance maturity at the top of Lower Syn-rift 1 unit for 105 (top left), 85 (top right), 36 Ma (lower left) and present day (lower right), for base case model. Co-ordinates on left and lower axes are UTM 58S in km; the right and upper axes are latitude (S) and longitude (E).

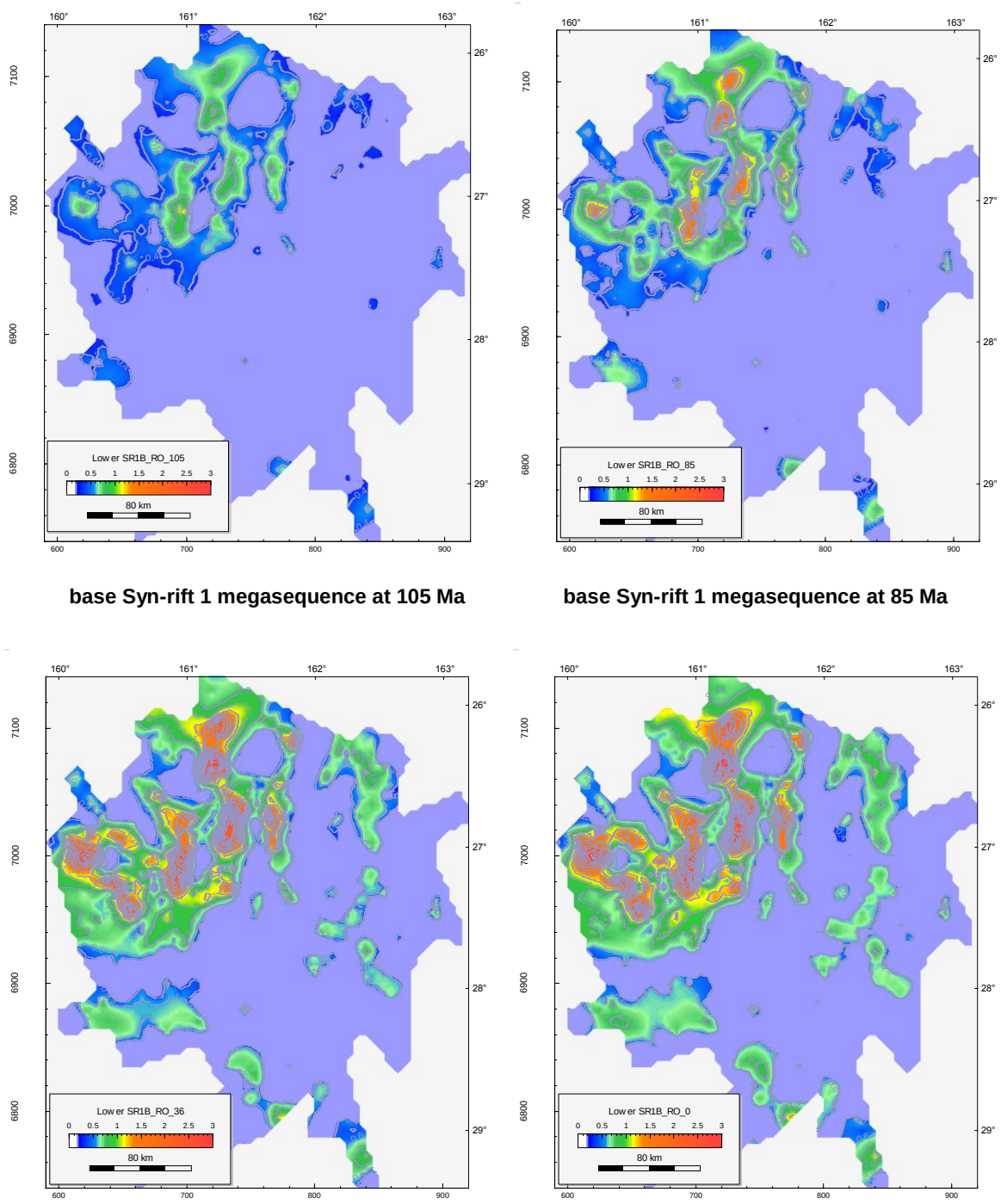

base Syn-rift 1 megasequence at 105 Ma

base Syn-rift 1 megasequence at 85 Ma

base Syn-rift 1 megasequence at 36 Ma

base Syn-rift 1 megasequence at 0 Ma

Figure 15 Predicted vitrinite reflectance maturity of base Syn-rift 1 megasequence for 105, (top left), 85 (top right), 36 Ma (lower left) and present day (lower right), for base case model. Co-ordinates on left and lower axes are UTM 58S in km; the right and upper axes are latitude (S) and longitude (E).

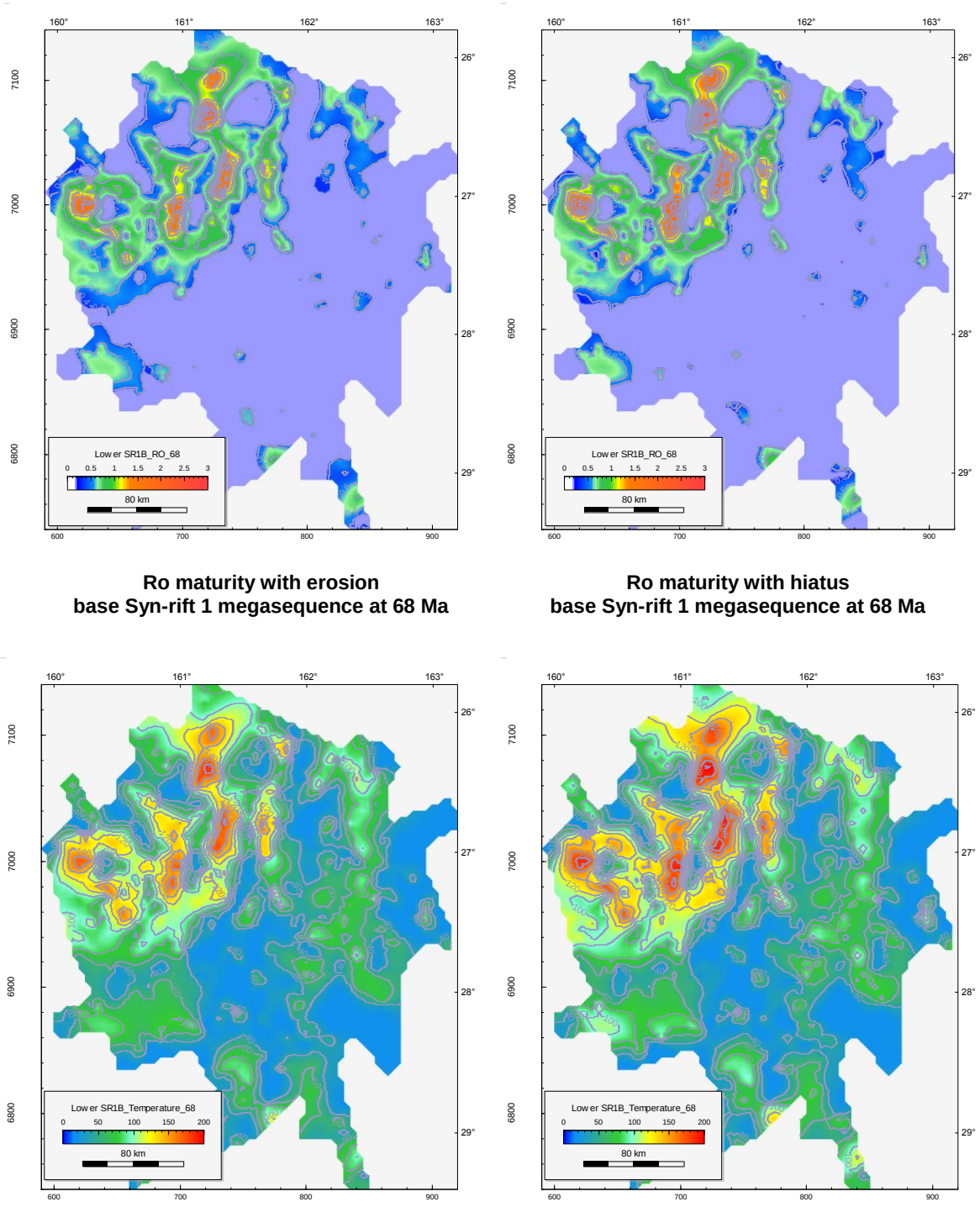

Ro maturity with erosion
base Syn-rift 1 megasequence at 68 Ma

Ro maturity with hiatus
base Syn-rift 1 megasequence at 68 Ma

Temperature with erosion
base Syn-rift 1 megasequence at 68 Ma

Temperature with hiatus
base Syn-rift 1 megasequence at 68 Ma

Figure 16 Comparison of erosion (left) and hiatus (right) base case models for predicted vitrinite reflectance maturity (upper) and temperatures (lower) of base Syn-rift 1 megasequence at 68 Ma. Co-ordinates on left and lower axes are UTM 58S in km; the right and upper axes are latitude (S) and longitude (E).

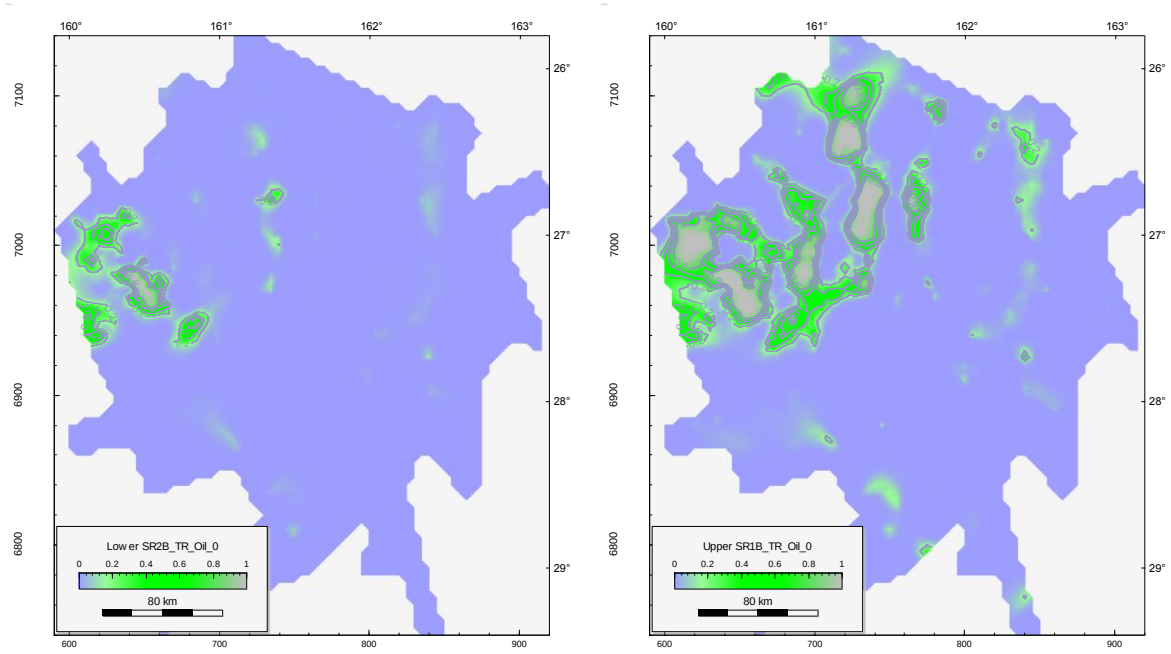

base Lower Syn-rift 2 unit at 0 Ma

base Upper Syn-rift 1 unit at 0 Ma

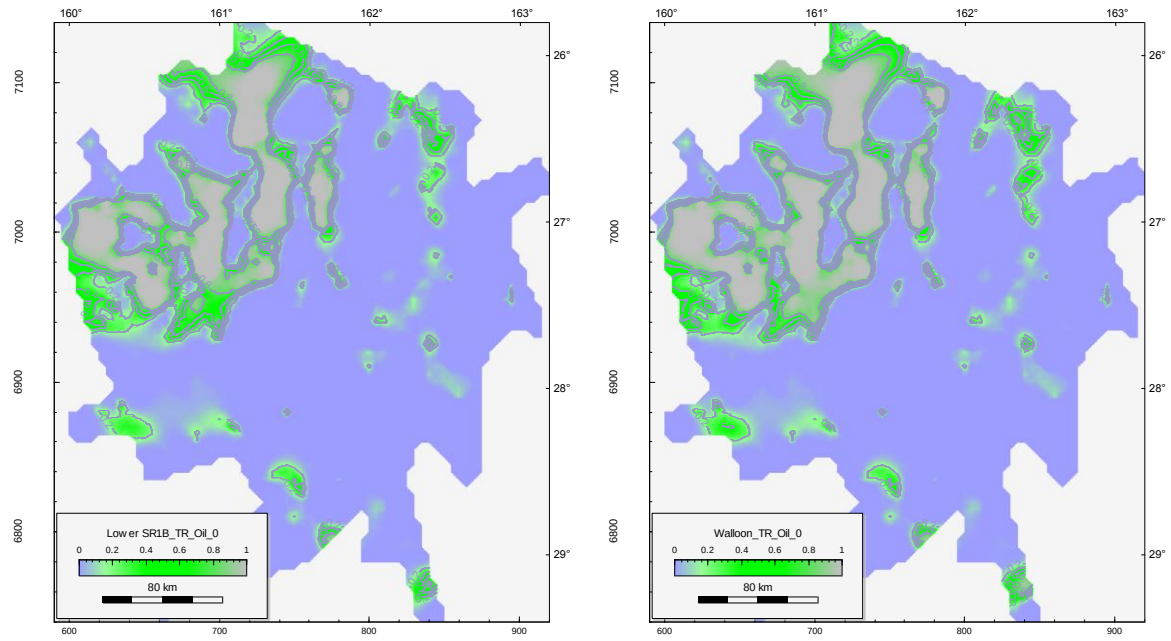

base Lower Syn-rift 1 unit at 0 Ma

base Walloon equivalent at 0 Ma

Figure 17 Predicted maturity using transformation ratio of oil (organofacies DE kinetics) at present day for base case model; base Lower Syn-rift 2 unit (top left), base Upper Syn-rift 1 unit (top right), base Lower Syn-rift 1 unit (bottom left), and base Walloon Coal Measures equivalent in upper part of the Pre-rift megasequence (bottom right). Co-ordinates on left and lower axes are UTM 58S in km; the right and upper axes are latitude (S) and longitude (E).

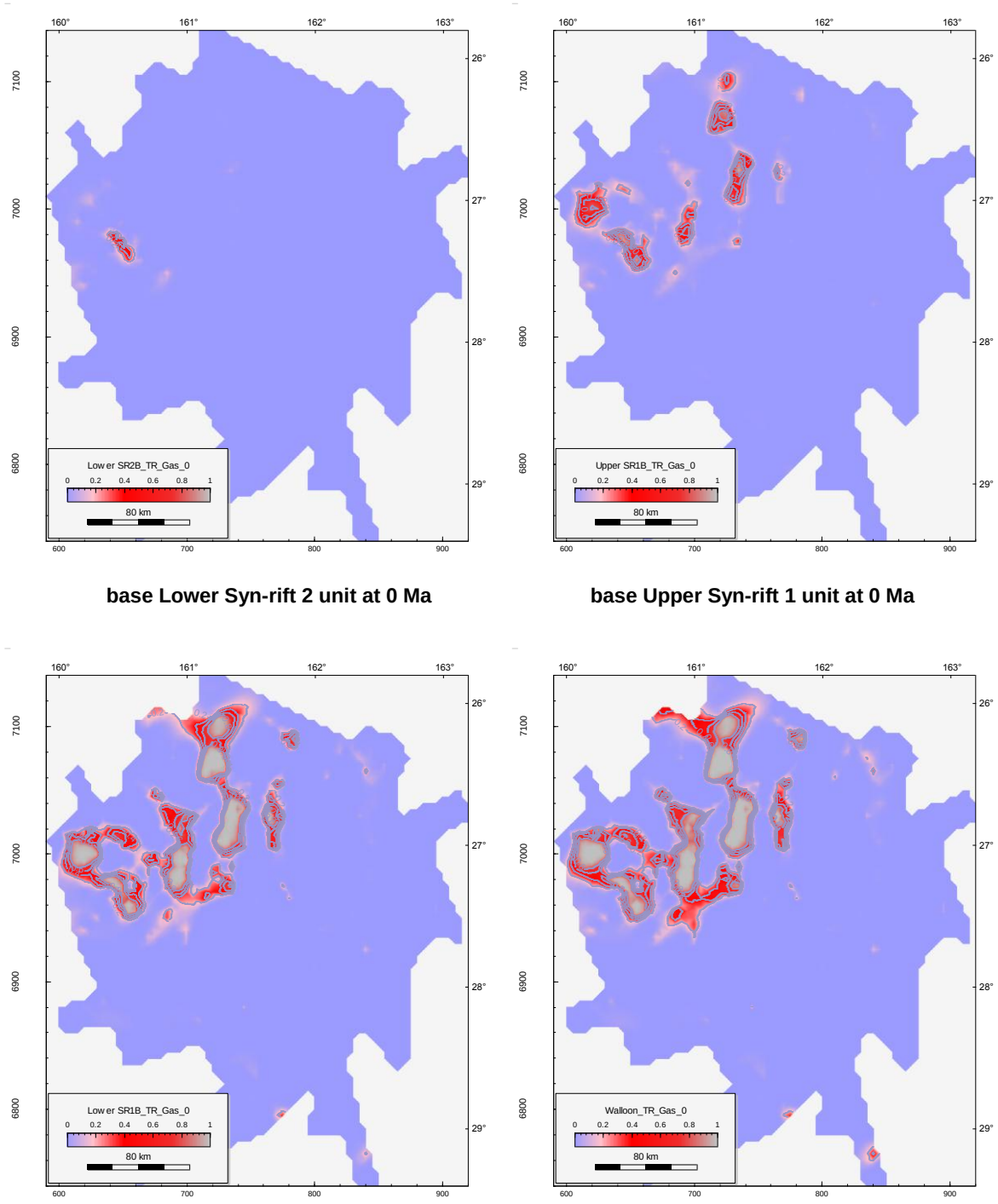

base Lower Syn-rift 2 unit at 0 Ma

base Upper Syn-rift 1 unit at 0 Ma

base Lower Syn-rift 1 unit at 0 Ma

base Walloon equivalent at 0 Ma

Figure 18 Predicted maturity using transformation ratio of gas (organofacies DE kinetics) at present day for base case model; base Lower Syn-rift 2 unit (top left), base Upper Syn-rift 1 unit (top right), base Lower Syn-rift 1 unit (bottom left), and base Walloon coal measures equivalent in upper part of the Pre-rift megasequence (bottom right). Co-ordinates on left and lower axes are UTM 58S in km; the right and upper axes are latitude (S) and longitude (E).

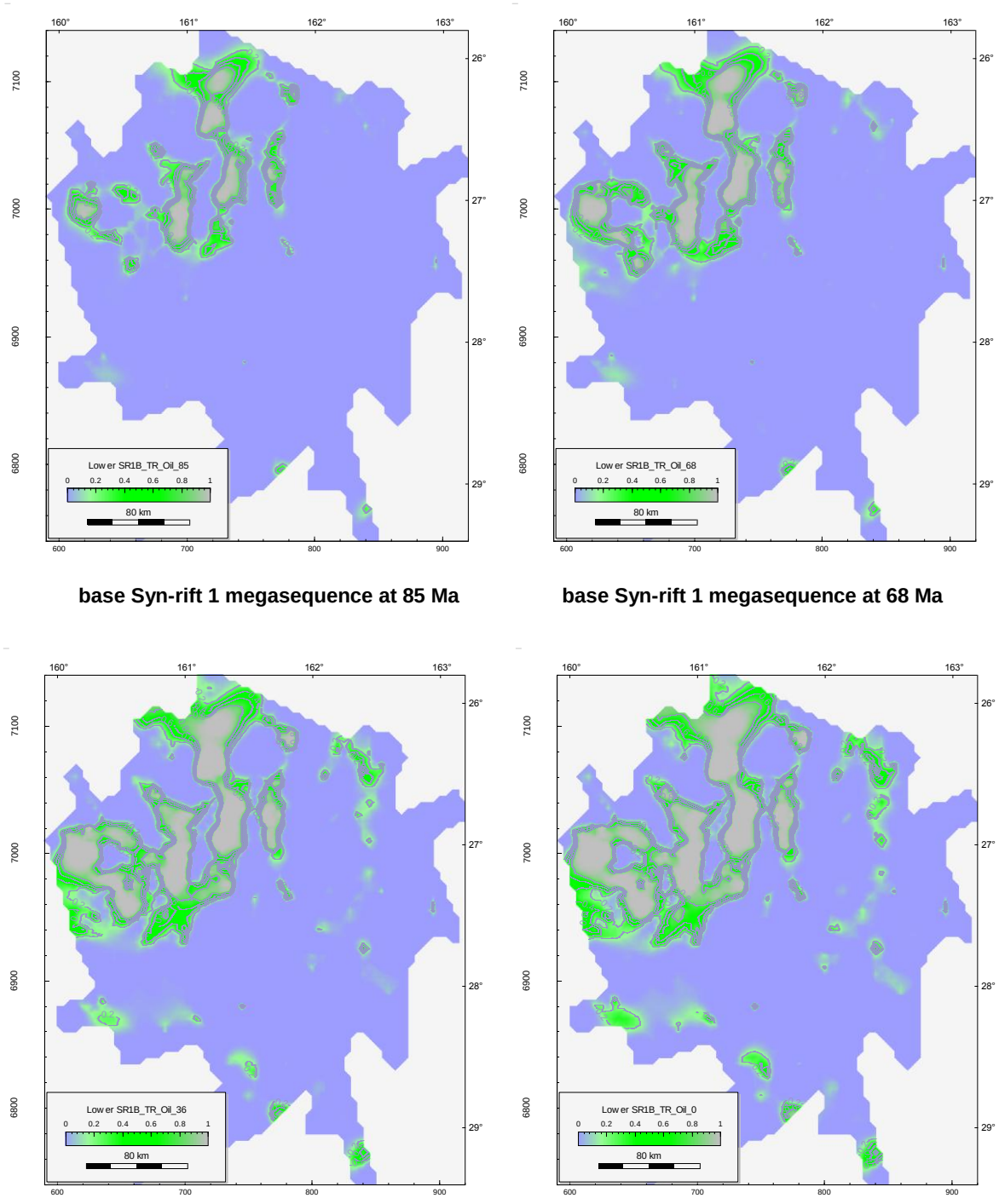

base Syn-rift 1 megasequence at 85 Ma

base Syn-rift 1 megasequence at 68 Ma

base Syn-rift 1 megasequence at 36 Ma

base Syn-rift 1 megasequence at 0 Ma

Figure 19 Predicted maturity using transformation ratio of oil generation (organofacies DE kinetics) at present day for base case model at the base of the Syn-rift 1 megasequence for 85 (top left), 68 (top right), 36 Ma (lower left) and present day (lower right). Co-ordinates on left and lower axes are UTM 58S in km; the right and upper axes are latitude (S) and longitude (E).

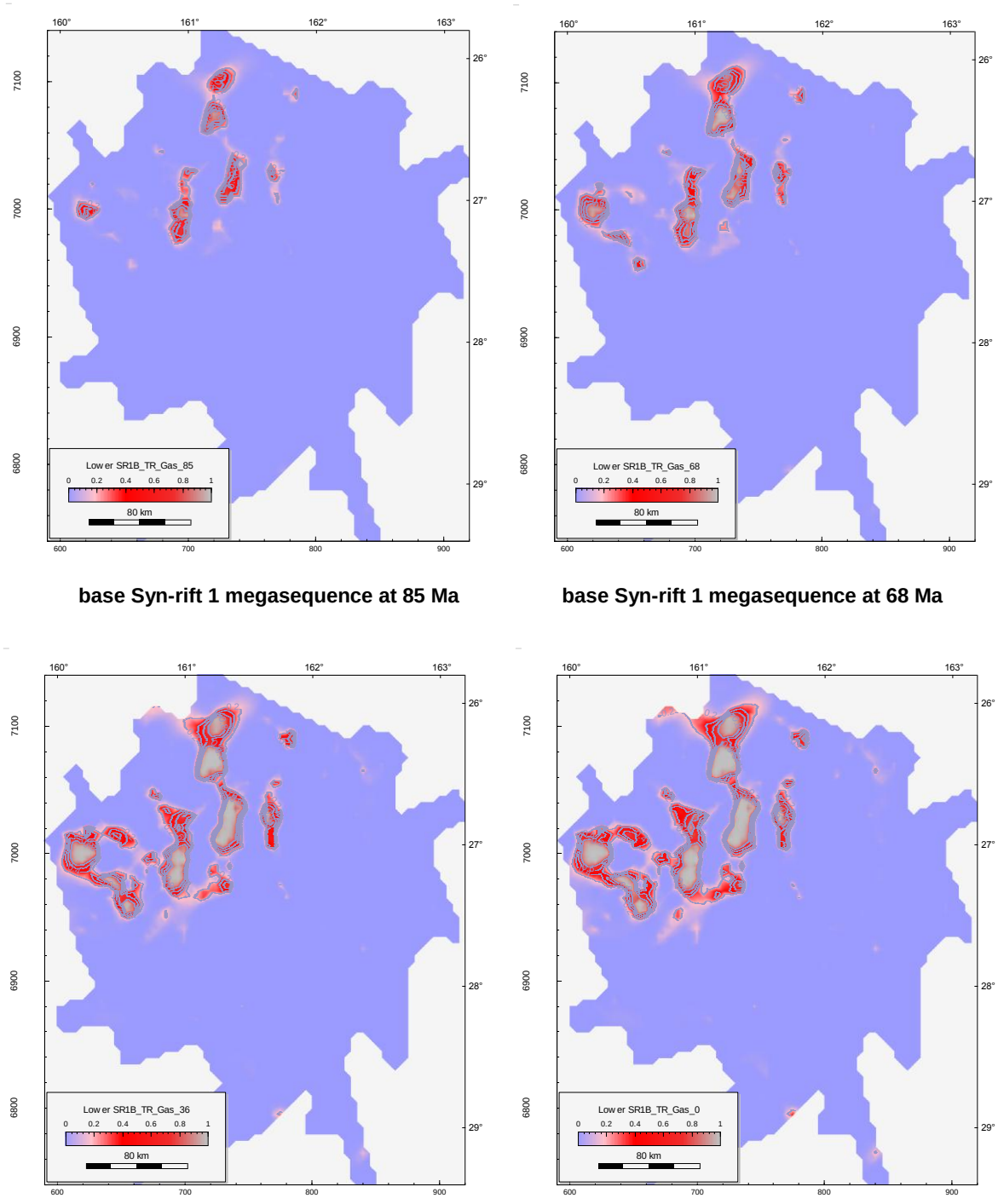

base Syn-rift 1 megasequence at 85 Ma

base Syn-rift 1 megasequence at 68 Ma

base Syn-rift 1 megasequence at 36 Ma

base Syn-rift 1 megasequence at 0 Ma

Figure 20 Predicted maturity using transformation ratio of gas generation (organofacies DE kinetics) at present day for base case model at the base of the Syn-rift 1 megasequence for 85 (top left), 68 (top right), 36 Ma (lower left) and present day (lower right). Co-ordinates on left and lower axes are UTM 58S in km; the right and upper axes are latitude (S) and longitude (E).

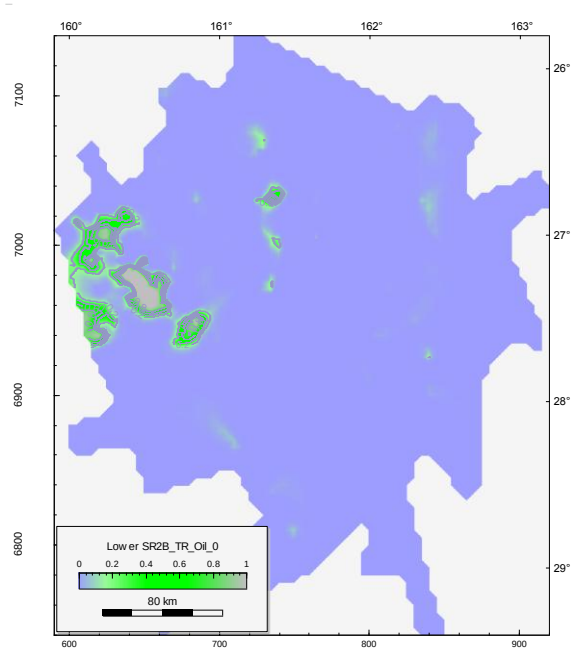

TR for oil
base Lower Syn-rift 2 unit at 0 Ma

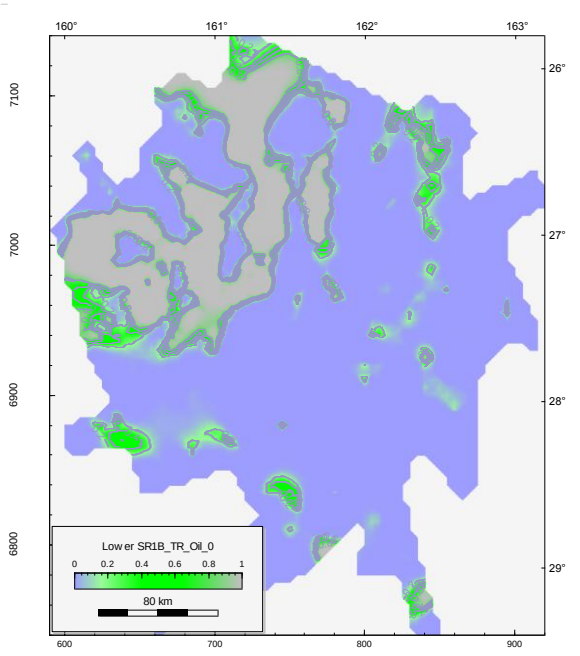

TR for oil
base Lower Syn-rift 1 unit at 0 Ma

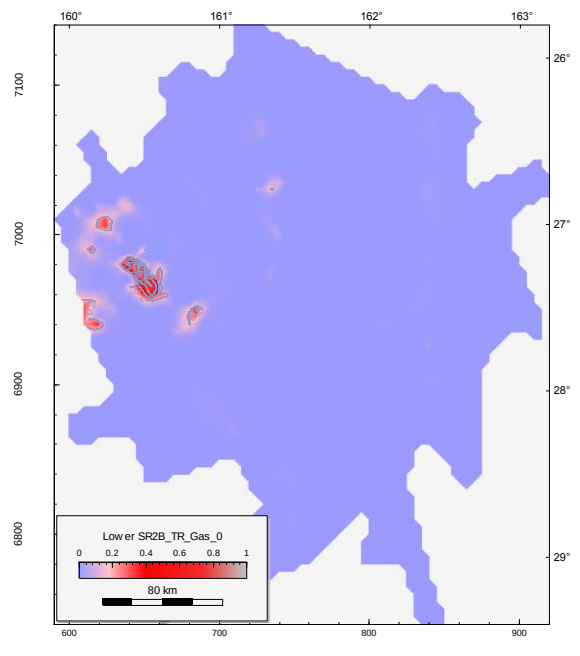

TR for gas
base Lower Syn-rift 2 unit at 0 Ma

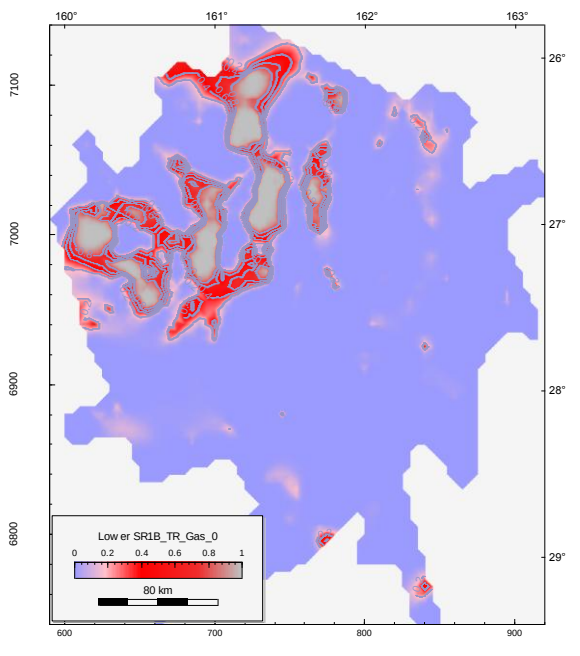

TR for gas
base Lower Syn-rift 1 unit at 0 Ma

Figure 21 Predicted maturity using transformation ratio of oil (upper) and gas (lower plots) (lacustrine organofacies C kinetics) at present day for base case model; base Lower Syn-rift 2 unit (left), and base Lower Syn-rift 1 unit (right). Co-ordinates on left and lower axes are UTM 58S in km; the right and upper axes are latitude (S) and longitude (E).

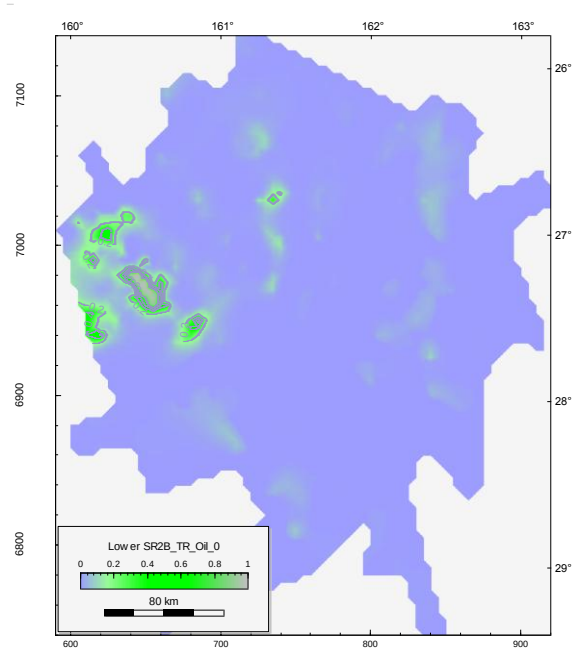

TR for oil
base Lower Syn-rift 2 unit at 0 Ma

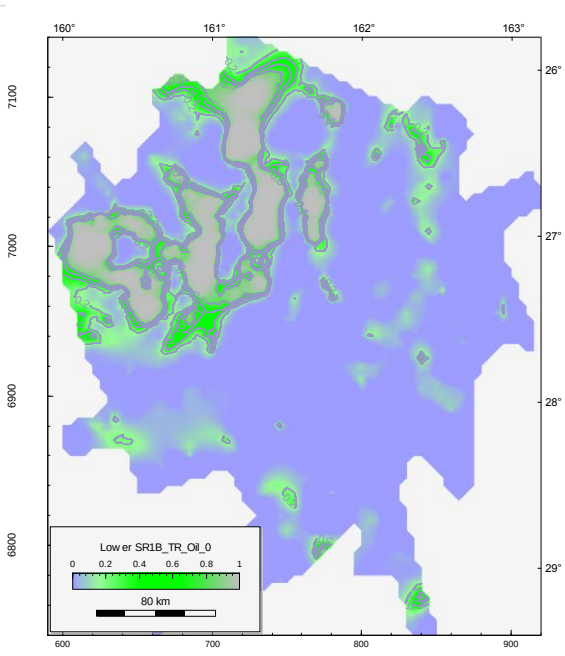

TR for oil
base Lower Syn-rift 1 unit at 0 Ma

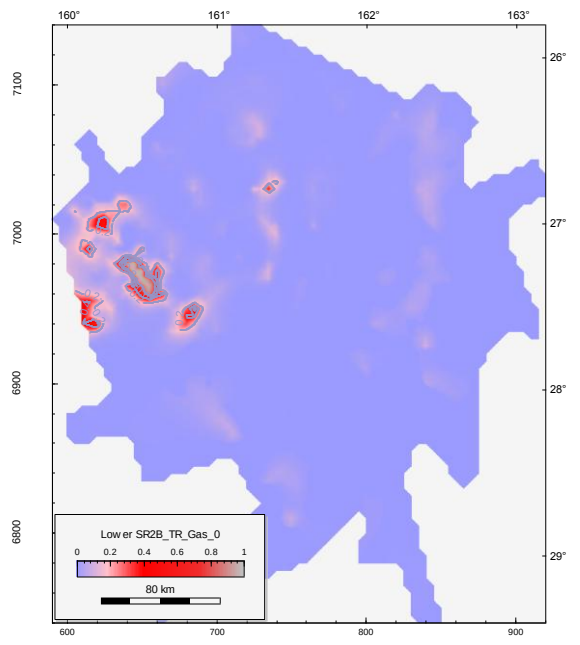

TR for gas
base Lower Syn-rift 2 unit at 0 Ma

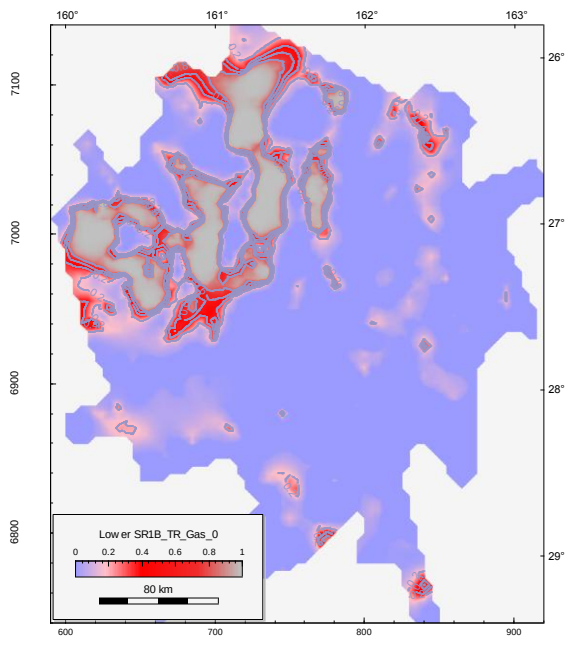

TR for gas
base Lower Syn-rift 1 unit at 0 Ma

Figure 22 Predicted maturity using transformation ratio of oil (upper) and gas (lower plots) (lacustrine shale, Woodleigh 2A kinetics) at present day for base case model; base Lower Syn-rift 2 unit (left), and base Lower Syn-rift 1 unit (right). Co-ordinates on left and lower axes are UTM 58S in km; the right and upper axes are latitude (S) and longitude (E).

2.3 MAPPED VOLUMETRICS

Predicted volumes expelled from the upper Pre-rift Walloon equivalent coaly source rock and the syn-rift coaly source rock units for specific times in the basin history are presented in Figures 23 to 26 for oil and Figures 28 to 29 for gas. The predicted total oil expelled is mapped in MMbbl/km^2 and gas, combining primary expelled gas and gas cracked from oil retained in the source rock, is mapped in Bcf/km^2. The time periods presented are based on ages of mapped and interpolated horizons (see Table 2); the properties assigned to respective source rocks that are used in the volumetric calculations are listed in Table 4. A comparison of predicted total oil volumes expelled from coaly source rocks throughout the stratigraphic succession for the base case model is presented in Figure 23. A similar comparison of the predicted total gas volumes expelled from coaly source rocks is presented in Figure 24. The Lower Syn-rift 1 unit is the most productive for both oil and gas, with the upper Pre-rift Walloon equivalent coal measures unit also expelling considerable volumes over a broad area. In contrast, the Upper Syn-rift 1 and Lower Syn-rift 2 units are relatively lean producers. Mapped volumetrics for the Upper Syn-rift 2 unit is not shown because this interval is modelled as not expelling either oil or gas.

2.3.1 Upper Pre-rift Walloon equivalent coaly source rock

Predicted expulsion through time of oil and gas from the upper Pre-rift Walloon equivalent coaly source rock is shown in Figures 25 and 26, respectively. The source rocks are modelled to expel oil early, with the rate of oil expulsion dropping slightly through to 36 Ma and further decreasing from 36 Ma onwards. The total gas expulsion rate shows a similar trend over this time period. Total volumes predicted to be expelled across the whole mapped region are:

a. 128 billion bbl of oil and 750 Tcf of total gas for the base case model (rifting plus Cenozoic magmatism)

b. 117 billion bbl of oil and 692 Tcf of total gas for the rift only model

c. 86 billion bbl of oil and 635 Tcf of total gas for the rift only plus erosion model

Basin-wide cumulative expelled volumes through time are illustrated in Figure 27. Given the lack of information on source rock richness and the approach of uniformly distributing source rock throughout specific units, it is to be expected that the primary petroleum producing areas will be related principally to depth of burial. However, a source rock richness and distribution overlay, if such information became available, would be a significant contribution to better understanding the distribution of active kitchens and the petroleum volumes expelled from them. Nevertheless, significant volumes are predicted to be expelled in the northwest Capel Basin with each of the different scenarios modelled, based on the assumed source rock properties (TOC 5%, HI 300 mg_{HC}/g_{TOC}, GOGI 0.37, Sth 100 mg_{OIL}/g_{TOC}). Given the thickness of the units and the uniform distribution of source rocks, these volumes should be treated as a maximum end-member for potential volumes likely to be generated and expelled.

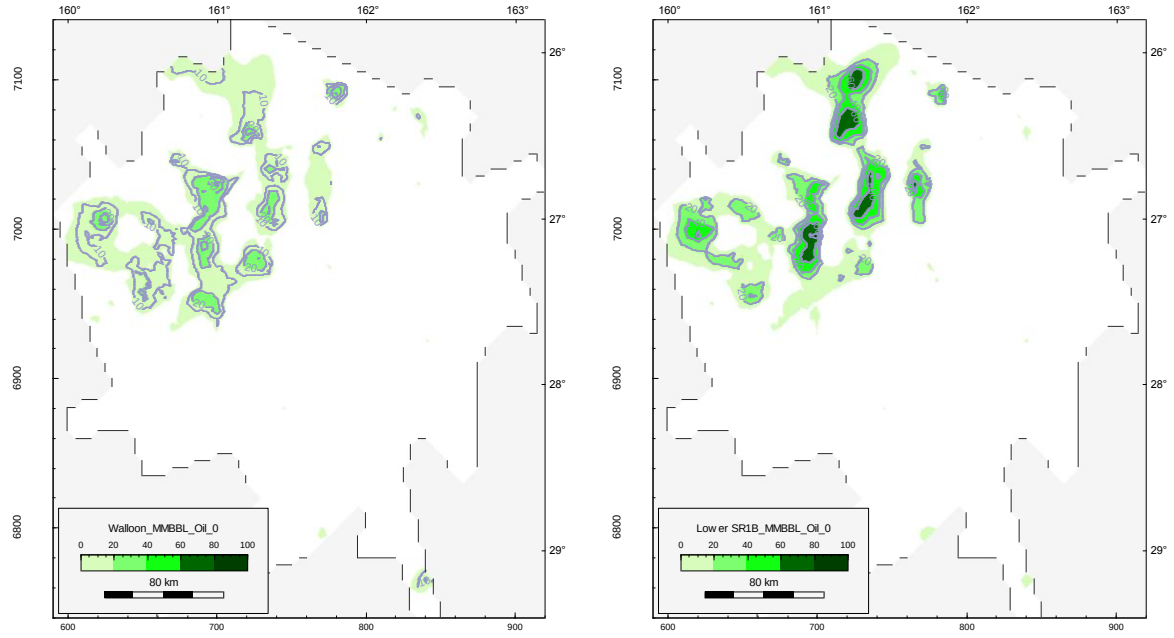

Walloon equivalent at 0 Ma **Lower Syn-rift 1 unit at 0 Ma**

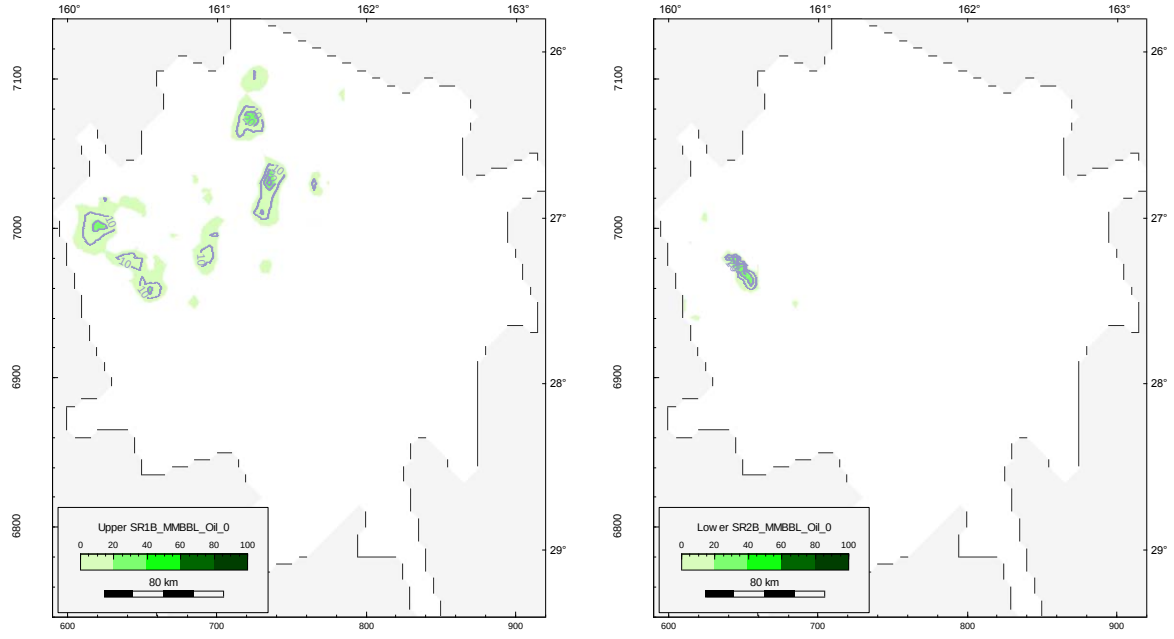

Upper Syn-rift 1 unit at 0 Ma **Lower Syn-rift 2 unit at 0 Ma**

Figure 23 Predicted total oil expelled (MMbbl/km^2) for base case model from upper Pre-rift Walloon Coal Measures equivalent (top left), Lower Syn-rift 1 coaly source rock unit (top right), Upper Syn-rift 1 coaly source rock unit (bottom left), and Lower Syn-rift 2 coaly source rock unit (bottom right). Co-ordinates on left and lower axes are UTM 58S in km; the right and upper axes are latitude (S) and longitude (E).

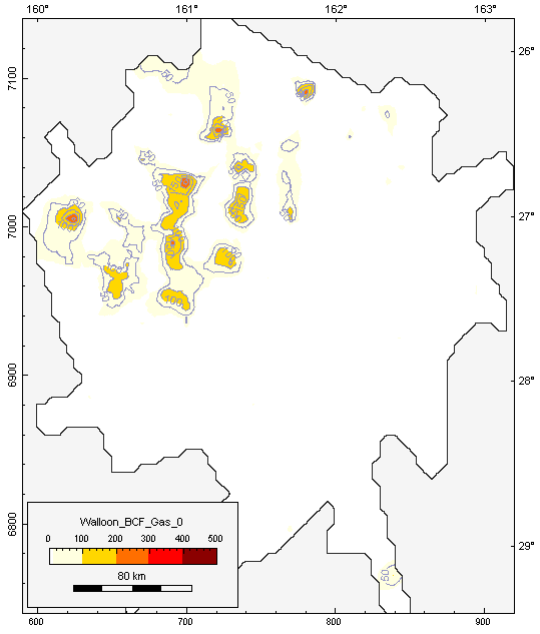

Walloon equivalent at 0 Ma

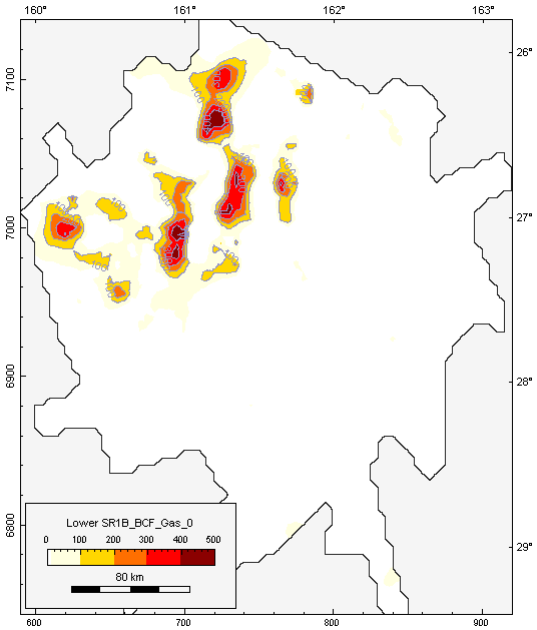

Lower Syn-rift 1 unit at 0 Ma

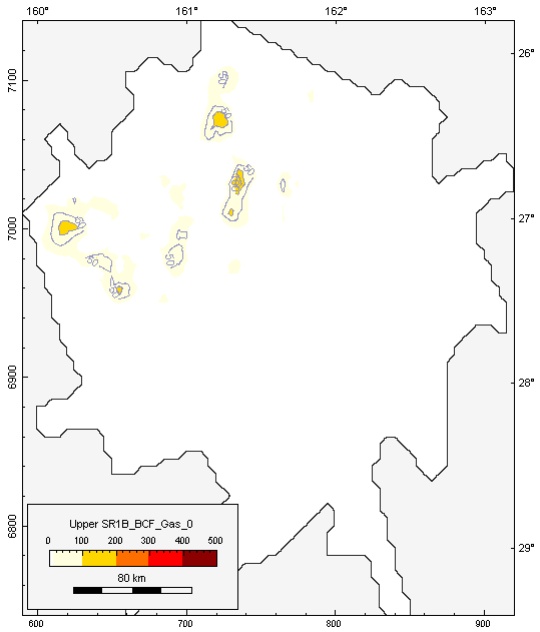

Upper Syn-rift 1 unit at 0 Ma

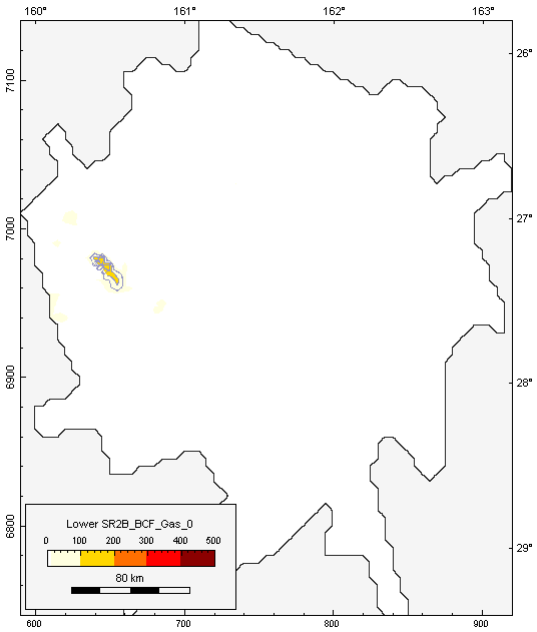

Lower Syn-rift 2 unit at 0 Ma

Figure 24 Predicted total gas expelled (Bcf/km^2) for base case model from upper Pre-rift Walloon Coal Measures equivalent (top left), Lower Syn-rift 1 coaly source rock unit (top right), Upper Syn-rift 1 coaly source rock unit (bottom left), and Lower Syn-rift 2 coaly source rock unit (bottom right). Co-ordinates on left and lower axes are UTM 58S in km; the right and upper axes are latitude (S) and longitude (E).

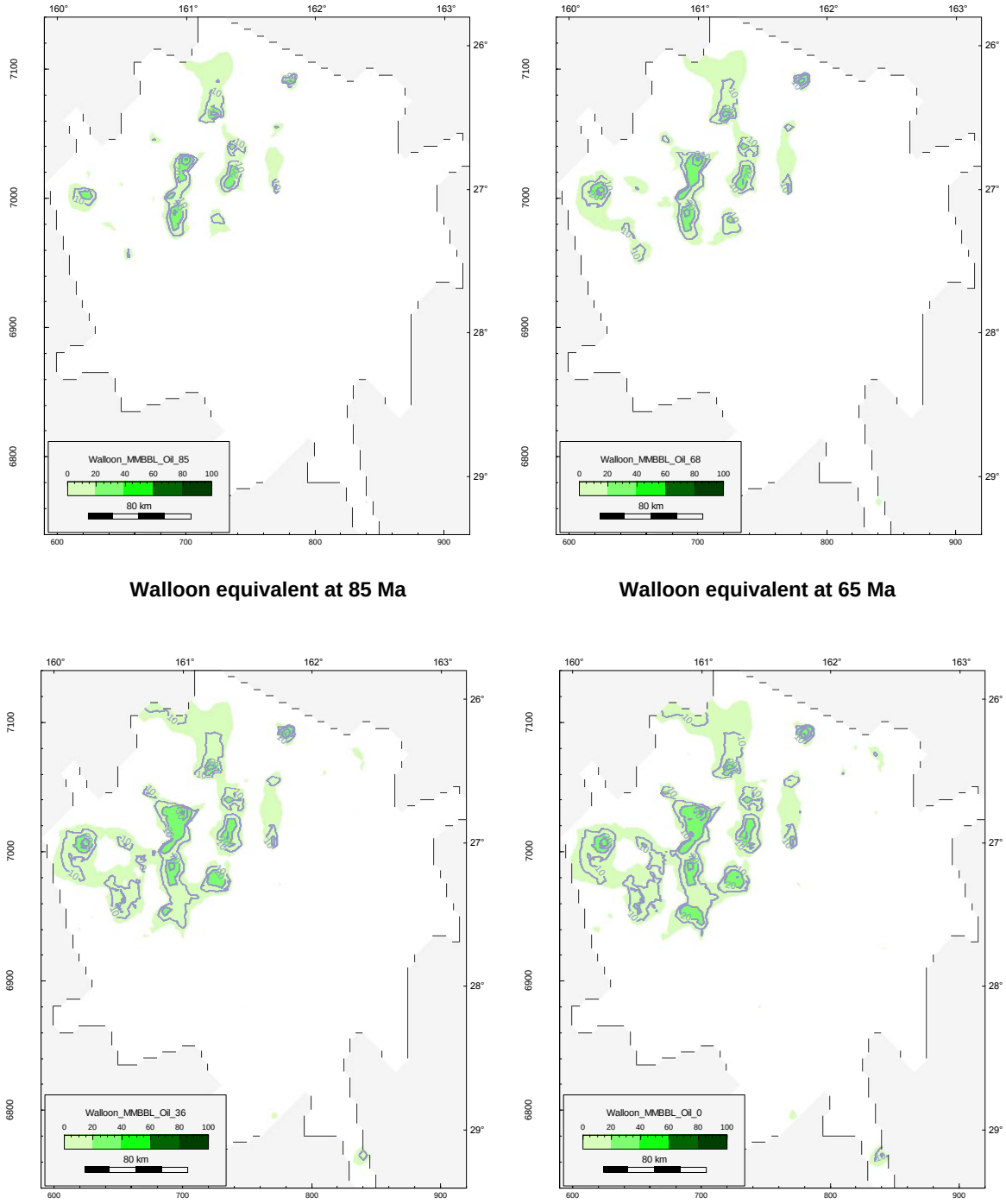

Walloon equivalent at 85 Ma

Walloon equivalent at 65 Ma

Walloon equivalent at 36 Ma

Walloon equivalent at 0Ma

Figure 25 Predicted cumulative oil expelled (MMbbl/km^2) for base case model from upper Pre-rift Walloon Coal Measures equivalent through time; 85 Ma (top left), 68 Ma (top right), 36 Ma (bottom left) and present day (bottom right) for coaly (organofacies DE) source rock kinetics (Pepper & Corvi 1995a). Co-ordinates on left and lower axes are UTM 58S in km; the right and upper axes are latitude (S) and longitude (E).

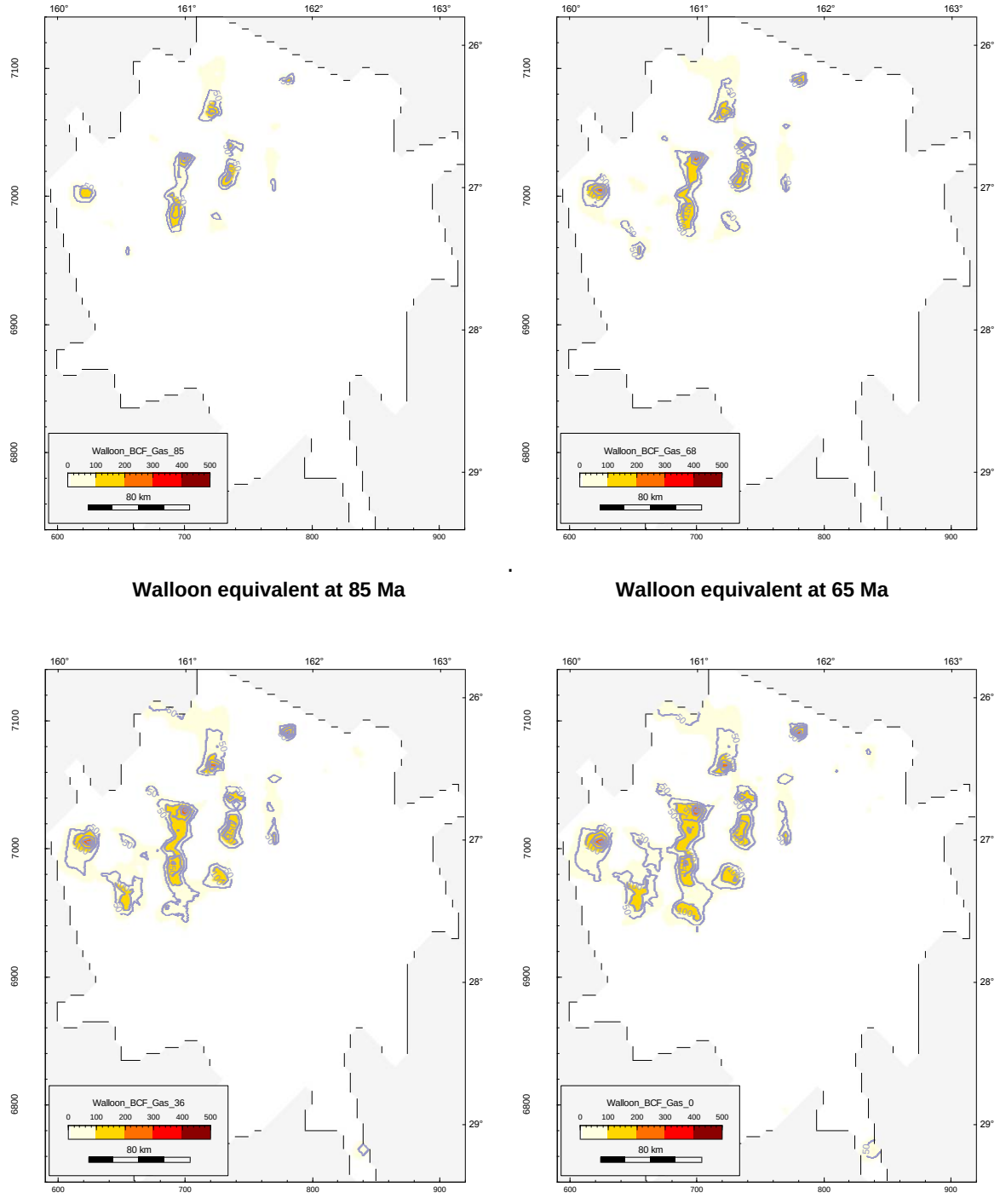

Walloon equivalent at 85 Ma

Walloon equivalent at 65 Ma

Walloon equivalent at 36 Ma

Walloon equivalent at 0 Ma

Figure 26 Predicted cumulative gas expelled (Bcf/km^2) for base case model from upper Pre-rift Walloon Coal Measures equivalent through time; 85 Ma (top left), 68 Ma (top right), 36 Ma (bottom left) and present day (bottom right) for coaly (organofacies DE) source rock kinetics (Pepper & Corvi 1995a). Co-ordinates on left and lower axes are UTM 58S in km; the right and upper axes are latitude (S) and longitude (E).

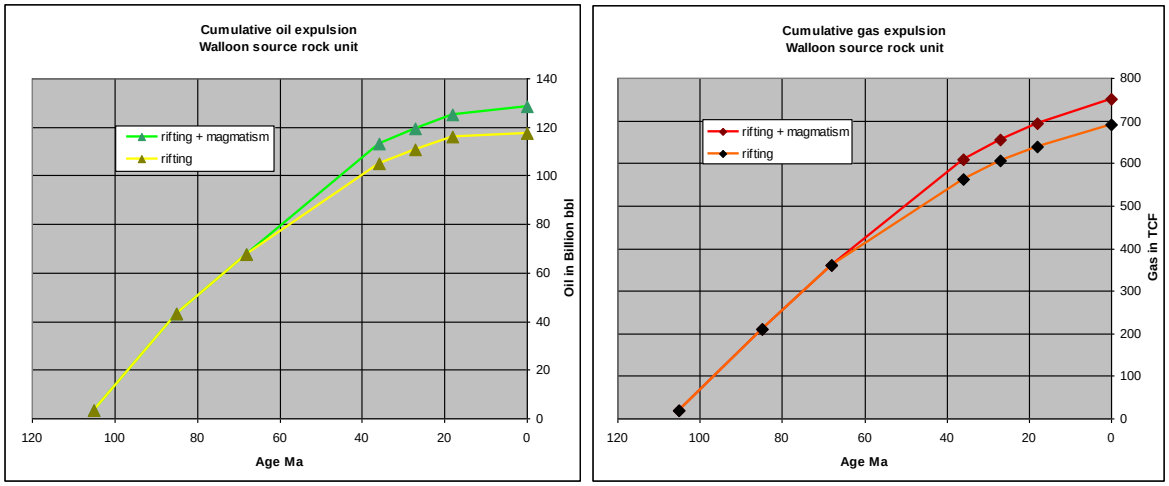

Figure 27 Cumulative oil and gas expelled from the upper Pre-rift Walloon equivalent coaly source rock unit for the rifting only and the rifting plus Cenozoic magmatism (base case) models.

2.3.2 Syn-rift 1 source rock

The Lower Syn-rift 1 source rock unit is thicker than the upper Pre-rift Walloon equivalent coal measures, and even though it has a lower TOC value, it is predicted to generate twice the volume of oil and gas. Predicted expulsion of oil and gas from the coal-rich Lower Syn-rift 1 source rock unit is shown in Figures 28 and 29, respectively. The Lower Syn-rift 1 rocks are, similar to the upper Pre-rift Walloon equivalent coal measures, modelled to expel oil and gas from Early Cretaceous through to the present day. However, the rate of expelled oil volumes decreases from 36 Ma onwards (Figure 30). Total volumes predicted to be expelled are:

a. 256 billion bbl oil and 1,500 Tcf total gas for the base case model (rifting plus Cenozoic magmatism)

b. 229 billion bbl oil and 1,370 Tcf total gas for the rift only model

c. 158 billion bbl oil and 1,250 Tcf total gas for the rift only plus erosion model

Figure 30 graphs the increase in expelled volumes at key time steps. Similar to the upper Pre-rift Walloon equivalent coal measures, and applicable to all source rocks modelled, the primary kitchens are the regions that have undergone significant burial during Cretaceous rifting. It is reasonable to expect this modelled distribution of generation and expulsion to be modified if further information on source rock richness and distribution becomes available. Based on the coaly source rock properties assumed (TOC 3%, HI 300 mg_{HC}/g_{TOC}, GOGI 0.37, Sth 100 mg_{OIL}/g_{TOC}), significant volumes are predicted to be expelled from the northwest Capel Basin with all three modelled scenarios. Once again, these volumes should be treated as a maximum end-member for potential volumes likely to be generated and expelled.

As an alternative to the presence of coaly source rocks, models including lacustrine source rocks were also developed for the Lower Syn-rift 1 and the Lower Syn-rift-2 units. The predicted total oil and gas expelled from these successions are presented using Pepper & Corvi (1995a) organofacies C kinetics in Figure 31 and Woodleigh 2A kinetics in Figure 32 (see Figure 6 for comparison of different kinetic parameters). Both kinetic data sets applied to the Lower Syn-rift 1 unit produce similar volumes of total gas, although the organofacies C kinetics produce 50% greater volumes of oil. Using the assumed source rock properties

(TOC 3%, HI 548 mg_{HC}/g_{TOC}, GOGI 0.16, Sth 100 mg_{OIL}/g_{TOC}) and lacustrine kinetic data, the Lower Syn-rift 1 unit, for the base case model (rifting plus Cenozoic magmatism) is predicted to expel 1,400 billion bbl oil and 1,600 Tcf total gas for the organofacies C kinetics, compared with 940 billion bbl oil and 1,830 Tcf total gas for the Woodleigh 2A kinetics.

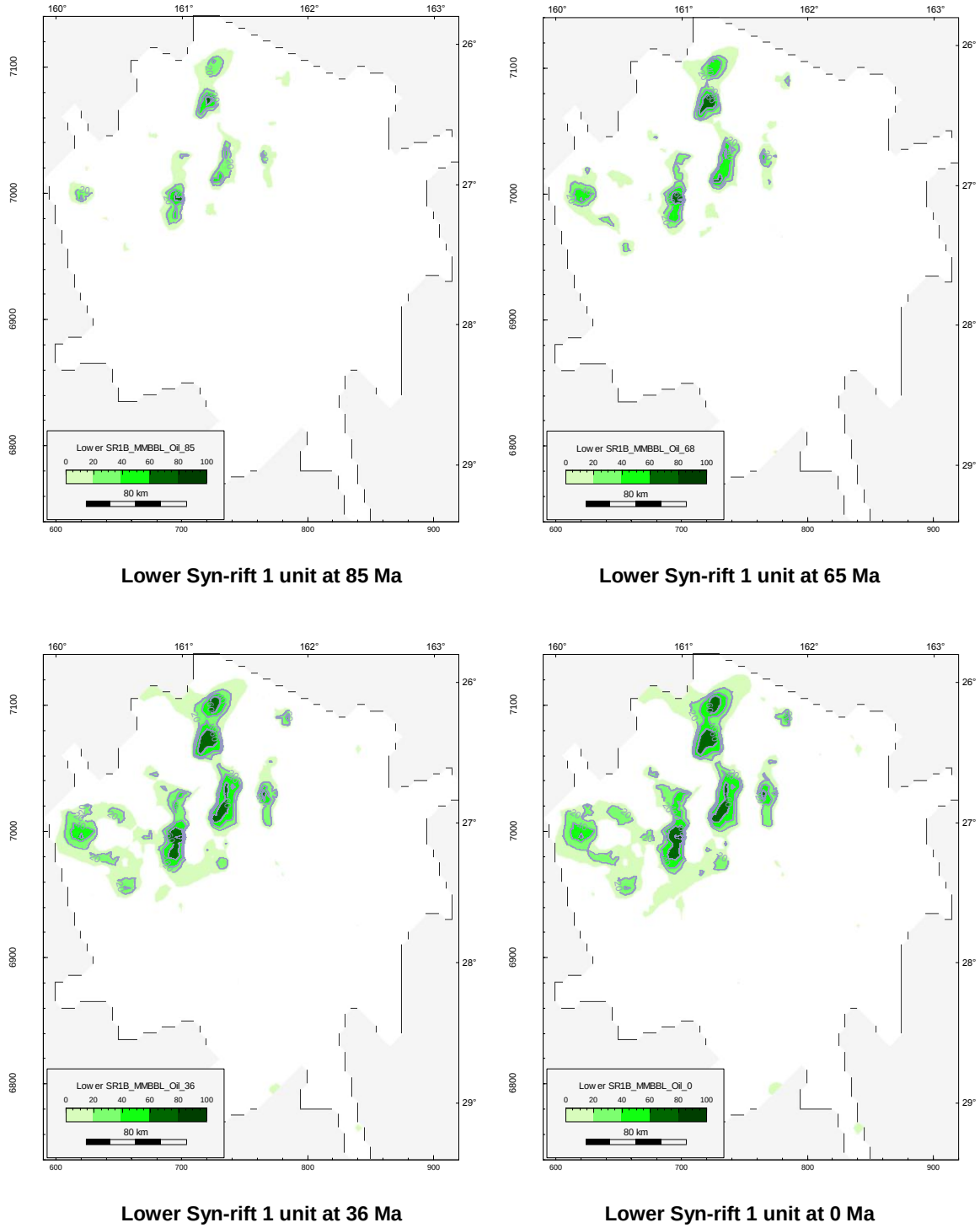

Lower Syn-rift 1 unit at 85 Ma

Lower Syn-rift 1 unit at 65 Ma

Lower Syn-rift 1 unit at 36 Ma

Lower Syn-rift 1 unit at 0 Ma

Figure 28 Predicted cumulative oil expelled ($MMbbl/km^2$) for base case model from Lower Syn-rift 1 coaly source rock unit through time; 85 Ma (top left), 68 Ma (top right), 36 Ma (bottom left) and present day (bottom right) for coaly (organofacies DE) source rock kinetics (Pepper & Corvi 1995a). Co-ordinates on left and lower axes are UTM 58S in km; the right and upper axes are latitude (S) and longitude (E).

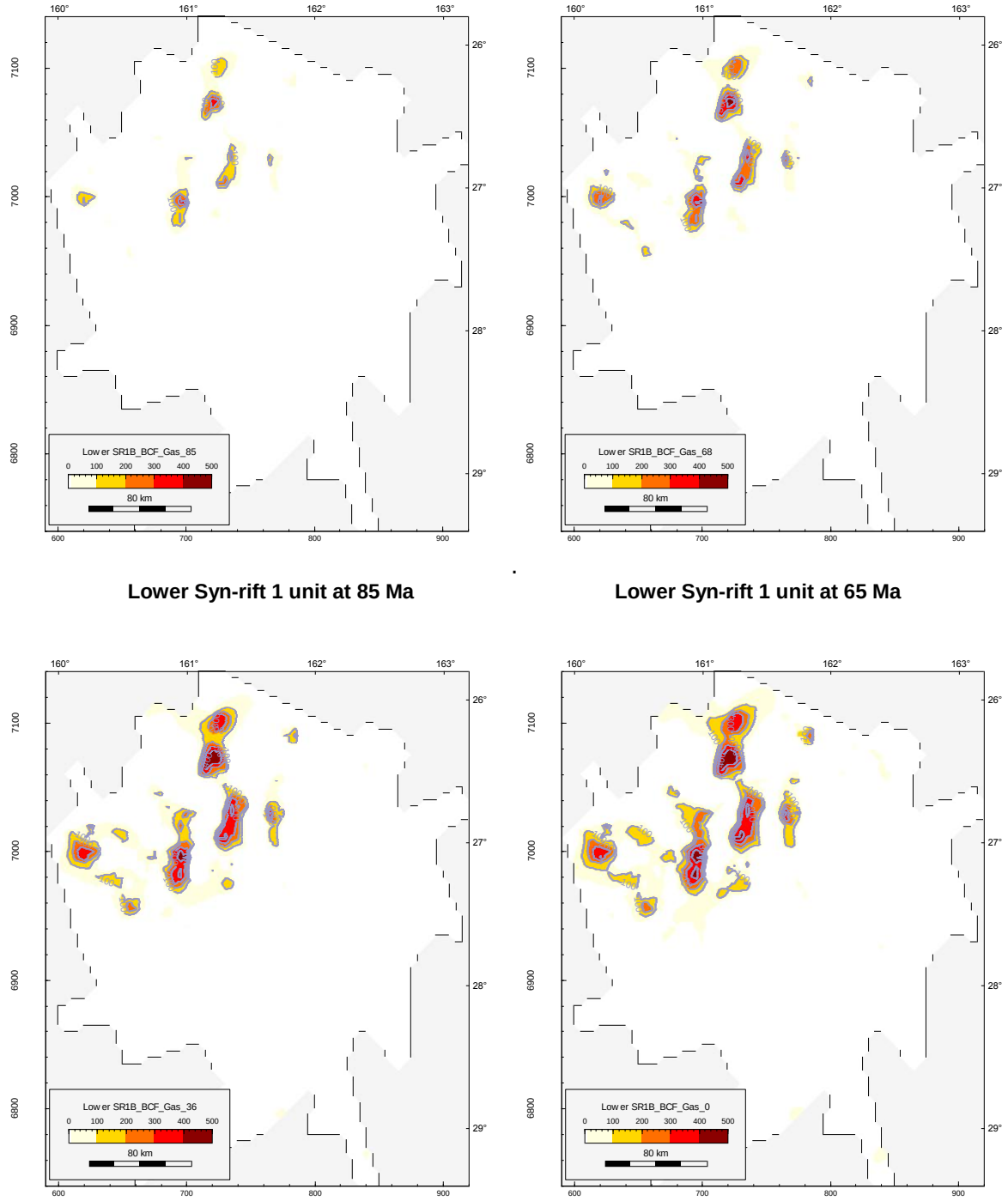

Lower Syn-rift 1 unit at 85 Ma

Lower Syn-rift 1 unit at 65 Ma

Lower Syn-rift 1 unit at 36 Ma

Lower Syn-rift 1 unit at 0 Ma

Figure 29 Predicted cumulative gas expelled (Bcf/km^2) for base case model from Lower Syn-rift 1 coaly source rock unit through time; 85 Ma (top left), 68 Ma (top right), 36 Ma (bottom left) and present day (bottom right) for coaly (organofacies DE) source rock kinetics (Pepper & Corvi 1995a). Co-ordinates on left and lower axes are UTM 58S in km; the right and upper axes are latitude (S) and longitude (E).

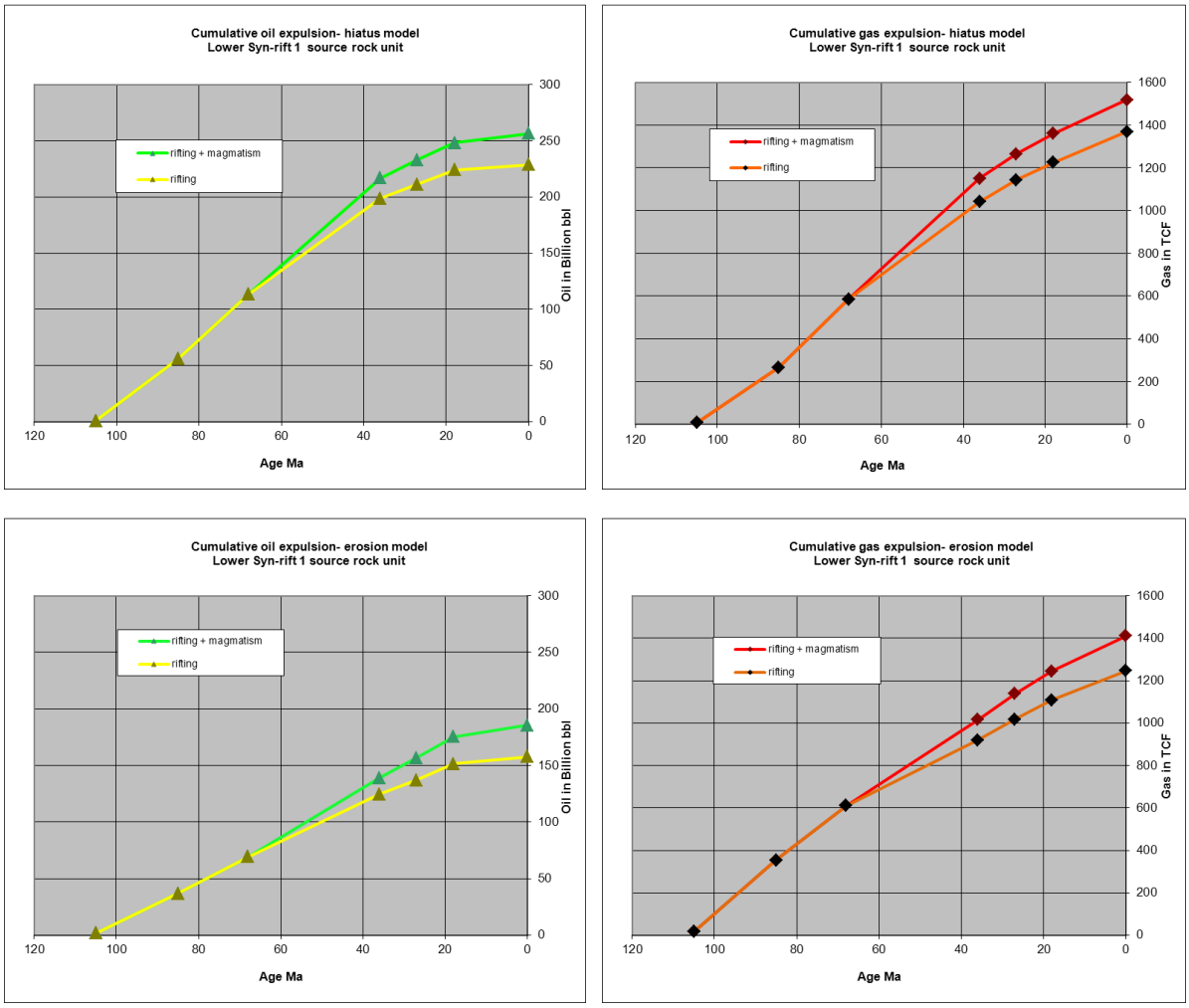

Figure 30 Cumulative oil and gas expelled from the Lower Syn-rift 1 coaly source rock unit for the rifting only and the rifting plus Cenozoic magmatism (base case) models for the hiatus scenarios (upper plots) and the deposition followed by equivalent erosion scenarios (lower plots).

The Upper Syn-rift 1 unit is modelled to be twice as thick, but leaner than the underlying Lower Syn-rift 1 unit, with 1% TOC distributed evenly throughout. As a result of the low TOC the predicted volumes of oil and total gas expelled amount to only 13% of those from the Lower Syn-rift 1 unit.

2.3.3 Syn-rift 2 source rock

The Syn-rift 2 megasequence is modelled to expel insignificant volumes across the whole mapped region; approximately 5 billion bbl oil and 30 Tcf total gas based on coaly source rock kinetics. Assuming lacustrine source rocks are present in the Lower Syn-rift 2 unit, then greater volumes (20 – 60 billion bbl oil and 40 – 50 Tcf total gas) are predicted for the base case model (Figures 31 and 32).

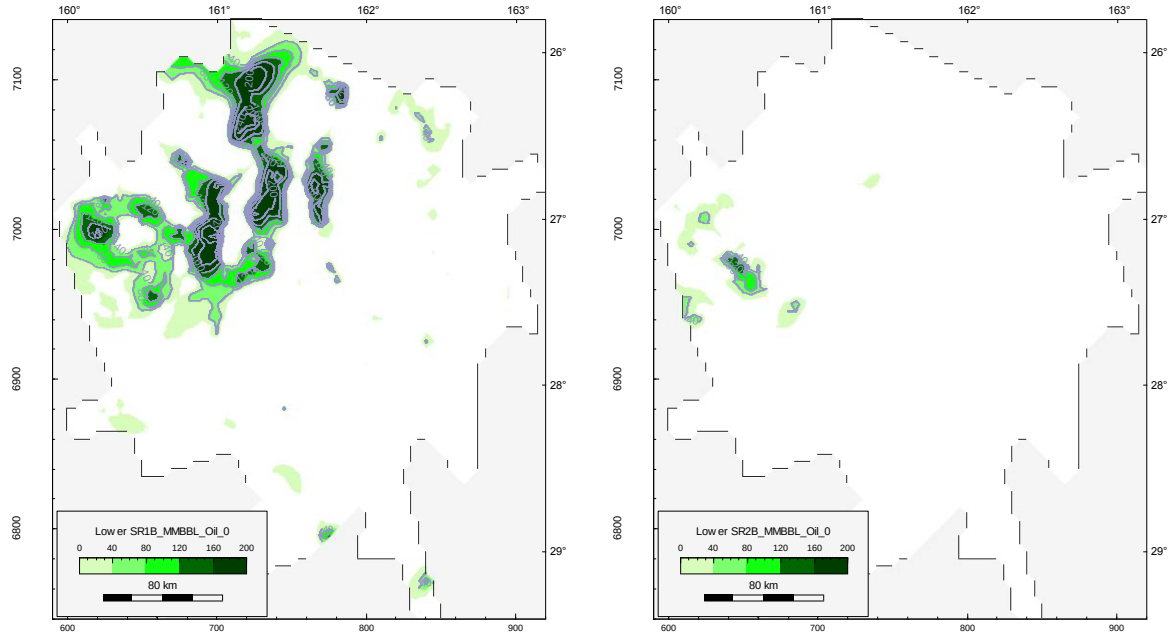

Lower Syn-rift 1 unit at 0 Ma **Lower Syn-rift 2 unit at 0 Ma**

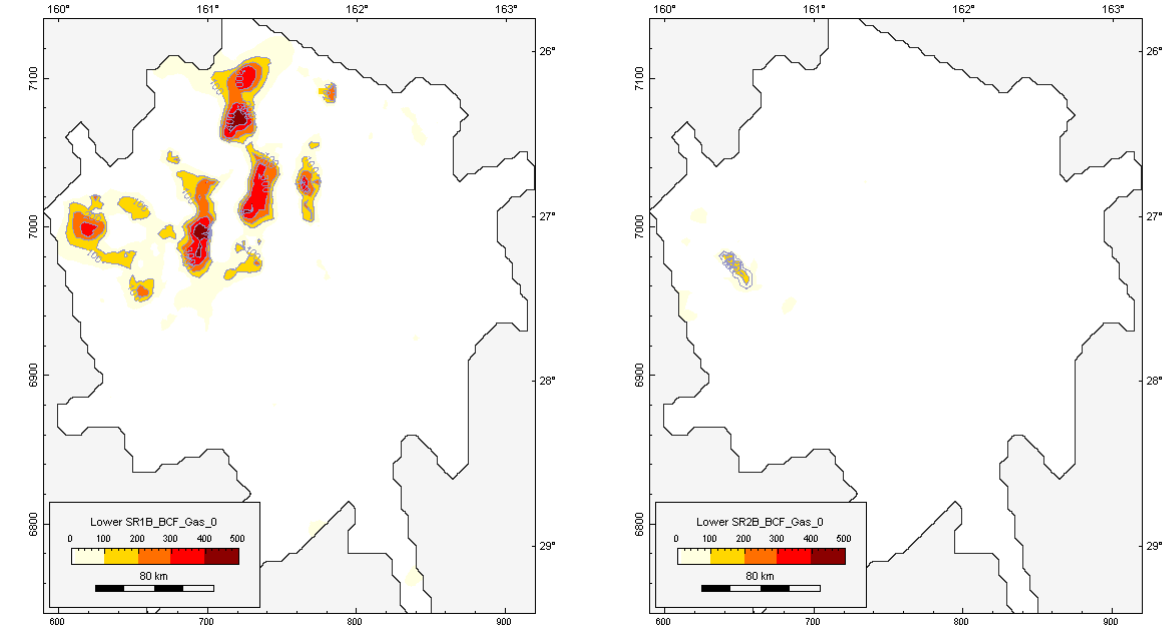

Lower Syn-rift 1 unit at 0 Ma **Lower Syn-rift 2 unit at 0 Ma**

Figure 31 Predicted total oil expelled (MMbbl/km^2) for base case model from Lower Syn-rift 1 lacustrine source rock unit (top left), and Lower Syn-rift 2 lacustrine source rock unit (top right); predicted total gas expelled (Bcf/km2) from Lower Syn-rift 1 lacustrine source rock unit (bottom left), and Lower Syn-rift 2 lacustrine source rock unit (bottom right) for lacustrine (organofacies C) source rock kinetics (Pepper & Corvi 1995a). Co-ordinates on left and lower axes are UTM 58S in km; the right and upper axes are latitude (S) and longitude (E).

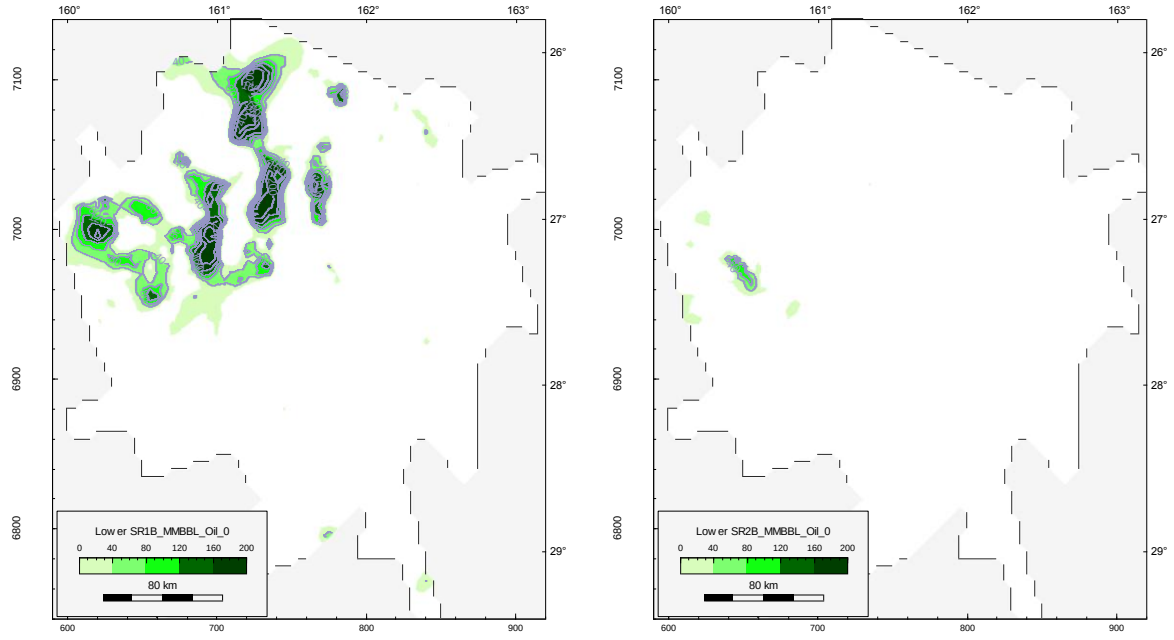

Lower Syn-rift 1 unit at 0 Ma **Lower Syn-rift 2 unit at 0 Ma**

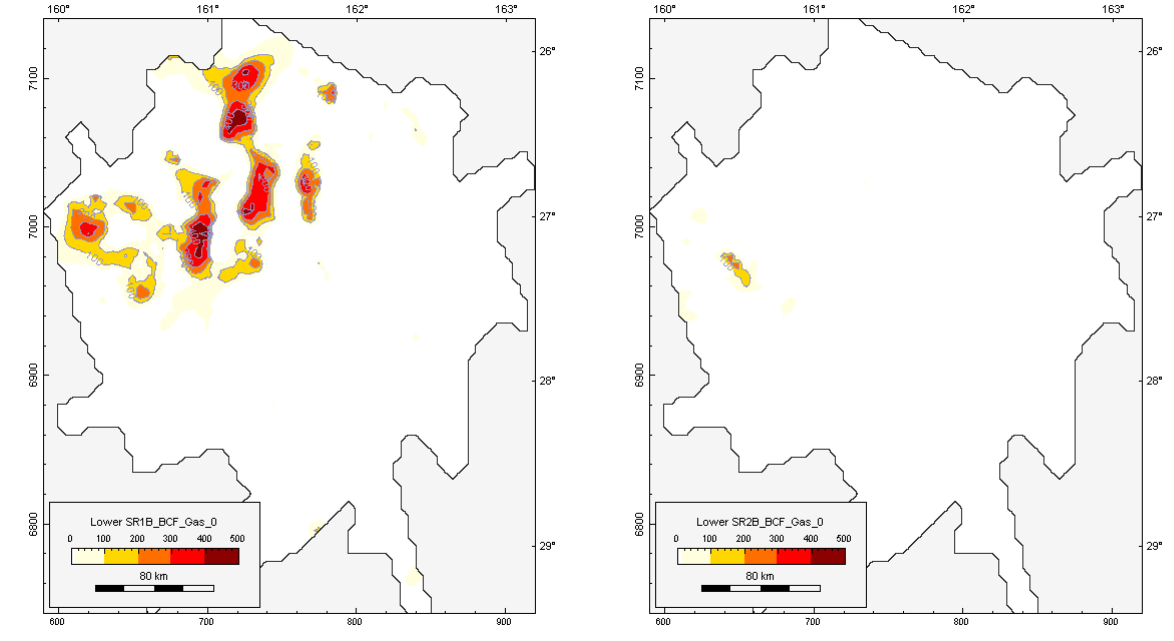

Lower Syn-rift 1 unit at 0 Ma **Lower Syn-rift 2 unit at 0 Ma**

Figure 32 Predicted total oil expelled (MMbbl/km^2) for base case model from Lower Syn-rift 1 lacustrine source rocks (top left), and Lower Syn-rift 2 lacustrine source rocks (top right); predicted total gas expelled (Bcf/km^2) from Lower Syn-rift 1 lacustrine source rock unit (bottom left), and Lower Syn-rift 2 sediments (bottom right) for Woodleigh 2A lacustrine source rock kinetics (Boreham 2010, pers. comm.). Co-ordinates on left and lower axes are UTM 58S in km; the right and upper axes are latitude (S) and longitude (E).

2.4 DISCUSSION ON VOLUMETRICS

Volumetric predictions are dependent on the accuracy of structural maps, assumed source rock distribution, and generation parameters used in the models. Without well calibration a greater certainty in the predicted petroleum generation history may be gained by including higher resolution seismic interpretation, which could also delineate seismic facies related to source rocks.

In general, the multi-1D basin modelling indicates that the Pre-rift and Syn-rift 1 megasequences have reached the oil or gas generation window within the deeper depocentres of the Capel and western Faust basins (Figures 17 – 22). Generation from the Syn-rift 2 megasequence is minor. Source rock maturity is modelled to increase from Early Cretaceous through to the present day; however, the rate of maturity increase slowed from 36 Ma to the present day. The slowing of maturation in the late Cenozoic is primarily due to a significant increase in water depth over this period (since about 36 Ma) and a decrease in sediment supply. During this time the average water depth across the whole region increased from about 160 m to 1600 m, causing a drop in temperature at the sea bed and a significant change in thermal boundary conditions. This temperature change effectively counters the effects of an additional 200 to 700 m (average 500 m) of burial that occurred since 36 Ma. For example, in the area of the maximum water depth increase (by 355 to 2859 m) the predicted average surface temperature drops from 20° to 4°C, shifting the thermal boundary condition at the surface by 16°C. Uncertainty in timing and amount of variation in paleo-water depth contributes to uncertainty in both the timing of source rock maturity and in the volumes of expelled petroleum throughout this period.

The primary petroleum producing areas are related principally to major depocentres, that are best developed in the western regions (Capel Basin). Assuming the base case modelling scenario of no erosion applies, and that coaly source rocks are present in the Pre-rift and both Syn-rift megasequences, the predicted volumes expelled from these depocentres exceeds 5 MMbbl/km^2 oil and and 25 Bcf/km^2 total gas from the Pre-rift megasequence, and 20 MMbbl/km^2 oil and 100 Bcf/km^2 total gas from the whole Syn-rift 1 megasequence (Figures 23 and 24). The maximum predicted yields range as high as 40 MMbbl/km^2 oil and 275 Bcf/km^2 total gas from the Pre-rift megasequence, and 100 MMbbl/km^2 oil and 630 Bcf/km^2 total gas from the whole Syn-rift 1 megasequence.

In terms of timing of expulsion, models predict that 80% of total hydrocarbon expulsion occurred before the end of the Eocene (Figures 27 and 30), with maximum expulsion taking place between the Maastrichtian and the Late Eocene (c. 68 – 36 Ma; Figures 28 and 29). However, some late-stage generation since 36 Ma is likely to have taken place across the major depocentres as those parts of the Syn-rift 1 source rock unit which were buried to shallow depths, began to enter the hydrocarbon generation window.

Post-rift magmatism may have significantly enhanced Late Cenozoic generation, if related to a significant increase in crustal heat flow, such as that arising from a mantle plume. The effects of Maastrichtian–Paleocene/Eocene and Late Oligocene–Miocene magmatic episodes were simulated in the models by the addition of heat pulses at the base of the lithosphere. This resulted in an increase in expelled volumes of about 11%, equating to additional volumes of over 35 billion bbl of expelled oil and 200 Tcf of total expelled gas from the whole modelled region (Figures 27 and 30).

Although the volumes of petroleum expelled from the source rock units are large, it should be recognised that:

- they should be considered a maximum end-member for potential expelled oil and gas volumes due to the uniformly distributed nature of generative organic matter within source rocks throughout each of the units; and,
- they do not reflect likely trapped volumes because no losses have been included.

In addition to leakage to the surface, losses might be related to residual saturation in carrier beds, blind migration pathways and small accumulations associated with migration from source to trap, and can represent a significant (>90%) proportion of the total expelled hydrocarbon volumes. Thus the amount available to charge prospects may be only a small fraction of this total – defining the migration efficiency of the basin (England 1994).

3.0 MAP-BASED CHARGE MODELLING

The objective of the map-based charge modelling (using Zetaware Trinity[2] software) is to provide a reconnaissance level investigation of migration pathways, identifying which traps have access to charge and the possible volumes of expelled petroleum capable of being trapped. Migration is traced on all mapped horizons between the top lower Post-rift (or top Lower Sag as identified on maps – see Table 2) and top Pre-rift (top Walloon equivalent coal measures), using potential charge volumes derived from multi-1D models for the time periods prior to, and following 36 Ma.

The estimates of trapped volumes given here make no allowance for migration losses and are based on the use of simple reservoir properties. They are intended to provide an initial assessment of potential migration pathways and traps that have access to charge. Trap sizes and predicted volume of accumulations are dependent on trap geometry, reservoir properties and seal effectiveness, all of which are generalised and should be considered as approximations in these models.

3.1 METHODOLOGY

The general methodology assesses migration on individual mapped surfaces based on simple buoyancy-controlled up-dip migration using both present day structure maps and modelled paleo-structure at 36 Ma. While the software allows for the incorporation of facies control (controlled by a capillary entry pressure value) and pressure effects (from potentiometric surfaces), these data were not available for this frontier region. Although, a simple sand facies map was developed for the Lower Post-rift (Lower Sag) unit (see Table 2). A crucial assumption in this methodology is that petroleum phases migrate vertically from source rock kitchens onto each migration surface, permitting migration to be assessed independently for each surface.

Trinity software is used to compile the input and output grids (625 x 625 m cells) for the BM1D modelling because of its flexibility in manipulating and managing grids. Inputs for the charge modelling consist of the following series of maps:

- Present day and paleo-structure surfaces on which to migrate petroleum
- Oil and gas expelled volume grids from BM1D software
- Sand facies map for Lower Post-rift (Lower Sag) unit.

These maps are assembled in a Trinity project that allows the interactive testing of secondary migration and accumulation. The results of these investigations are dependent on the following assumptions with respect to migration:

- The source is limited by the predicted distribution and volume of expelled oil and gas for each time period based on the BM1D output maps
- Migration is controlled by buoyancy driven flow on structural surfaces, unless stated otherwise
- No losses occur during migration
- The sides of the model are open, allowing flow out of the model.

[2] Interactive petroleum system analysis and risking software by Zetaware, Inc. http://www.zetaware.com

The predicted accumulations are dependent on the following assumptions:

- Reservoir properties controlling accumulation size assume 100 m thick sand, 25% porosity and 60% hydrocarbon saturation for all horizons
- Seals are considered adequate to support no more than a 200 m hydrocarbon column, after which they leak
- All quoted volumes are at standard temperature pressure (STP) unless otherwise stated.

The ratio of oil and gas in each trap is defined by the gas-oil ratio (GOR) of fluids initially charging the trap and the contribution of processes leading to seal leakage or trap-volume controlled spillage (e.g., gas tends to leak, oil tends to spill in the model). It should be clearly understood that since the reservoir and seal properties are generalised (using those parameters identified above), this assessment does not provide definitive volume estimates for accumulations, or prove the viability of structural containment.

3.2 FLOW-PATH MODEL

Colwell et al. (2010) and Hashimoto et al. (2010) suggested potential reservoir sandstones could occur in both Syn-rift and lower Post-rift successions (Table 1). The Syn-rift 1 megasequence and Lower Syn-rift 2 unit are most likely to include fluvial system rocks with potential as reservoir formations. Seismic interpretation suggests that the Upper Syn-rift 2 unit and lower Post-rift megasequence possibly contain well-sorted deltaic, shoreline and turbidite sandstones (Hashimoto et al. 2010). Seals may include fine-grained estuarine, pro-delta, shelf and bathyal mud deposited as part of a transgressive systems tract formed during the initial stages of marine transgression and fine-grained calcareous bathyal sediments of the upper parts of the Post-rift megasequence (Colwell et al. 2010, Hashimoto et al. 2010).

The unconformity at the base of the Oligocene Post-rift succession (Figure 2) is related to tectonic events (Sutherland et al. 2010) and is represented by a 40 – 36 Ma hiatus in the model. This event is recognised as a significant episode in basin history, causing a change in sedimentation patterns and water depth across both basins. In the flow-path modelling our approach has been to: firstly apply the volume of oil and gas expelled up to the Oligocene on each of the 36 Ma-aged paleo-structure maps and model migration and entrapment; and secondly, to apply only oil and gas expelled since 36 Ma to present day structural maps. While it could be argued that volumes expelled before 36 Ma, and any accumulations existing at 36 Ma, may contribute to present day entrapped volumes, the modelling exercise indicates that these early expelled products were most likely lost from the system (see discussion in Section 4.3). No migration loss factor has been applied since the aim of this charge modelling component is to identify the likelihood of accumulations assuming adequate volumes for charge exist.

Within the Post-rift megasequence, the Maastrichtian-aged Lower Post-rift (Lower Sag) unit is identified as a relatively thin potential reservoir. An interpreted sand/mud facies map was developed from available data for this unit. A “sand” facies was assumed for water depths less than 50 m on the 69 Ma water depth map. Bald highs (isopach values less than 1 m) were assigned a no-flow or “mud” facies and then combined with the sand facies map. Finally, fault data representing major (basement involved) faults mapped on the top of the Lower Post-rift (Lower Sag) unit were added to act as lateral seals. The resulting facies map

is shown in Figure 33. For other potential reservoir units a no-flow facies was assigned in regions of zero isopach although no sand facies were included due to the lack of information.

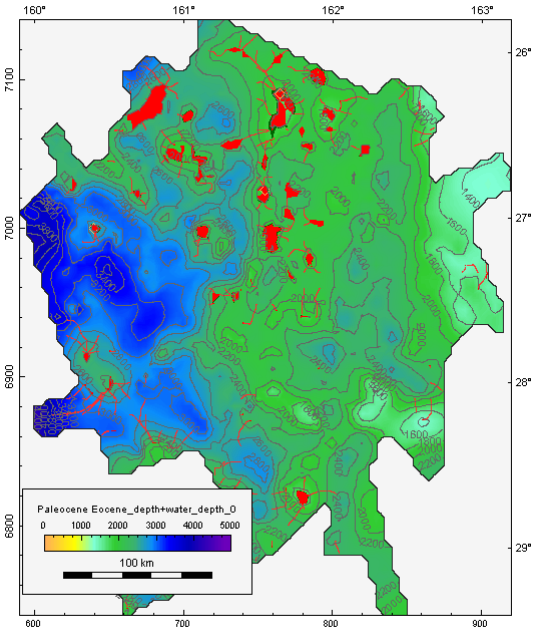

Structure and accumulations
top Lower Post-rift (Lower Sag) at 0 Ma

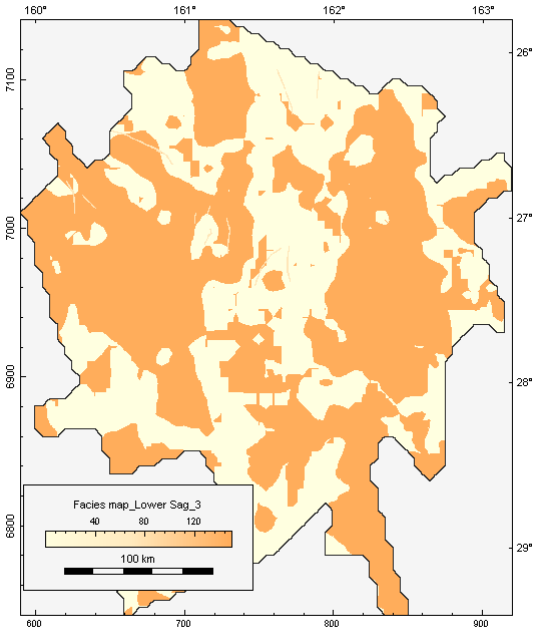

Sand facies map
top Lower Post-rift (Lower Sag) at 0 Ma

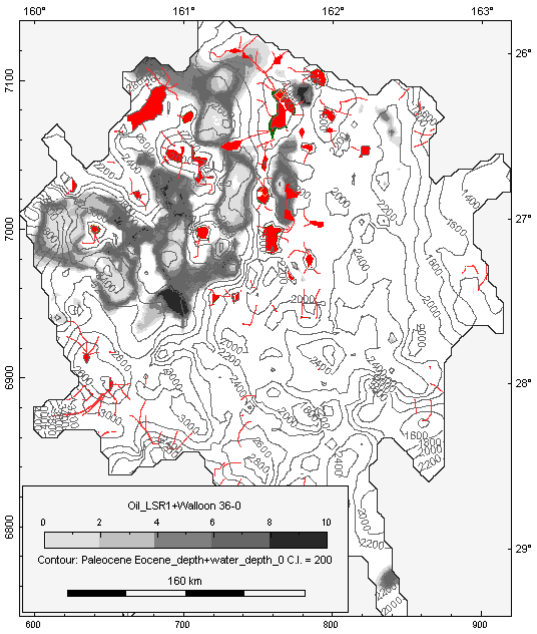

Expelled oil volumes and accumulations
top Lower Post-rift (Lower Sag) at 0 Ma

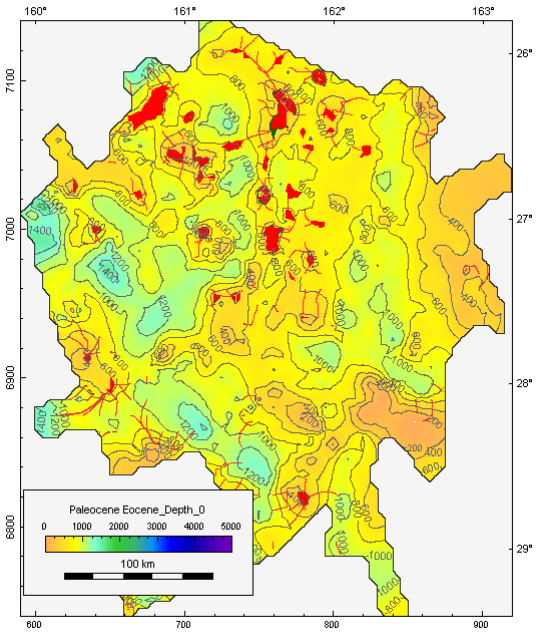

Burial depth and accumulations
top Lower Post-rift (Lower Sag) at 0 Ma

Figure 33 Migration results from flow-path modelling using sand facies control on the top Lower Post-rift (Lower Sag) unit at the present day; structural map with accumulations (top left), facies showing sands as yellow and no-flow zones as orange (top right), structural contours with accumulations and expelled oil volumes (MMbbl/km^2) for the period since 36 Ma as a grey-scale overlay (bottom left), present day burial depth with accumulations (bottom right). Note that legends on maps refer to the base of the overlying unit; in this case the Paleocene Eocene unit.

3.3 CHARGE MODEL RESULTS

3.3.1 Post-rift sequences

By the end of the Eocene (c. 36 Ma) the Lower Post-rift (Lower Sag) unit was variably buried up to depths of 1,200 m, although many of the mapped structural highs remained with little cover and it is unlikely an effective seal was present over structural highs. No accumulations are expected to be retained within this unit at this time. Results of the flow-path modelling for the present day on the top Lower Post-rift (Lower Sag) structure (68 Ma) are presented in Figure 33. Accumulations are located mainly in the north and eastern Capel and western Faust basins, and modelled as dominantly gas with volumes generally about 5 to 9 Tcf at burial depths of 400–700 m. Seal effectiveness has been fixed in this model to allow a maximum 200 m column to be contained. However, it is likely that this may be over-predicting the seal effectiveness of the overlying rocks given their relatively shallow depth of burial. Reducing the seal effectiveness decreases the predicted trapped volumes although the distribution of predicted accumulations remains the same.

Figures 33 and 34 allow comparison of migration with and without the application of a sand facies control for the Lower Post-rift (Lower Sag) unit at the present day. By allowing unrestricted flow on this surface, models predict larger accumulations (Figure 34) extending further to the west and south than models with sand facies control (Figure 33). However, this only provides one end-member for migration, assuming laterally continuous and connected high quality reservoir facies are present across the model area; which is unlikely to be the case. Predicted accumulations with unrestricted flow (no sand facies control) generally tend to be larger and with greater proportions of oil; although, seal effectiveness remains a containment risk as mentioned above.

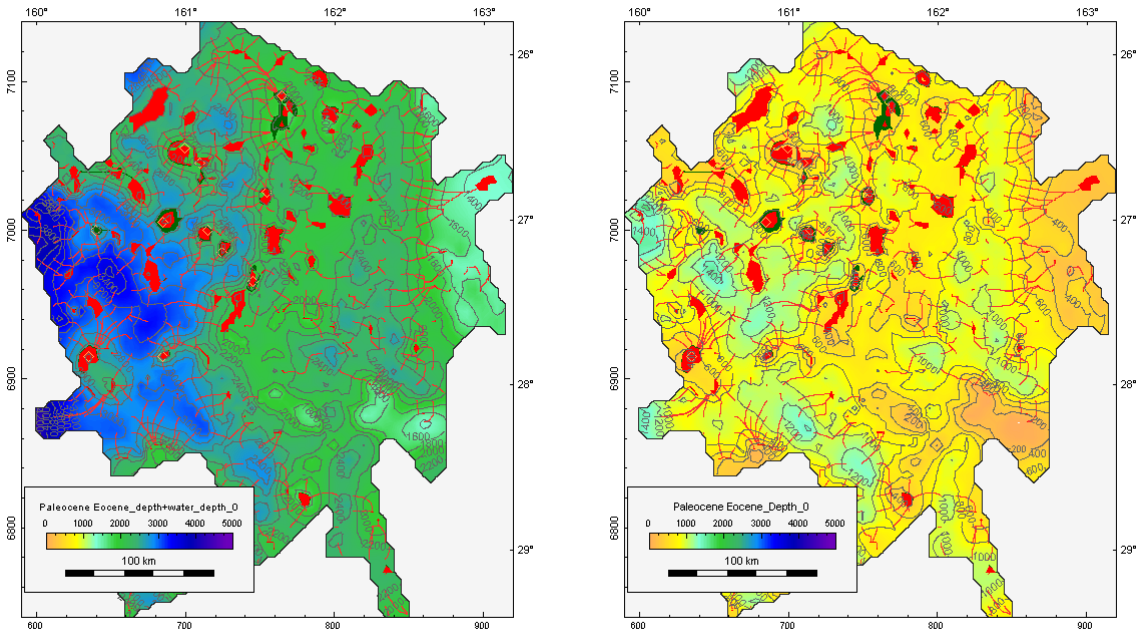

Figure 34 Migration results from flow-path modelling without using sand facies control on top Lower Post-rift (Lower Sag) unit at the present day; structural map with accumulations (left), present day burial depth with accumulations (right). Note that legends on maps refer to the base of the overlying unit; in this case the Paleocene Eocene unit.

3.3.2 Syn-rift sequences

Possible reservoir rocks in the Upper Syn-rift 2 unit include deltaic, shoreline and turbidite sandstones. Without migration facies constraints the models can only provide the best-case end-member for petroleum migration and accumulation, because they assume the existence of laterally continuous and connected reservoir facies across the model area. In reality, migration routes are likely to be less developed and more restricted resulting in fewer and smaller predicted accumulations. Flow-path models are presented for this succession, although the resultant mapped accumulations should be interpreted with care bearing in mind the simplifications and assumptions used in the models.

Migration modelling suggests numerous large oil accumulations at the end of the Eocene (36 Ma), however the crestal depth of burial for accumulations at this time is less than 400 m and it is unlikely an adequate seal existed. Equivalent flow-path models for the present day on the top Upper Syn-rift-2 (70 Ma) unit are shown in Figure 35. Accumulations are predicted across the Capel Basin and in the west Faust Basin generally containing 2 to 3 billion bbl (up to 8 billion bbl) of oil, and 7 to 13 Tcf gas. Such large accumulations are unlikely to be contained, since burial depths remain relatively shallow, at 400 – 800 m. Reducing the modelled seal capacity to an arbitrary 100 m column height decreases the largest accumulations to 2 billion bbl oil and 4 Tcf gas.

The Lower Syn-rift 2 unit and Syn-rift 1 megasequence may include fluvial systems with variable potential as reservoir formations. Nearly all predicted accumulations at the end of the Eocene (at 36 Ma) are located in structures with burial depths generally less than 500 m so are unlikely to be contained. There is a good probability that petroleum migrating into such structural traps has leaked to the surface. Flow-path models with predicted accumulations for the present day are presented in Figure 36 for the base of the Upper Syn-rift 2 unit (or middle Syn-rift 2 megasequence). The larger accumulations average 3 billion bbl oil and 10 Tcf gas at burial depths of 400 – 900 m, although some deeper accumulations are predicted at burial depths of 1200 -1600 m in the west Capel Basin. Deeper structures are likely to carry less of containment risk, and may prove to be better exploration targets. In addition, stratigraphic plays (not assessed as part of this project) may also provide an important contribution to the petroleum potential of the basins.

A representation of predicted present day accumulations for the deeper Syn-rift 1 megasequence is presented in Figure 37. Burial at the present day for accumulations in the west Capel Basin at the base of the sequence is up to 2,200 m, but many of the larger structural traps are only buried by between 400 and 800 m of overburden. This model utilises only oil and gas expelled from the Walloon equivalent coal measures for flow-path modelling so predicted accumulations are smaller than for overlying intervals, varying between 1 and 5 Tcf of gas at this level. Notably many of the accumulations are located on the same structural highs as the other levels examined (see Figure 4), hence the similarity in burial depths.

3.4 DISCUSSION ON MIGRATION

Map-based charge modelling has provided a reconnaissance level understanding of migration pathways on mapped horizons between the lower Post-rift (top Lower Post-rift (Lower Sag) unit) and Pre-rift megasequences (top Walloon equivalent coal measures unit). The modelling assumed simple reservoir properties with no migration losses to estimate possible trapped volumes in structural highs. The charge and volumetric assessment could be further refined using higher density seismic data, reservoir facies maps and actual, rather than assumed, rock property data for reservoir and seal units. In addition, the flow-path

models for different levels use the same volumes of expelled petroleum and 3D modelling is required to fully account for losses and dependencies related to vertical migration between levels. Future 3D modelling may be justified when more data, providing further geological constraints, becomes available.

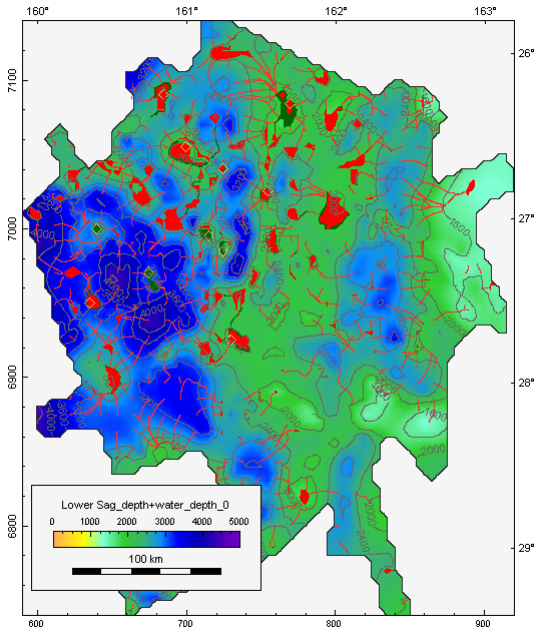

Structure and accumulations
base Lower Post-rift (Lower Sag) at 0 Ma

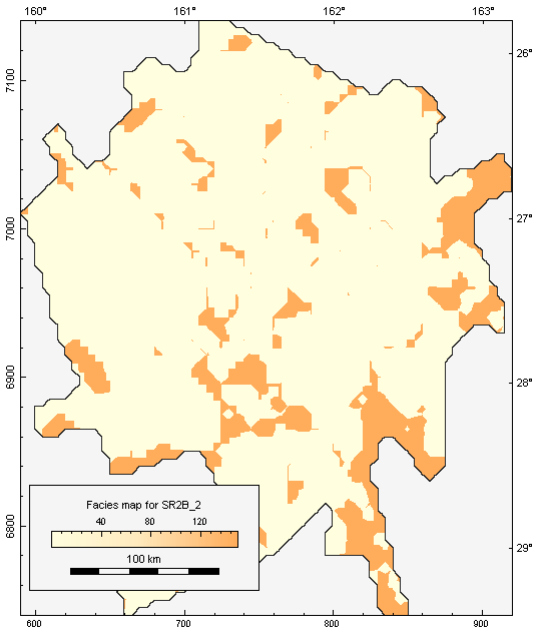

No-flow 'facies' map
base Lower Post-rift (Lower Sag) at 0Ma

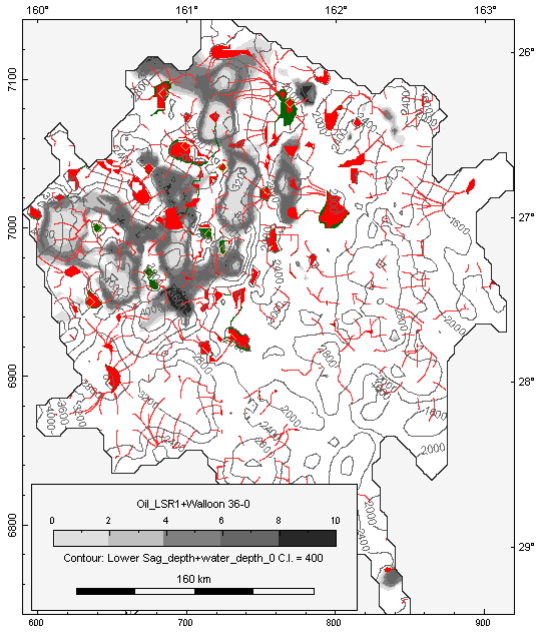

Expelled oil volumes and accumulations
base Lower Post-rift (Lower Sag) at 0 Ma

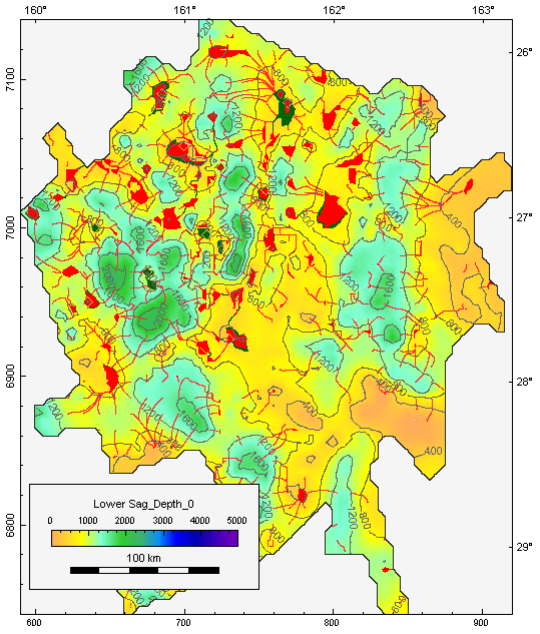

Burial depth and accumulations
base Lower Post-rift (Lower Sag) at 0 Ma

Figure 35 Migration results from flow-path modelling on the base of the Lower Post-rift (Lower Sag) unit at the present day; structural map with accumulations (top left), no-flow 'facies' zones shown as orange (top right), structural contours with accumulations showing expelled oil volumes (MMbbl/km^2) for the period since 36 Ma as a grey-scale overlay (bottom left), present day burial depth with accumulations (bottom right). Note that legends on maps refer to the base of the overlying unit; in this case the Lower Post-rift (Lower Sag) unit.

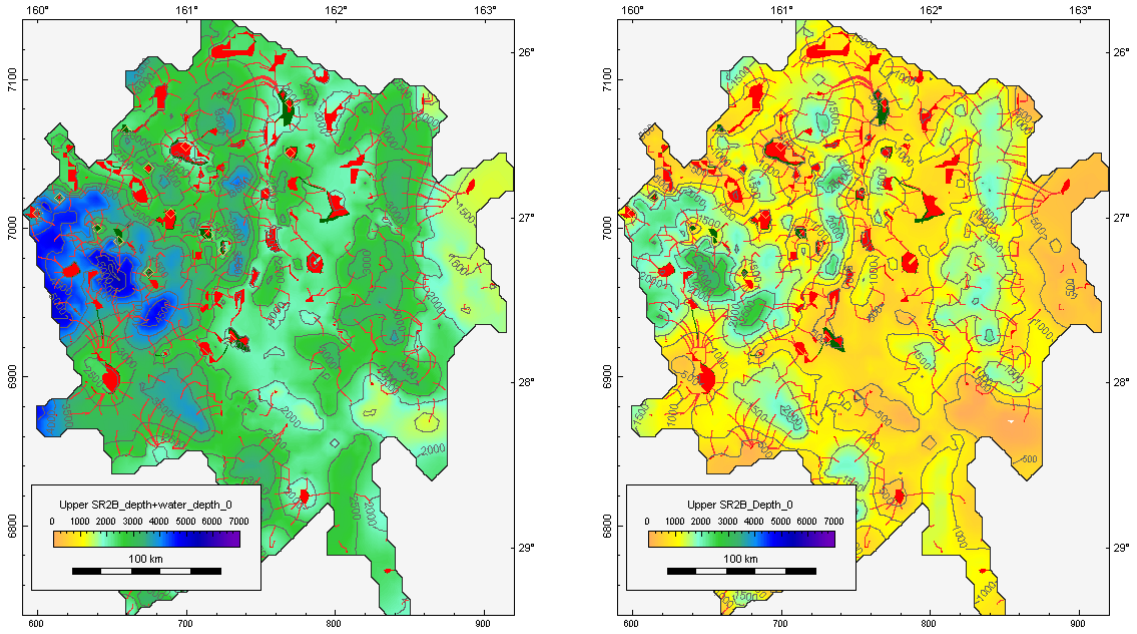

Figure 36 Migration results from flow-path modelling using no sand facies control on the base of the Upper Syn-rift 2 (top Lower Syn-rift 2) at the present day; showing structural map with accumulations (left), and present day burial depth with accumulations (right).

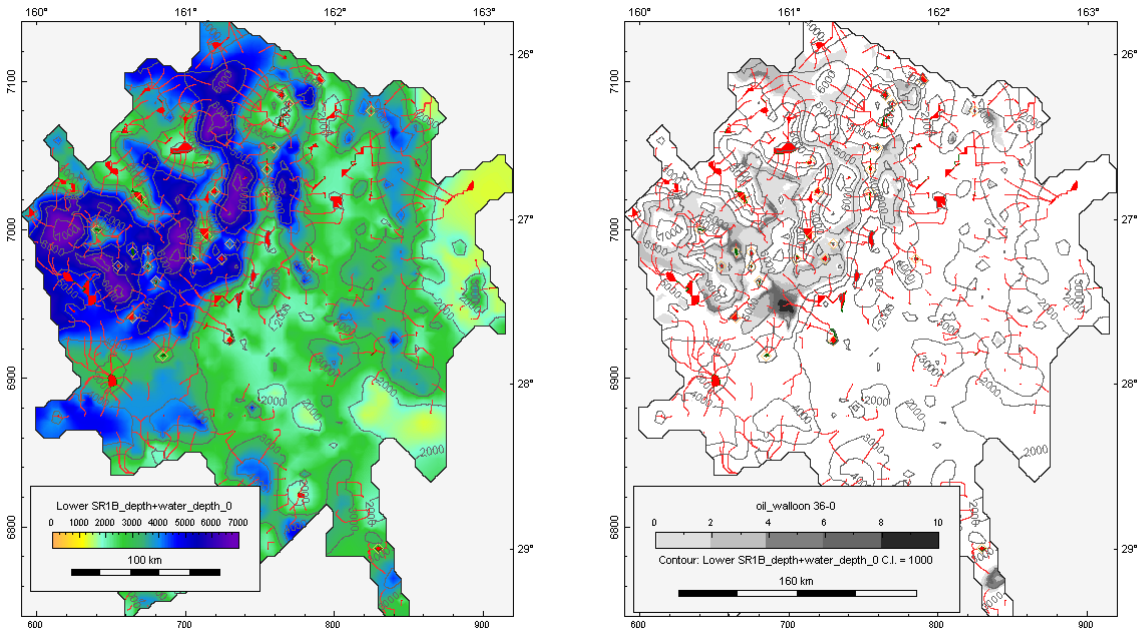

Figure 37 Migration results from flow-path modelling on base Lower Syn-rift 1 unit (top Pre-rift megasequence) at the present day; showing structural map with accumulations (left), and structural contours with accumulations and expelled oil volumes (MMbbl/km2) from the Walloon coal measures for the period since 36 Ma as a grey-scale overlay (right).

In terms of the petroleum systems, the Capel and Faust basins have been characterised by two key periods, pre-Oligocene (prior to 36 Ma in models) and Oligocene through Neogene times. A primary assumption for the modelling is that source rocks exist with adequate petroleum potential within the Pre-rift and Syn-rift megasequences. While 80% of the total volume of oil and gas is predicted to have been generated and expelled before the Oligocene

(before 36 Ma), our models predict there are still sufficient volumes expelled since 36 Ma to charge mapped structural traps. Using an approach whereby total expelled oil and gas volumes are "migrated across" individual mapped horizons, the flow-path models predict oil accumulations of generally 2 to 3 billion bbl and up to 8 billion bbl, with gas accumulations of about 10 Tcf (5 to 13 Tcf). For comparison, arbitrarily applying a 90% loss of expelled volumes yields models with average sized accumulations of 200 to 500 Mbbl oil and 2 to 4 Tcf gas.

A key risk however, is containment with many of these predicted accumulations located at burial depths of less than 1,000 m. Seal effectiveness risk is considered greater for structural traps charged prior to 36 Ma due to overburden thicknesses of generally less than 400 m mapped for the Late Eocene. Because of the risks associated with seal effectiveness over large but shallow structural highs, more favourable petroleum targets may be located in deeper structural and stratigraphic traps within the Cretaceous and Paleogene succession.

Given the reconnaissance-level scope of this study, and the lack of suitable lithostratigraphic data, no stratigraphic traps have been modelled. Nevertheless the simple flow-path modelling does indicate the potential for charge of structural traps in the Capel and western Faust basins and highlights the key risks.

The application of a simplistic sand/mud facies control reduced total accumulated volumes by a third, and restricted predicted accumulations to the eastern Capel and western Faust basins. Clearly the presence of suitable reservoir facies is a risk in any charge study and before more detailed assessment is undertaken further analysis on possible sand distribution will be necessary.

Proving that a viable petroleum system is present in the Capel and Faust basins will ultimately require drilling and testing. Until this is undertaken, recommendations to improve our understanding of the basin's petroleum systems include:

- Higher density seismic investigation with appropriate data processing and analyses to:
  - further delineate potential trapping structures,
  - outline possible reservoir facies,
  - map likely source rock intervals, and
  - identify migration pathways, including those associated with faults and fractures.
- Correlation studies with sample data to define key source, reservoir and seal rock properties.
- Probabilistic petroleum systems analysis to identify and better constrain locations and sizes of potential accumulations.

4.0 REFERENCES

Armstrong, P.A., Chapman, D.S., Funnell, R.H., Allis, R.G., Kamp, P.J.J. 1996. Thermal modelling and hydrocarbon generation in an active-margin basin: The Taranaki Basin, New Zealand. American Association of Petroleum Geologists Bulletin 80, 1216–1241.

Boreham, C.J., Blevin, J.E., Radlinski, A.P. and Trigg, K.R. 2003. Coals as a source for oil and gas, a case study from the Bass Basin, Australia. The APPEA Journal 45, 117-148.

Bryan, S.E., Constantine, A.E., Stephens, C.J., Ewart, A., Schon, R.W. and Parianos, J. 1997. Early Cretaceous volcano-sedimentary successions along the eastern Australian continental margin: implications for the breakup of eastern Gondwana. Earth and Planetary Science Letters 153, 85–102.

Colwell, J., Foucher, J-P., Logan, G. and Balut, Y. 2006. Partie 2, Programme AUSFAIR (Australia–Fairway basin bathymetry and sampling survey) Cruise Report. *In:* Les rapports de campagnes à la mer, MD 153/AUSFAIR–ZoNéCo 12 and VT 82/GAB on board R/V Marion Dufresne, Institut Polaire Français Paul Emile Victor, Plouzané, France, Réf : OCE/2006/05.

Colwell, J.B., Hashimoto, T., Rollet, N., Higgins, K., Bernardel, G. and McGiveron, S. 2010. Interpretation of seismic data, Capel and Faust basins, Australia's remote offshore eastern frontier. Geoscience Australia Record 2010/06.

England, W.A., 1994. Secondary migration and accumulation of hydrocarbons. *In:* Magoon, L.B. and Dow W.G. (eds.) The petroleum system – from source to trap. American Association of Petroleum Geology Memoir 60, 211–217.

Funnell, R.H., Stagpoole, V.M., Nicol, A., McCormack, N.M. and Reyes, A.G. 2004. Petroleum generation and implications for migration: A Maui Field charge study, Taranaki Basin. 2004 New Zealand Petroleum Conference Proceedings, 7th -10th March 2004, Auckland, New Zealand.

Grim, P.J., 1969. Heat flow measurements in the Tasman Sea. Journal of Geological Research 74, 3933–3934.

Hashimoto, T., Rollet, N., Stagpoole, V., Higgins, K., Petkovic, P., Hackney, R., Funnell, R., Logan, G.A., Colwell, J. and Bernardel, G. 2010. Geology and evolution of the Capel and Faust basins: petroleum prospectivity of the deepwater Tasman Sea frontier. 2010 New Zealand Petroleum Conference, Ministry of Economic Development, Wellington.

Hashimoto, T., Rollet, N., Higgins, K., Bernardel, G. and Hackney, R., 2008. Capel and Faust basins: Preliminary assessment of an offshore deepwater frontier region. *In:* Blevin, J.E., Bradshaw, B.E. and Uruski, C. (eds), Eastern Australasian Basins Symposium III: Energy security for the 21st century, Petroleum Exploration Society of Australia Special Publication, 311–316.

Higgins, K.L., Hashimoto, T., Hackney, T., Petkovic, P. and Milligan, P. 2011. 3D geological modelling and petroleum prospectivity assessment in offshore frontier basins using GOCAD^{TM}: Capel and Faust basins, Lord Howe Rise. Geoscience Australia Record 2011/02.

King, P.R. and Thrasher, G.P. 1996. Cretaceous–Cenozoic geology and petroleum systems of the Taranaki Basin, New Zealand, Institute of Geological and Nuclear Sciences Monograph 13.

Morin R.H. and Von Herzen R.P. 1986. Geothermal measurements at deep sea drilling project site 587. *In:* Kennett, J.P., von de Borch, C.C., et al., Initial Reports DSDP 90 Washington (U.S. Govt. Printing Office), 1317–1324.

Norvick, M.S., Smith, M.A. and Power, M.R. 2001. The plate tectonic evolution of eastern Australasia guided by the stratigraphy of the Gippsland Basin. *In*: Hill, K.C. and Bernecker, T., (eds.) Eastern Australasian Basins Symposium: a refocussed energy perspective for the future, Petroleum Exploration Society of Australia Special Publication, 15–24.

Norvick, M.S., Langford, R.P., Rollet, N., Hashimoto, T., Higgins, K.L. and Morse, M.P. 2008. New insights into the evolution of the Lord Howe Rise (Capel and Faust basins), offshore eastern Australia, from terrane and geophysical data analysis. *In*: Blevin, J.E., Bradshaw, B.E. and Uruski, C. (eds.) Eastern Australasian Basins Symposium III: Energy security for the 21st century, Petroleum Exploration Society of Australia Special Publication, 291–310.

O'Brien, P.E., Powell, T.G. and Wells, A.J. 1994. Petroleum potential of the Clarence-Moreton Basin. *In*: Wells, A.T. and O'Brien, P.E. (eds.) Geology and petroleum potential of the Clarence-Moreton Basin, New South Wales and Queensland. Australian Geological Survey Organisation Bulletin 241, 277–290. Australian Government Publishing Service, Canberra.

Pepper, A.S. and Corvi, P.J., 1995a. Simple kinetic models of petroleum formation. Part 1: oil and gas generation from kerogen. Marine and Petroleum Geology 12, 291–319.

Pepper, A.S. and Corvi, P.J. 1995b. Simple kinetic models of petroleum formation. Part III: modelling an open system. Marine Petroleum Geology 12, 417–452.

Pepper, A.S. and Dodd, T.A. 1995. Simple kinetic models of petroleum formation. Part II: oil–gas cracking. Marine and Petroleum Geology 12, 321–340.

Powell, T.G., Boreham, C.J., Smyth, M., Russell, N.J. and Cook, A.C. 1991. Petroleum source rock assessment in non-marine sequences: pyrolysis and petrographic analysis of Australian coals and carbonaceous shales. Organic Geochemistry 17, 375–394.

Sutherland, R., Collot, J., Lafoy, Y., Logan, G.A., Hackney, R., Stagpoole, V.M., Uruski, C.I., Hashimoto, T., Higgins, K., Herzer, R.H., Wood, R.A., Mortimer, N. and Rollet, N. 2010. Lithosphere delamination with foundering of lower crust and mantle caused permanent subsidence of New Caledonia Trough and transient uplift of Lord Howe Rise during Eocene and Oligocene initiation of Tonga-Kermadec subduction, western Pacific. Tectonics 29, TC2004, doi:10.1029/2009TC002476.

Van de Beuque, S., Stagg, H.M.J., Sayers, J., Willcox, J.B. and Symonds, P.A. 2003. Geological framework of the northern Lord Howe Rise and adjacent areas. Geoscience Australia Record 2003/01.

Von Herzen, R.P. 1973. Geothermal measurements, Leg 21. *In:* Burns, R.E., Andrews, J.E., et al., Initial Reports DSDP 21 Washington (U.S. Govt. Printing Office), 443–457.

Willett, S.D. 1988 Spatial variation of temperature and thermal history of the Uinta Basin. Unpublished PhD thesis, Univ. of Utah.

Wood, R.A., Funnell, R.H., King, P.R., Matthews, E., Thrasher, G.P., Killops, S.D. and Scadden, P.G. 1998. Evolution of the Taranaki Basin - hydrocarbon maturation and migration with time. *In:* 1998 New Zealand Petroleum Conference Proceedings, 307–316. The Publicity Unit, New Zealand Crown Minerals, Ministry of Commerce; Wellington.